ARTERIAL SIGNAL COORDINATION

WITH UNEVEN DOUBLE CYCLING

A Dissertation

by

HONGMIN ZHOU

Submitted to the Office of Graduate and Professional Studies of
Texas A&M University
in partial fulfillment of the requirements for the degree of

DOCTOR OF PHILOSOPHY

Chair of Committee,	H. Gene Hawkins
Committee Members,	Luca Quadrifoglio
	Martin A. Wortman
	Yunlong Zhang
Head of Department,	Robin Autenrieth

August 2016

Major Subject: Civil Engineering

ABSTRACT

In arterial coordination, high traffic volume at large intersections often requires a long cycle length to achieve good two-way progression. This long cycle length, however, often causes excessive delay at some minor intersections where the traffic volume is low on cross streets. This research proposed mathematical optimization models to enable uneven double cycling (UDC) in arterial signal coordination to address this issue.

The study first developed a basic UDC model to maximize two-way bandwidths and minimize average delay of cross streets at UDC intersection. The concept of nominal red was introduced to describe bandwidth geometry at UDC intersections. Disjunctive programming technique was used to convert a mixed integer nonlinear programming problem into a mixed integer quadratic programming problem for computation efficiency. The study further improved the basic UDC model to consider pedestrian needs and enhanced the modeling through multicriterion optimization. The additional objectives included minimal arterial average delay and minimal arterial number stops at UDC intersections, maximal variable bandwidth, and maximal secondary bandwidth.

With all the mathematical models ready, numerical experiments in the study explored factors affecting the applicability of the UDC control scheme. Results of the numerical experiments provided thresholds of parameters for determining UDC applicability. A rule of thumb was that when the green time of an intersection in the peak direction is longer than that at the critical intersection by at least the sum of minimum green time

and per phase lost time, UDC control might be beneficial at this intersection. The research then conducted a case study to evaluate the performance of various models on the field data of an arterial with four intersections. Comparing with conventional SC control under fixed timing, the UDC models significantly reduced delay at UDC intersections for both through and left turn movements, and reduced number stops at SC intersections. UDC control under actuated operation overcame the shortcoming of increasing arterial number of stops compared with fixed timing.

Finally, the advantages and disadvantages of UDC control were summarized, and preliminary guidelines were provided for UDC implementation. Future study topics were also recommended.

DEDICATION

To my parents, my husband, and three lovely kids

ACKNOWLEDGEMENTS

I would like to thank my committee chair and adviser, Dr. Hawkins, for his guidance and support throughout the course of my academic studies. He has been supportive no matter what decision I make and considerate during my tough times. I am also thankful for my committee member, Dr. Zhang, for admitting me to Texas A&M University and providing valuable comments and suggestions for my research. It has been a great experience to study here. Many sincere thanks to my committee members, Dr. Quadrifoglio, and Dr. Wortman for discussing with me in solving my academic problems. I also gratefully acknowledge Dr. Nadeem Chaudhary for his guidance on this research, Mr. John Black, Mr. Wayne Kurfees, and Dr. Tom Urbanik for their suggestions on initializing this research topic.

I would also like to show my deepest appreciations to so many of great people with whom I have befriended during my doctoral study at the Texas A&M University and the Texas A&M Transportation Institute. Thank Dr. Xiaosi Zeng for being a great friend and discussing many technical details in this research with me; thank Mr. Robert Benz and Mr. Anthony Voigt for providing financial support for me and introducing me to great people; thank Ms. Ying Li for being a sincere company and enriching my life experience.

Finally, thanks to my parents for their unconditional love, to my husband for his patience and love, and to my three lovely kids for being the motivation to finish my Ph.D study.

NOMENCLATURE

ArtLT	Arterial Left Turn
AtC	Arterial to Cross street traffic ratio
BB	Branch and Bound
CF	Coordinability Factor
Crst	Cross Street
CrstLT	Cross street Left Turn
CTM	Cell Transmission Model
FHWA	Federal Highway Administration
GA	Genetic Algorithm
HCM	Highway Capacity Manual
IQA	Incremental Queue Accumulation
LOS	Level of Service
LWR	Lighhill-Whitham-Richards
MILP	Mixed Integer Linear Programming
MINLP	Mixed Integer Nonlinear Programming
MIQP	Mixed Integer Quadratic Programming
MOE	Measure of Effectiveness
MUTCD	Manual on Uniform Traffic Control Devices
NEMA	National Electrical Manufacturers Association
PI	Performance Index
PROS	Perceived Progression Opportunity

PSD	positive semi-definite
SC	Single Cycling
UDC	Uneven Double Cycling
UtS	Traffic ratio between UDC intersection to SC intersection
Xc	Volume to Capacity ratio

TABLE OF CONTENTS

Page

LIST OF FIGURES

Page

LIST OF TABLES

Page

CHAPTER I

INTRODUCTION

BACKGROUND

As traffic volume has increased over the past two decades, the total hours of national urban traffic delay has been more than doubled [*1*]. Traffic agencies are using long cycle lengths (often over 150 seconds) during peak hours to provide adequate two-way arterial progression between large major-major intersections (high-volume on both roads) and to alleviate congestion at the critical intersections. However, conventional arterial coordination using a long cycle length can cause excessive delay for drivers on the minor cross streets at major-minor intersections (low-volume on the minor street). Traffic agencies have used half of the background cycle length at some of these major-minor intersections, where the second half cycle repeats exactly the same services (phasing sequences and splits) as the first half cycle, to reduce delay. With the introduction of 16-phase controllers, Kurfees proposed to address this issue with a more flexible tool, the "*uneven double cycling*" (UDC) control scheme [*2*], where the key phases in a cycle are repeated twice during the background cycle, but with different phase lengths. Figure 1 illustrates two examples of phase sequences and splits using a UDC scheme.

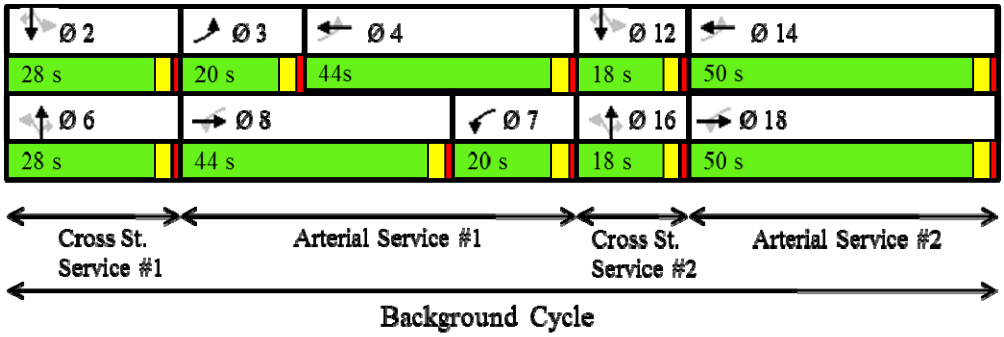

1a. UDC example with protected left turn on both streets

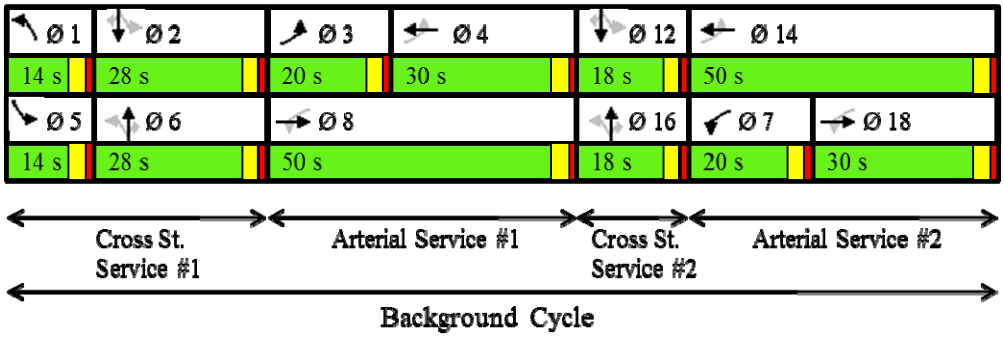

1b. UDC example with protected left turn on arterial only

Figure 1. Phase sequence and splits using a UDC scheme

The UDC scheme shown in Figure 1 services all through movements twice (typically with unequal phase lengths) and typically services the protected left-turn once per background cycle (if at all) at the major-minor intersection. The Signal Timing Manual [*3*] categorizes this control scheme as the repeated phase service or conditional service for through phases. Compared with half cycling, the UDC scheme is able to reduce delay on minor cross streets without impeding the passage of the green band in either direction on the arterial street and is potentially applicable to more traffic and geometric scenarios.

However, few studies have addressed UDC development procedures or the method of optimizing coordination. At present, the UDC timing scheme is developed manually [*2*] and thus might not be optimal. This dissertation proposes a UDC-enabled arterial coordination optimization method that maximizes two-way progression and minimizes signal delay and arterial number of stops.

RESEARCH OBJECTIVES AND TASKS

Arterial signal coordination with the UDC control scheme differs from conventional coordination with only single cycling (SC). Firstly, the underlying reason of enabling UDC is to reduce unnecessary delay on minor cross streets when the background cycle length is very long. This intuitively signals the need to account for minimized delay on cross streets in the objective function, which is usually not a concern in conventional coordination optimization. Secondly, serving through traffic twice and left turn traffic once in the background cycle makes a phasing scheme different from traditional signal timing. This requires the addition of new decision variables in formulating signal offsets and adds complexity to the modeling. Thirdly, the UDC scheme splits a single long through green phase into two separated short phases, which reduces the available green time for arterial progression and might not be beneficial for all traffic conditions. This justifies the consideration of additional objectives of minimal arterial disutilities and the evaluation of model performance under various traffic and operation scenarios for preliminary guidelines. These issues are targeted throughout the research.

The research focuses on off-line signal timing optimization given the fact that the real-time operation system is not widely implemented yet. Deterministic programming is commonly adopted for off-line optimization, although traffic variation is often a concern for the evaluation of model performance. Under such scope to solve the above issues, this research sets the goal as (1) to develop off-line deterministic mathematical models that efficiently generates arterial coordination signal timing plans serving the UDC control scheme; and (2) to develop preliminary guidelines for UDC application. The research has the following tasks in respective chapters of the this dissertation to achieve the goal

- Study the mechanism of UDC control scheme and thoroughly review the literature on arterial signal coordination methods for optimization strategies and on traffic representation method for objective formulation and performance evaluation. These work is presented in Chapter II;
- Develop a basic model to enable UDC control in arterial coordination in Chapter III;
- Improve the basic UDC model to consider multicriterion optimization in Chapter IV;
- Conduct numerical experiments in Chapter V and case study in Chapter VI to evaluate performance of the UDC models; and
- Provide preliminary guidelines for UDC implementation and suggest topics for future study in Chapter VII.

CHAPTER II

LITERATURE REVIEW

This chapter first provides an overview of the basics of arterial signal coordination for the reasoning behind UDC. A comprehensive review on the literature then covers a variety of off-line optimization strategies, traffic representation methods, their applications, and relevant studies.

MECHANISM OF UNEVEN DOUBLE CYCLING

The Manual on Uniform Traffic Control Devices (MUTCD) [*4*] defines a traffic control signal as any highway traffic signal by which traffic is alternatively directed to stop and permitted to proceed. The MUTCD provides guidance that traffic signals within 0.5 miles apart along a corridor should be coordinated unless operating in different cycle lengths. The purpose of arterial signal coordination is to permit continuous movement along the arterial with minimum stops and delays to reduce fuel consumption and improve air quality [*3*]. Under coordination, cycle lengths should normally be the same for all participating signalized intersections to maintain a consistent time based relationship. This common cycle length is called the background cycle length, which is often dictated by the critical intersection with the longest natural cycle length among all coordinated intersections. Since the natural cycle length is determined by the minimum delay requirement, increasing it at a noncritical intersection to the background cycle

length for coordination may bring unnecessary delay to uncoordinated movements at this intersection. Because the noncritical intersection has longer green phase durations than the critical intersection for coordinated through movements, when the difference between the two, defined as the slack time [*5*], is long enough, it is possible to split the long through green time into two separated phases while still maintaining a good coordination quality.

Figure 2 illustrates how UDC scheme can reduce unnecessary delays. Consider a major-minor intersection with westbound and northbound being the peak direction on arterial and cross street, respectively. Under SC, the westbound through phase (∅4) is 80 seconds and the northbound through phase (∅6) is 46 seconds. The coordinated through phase ∅4 has a slack time of, say, 35 seconds, in excess of that at the critical intersection. For a vehicle arriving at the end of northbound through green phase ∅6, the wait time is about 114 seconds (indicated as the red bar in Figure 2) before it leaves the stop bar. Under UDC, the long coordinated phase of 80 seconds is split into two phases of 30 seconds (∅4) and 50 seconds (∅14). The 50-second ∅14 is the new coordinated phase which is still longer than the westbound green phase of 45 seconds at the critical intersection and is possibly long enough for good progression. Meanwhile, the northbound coordinated through phase ∅6 is split into two phases of 28 seconds (∅6) and 18 seconds (∅16). For the same vehicle arriving at the end of the northbound through green, it only needs to wait for 50 seconds before leaving the stop bar. This

mechanism holds the same for the off-peak directions of eastbound and southbound and reduces through delay on cross streets without affecting the capability of coordination.

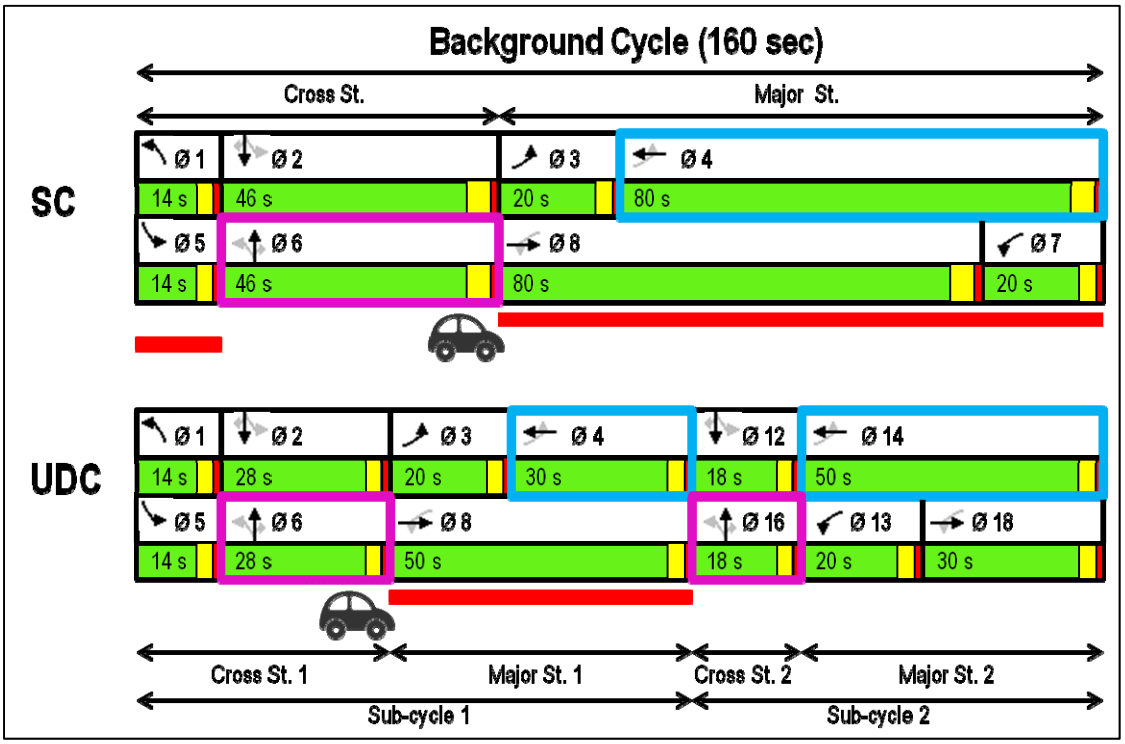

Figure 2. UDC mechanism of reducing delay on cross streets

Note that the repeated phases ∅4 and ∅14 (or ∅6 and ∅16) run as overlap with each other, whereas the left turn phases are serviced only once. This unique feature differentiates UDC from half cycling and thus requires advance signal controller (e.g., 16-phase controller) as opposed to repeat all phases exactly the same using the NEMA (8-phase) controller.

While the UDC control scheme reduces cross street delay by servicing through movement twice in a background cycle, there is very limited study in the literature about optimizing UDC coordination timing plans. Currently, the UDC timing scheme has been developed manually in the commercial signal timing software package Synchro [*2*, *6*]. Figure 3 shows a Synchro output of time-space diagram of an arterial (Campbell Rd in Richardson, TX) with SC control at end major-major intersections (at N Jupiter Rd and N Plano Rd) and UDC control at two major-minor intersections (at Owens Blvd and Yale Blvd) in between. Eastbound and westbound green bands pass through the intersection at Owens Blvd in the same sub-cycle of a long green phase leaving the other sub-cycle uncoordinated. On the contrary, the eastbound green band passes through the intersection at Yale Blvd in the sub-cycle of a long green phase whereas the westbound green band passes through the sub-cycle of a short green phase.

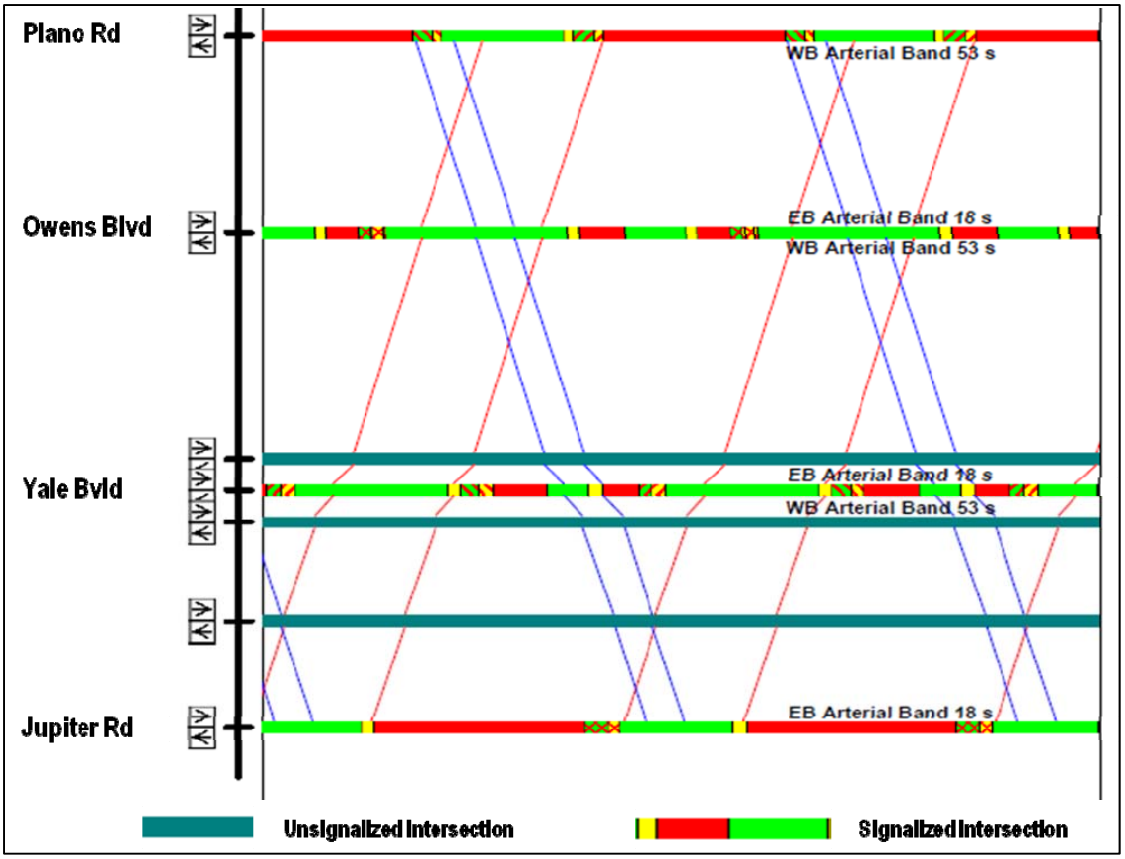

Figure 3. Example of time-space diagram with UDC control

(Generated by Synchro [*6*])

Developing the coordination timing plans with UDC scheme in Synchro is an iterative process of on-screen adjustments of the following settings for each candidate UDC intersection.

- Length of green phases of the twice-serviced through movements; and
- Association of the once-serviced left-turn movement, leading or lagging, with one of the through services.

Such a process is cumbersome and might not yield optimal solutions, and few studies have addressed mathematical methods of optimizing coordination considering UDC control.

STRATEGIES OF COORDINATION OPTIMIZATION

From the aforementioned purpose of signal coordination, the objectives of signal coordination may include (1) continuous traffic movements, (2) minimum delays and stops, and (3) reduced fuel consumption. Each of the objectives has its own quantitative representation in the objective function, and a number of studies target one or more of these objectives for their coordination optimization. Since fuel consumption is often associated with traffic progression and delay/stops and is less of a concern in this research, this section focuses on the first two optimization strategies.

For continuous traffic movements, the concept of bandwidth describes the proportion of background cycle length in which a vehicle can travel throughout the arterial at a determined progression speed [*3*]. This is the most widely used objective for signal synchronization. One of the earliest studies by Bowers [*7*] uses a graphic method to manually design time-space diagram to find the maximum bandwidth with constant speed and green times being the same for all intersections. Brooks' computerized model [*8*] indirectly maximizes bandwidth by minimizing bandwidth interferences and defines the master (critical) intersection as the one with shortest arterial through green phase. The model relaxes constraints of Bowers' model for unequal green times and varying

speed. The PASSER-II program [*9*] extends Brooks' model to optimize phasing sequence for left turn movements. Morgan and Little's model [*10*] uses a half-integer technique to optimize offsets at multiple of half length of the background cycle for maximized bandwidth. A more generalized formulation of the bandwidth maximization is Little's mixed integer linear programming (MILP) model [*11*]. The model describes a bandwidth geometry and optimizes cycle length and design speed.

Little's model sets the benchmark for maximal bandwidth based coordination methods, and a number of studies improves coordination capability based on the model. The MAXBAND program [*12*] is an extension of Little's model to allow overlap and the selection of phasing sequence for left turn phases and can handle a simple triangular network. The MAXBAND-86 program generalizes the capability of network optimization to closed network [*13*, *14*]. The MULTI-BAND approach [*15*, *16*] generates variable bandwidths for both directions to accommodate various traffic on different links, which is then applied for network coordination in the MULTI-BAND-96 program [*17*]. The circular phasing scheme proposed Chaudhary *et al*. [*18*] services movements on four approaches clockwise or counter-clockwise in a four-phase sequence (main1-cross1-main2-cross2) to increase bandwidth. One problem of these bandwidth-based approaches is that the bandwidth tends to decrease as the number of intersections increases [*19*]. The system partition technique proposed by Tian and Urbanik [*20*] overcomes this issue by maximizing bandwidth for the peak direction and providing

sufficiently large bandwidths within individual subsets of intersections on the other direction.

In an effort to promote systematic optimization of signal timing in urban areas [*21*], the U.S. Federal Highway Administration (FHWA) adopts the delay-based optimization strategy originally developed by the U.K. Transport and Road Research Laboratory in the TRANSYT-7F program [*22*]. The original version of this program, TRANSYT, mainly uses a linear combination of delay and the number of stops as the objective function. It performs a macroscopic simulation of traffic flow within small time increments while signal timing parameters are varied. The decision variables include cycle length, green split, offset, and phase sequences. Another delay-base coordination program is Synchro [*6*]. It calculates intersection and approach delays using a percentile delay method [*23*]. It is capable of optimizing cycle length, green split, offset, and phase sequences by minimizing delay and stops [*24*]. Not many efforts have been made on the delay-based coordination method.

The bandwidth-based programs oversimplify traffic flow condition in the modeling and may result in unnecessary delay for cross-street traffic, whereas the delay/stop-based programs often do not provide good progression quality [*5*]. This leads to the multiobjective coordination strategy where a combination of two or more objectives dominant the optimization results. A new approach proposed by Wallace and Courage [*25*] is to maximize the perceived progression opportunity (PROS) by the driver outside

the green band. PROS is quantified as the number of successive green signals a driver encounters at the design speed without stopping. This method indirectly consider maximal bandwidth and minimal delay/stops as the objective and yields better results than optimizing each of the two objectives individually. A direct approach is to concurrently use delay-based and bandwidth-based programs for the optimization, which gives substantial benefits [*26*, *27*]. This motivates the corporation of both objectives in the model formulation. One attempt is to constrain the delay-based program with a bandwidth solution [*28*, *29*]. This method reveals that adjusting signal offsets and green times at the same time improves the arterial performance significantly. The saw-tooth pattern of bandwidth geometry proposed by Tsay and Lin [*30*] divides the front portion of slack time into two parts for queue clearance time and incoming flow clearance time. This is equivalent to adding minimal queue length to the formulation and thus brings the advantages of both delay-based and bandwidth-based strategies together. The COMBAND program [*5*] formally formulates a multiobjective function to minimize arterial total delay/stops and maximize bandwidth and arterial throughput. This method estimates uniform delay using two piecewise-linear components for computational efficiency. The enhanced version of the saw-tooth pattern model [*31*] maximizes the number of intersections vehicles, both from arterial and cross streets, can pass through without stopping. This resultant model is a mixed integer nonlinear programming problem.

Being improved over the years, current TRANSYT-7F and Synchro can optimize even more objectives [*23*]. In TRANSYT-7F [*32*], the objective function, named as the performance index (PI), may be a combination of delay and stops, fuel consumption, and/or optionally selected excessive maximum back of queue, excess operating costs, or progression opportunities. While optimizing delay-based objectives, Synchro incorporates a coordinability factor (CF) for each link between adjacent intersections to evaluate if synchronizing the two intersections would be beneficial. The calculation of CF is empirical and considers several factors, including link travel time, link traffic volume, link distance, vehicle platoon, vehicle queuing, and cycle lengths. Note that both programs are capable of optimizing half cycling but not UDC.

TRAFFIC REPRESENTATION METHODS

Different optimization strategies may target different performance measures, but all of them share a common requirement for traffic demand information. Depending on the available information, various traffic representation methods have been incorporated in signal optimization models. Traffic presentation methods consist of two major categories: analytical models and simulation models. The latter further includes macro-simulation and micro-simulation methods.

Analytical traffic representation often assumes certain distribution of traffic arrivals and discharges and then derives equations for calculating delays or stops. One of the earliest models calculating delay is the famous Webster's formulation [*33*]. The model assumes

Poisson traffic arrival rates and uniform discharging headways to derive an equation for average delay. This equation consists of three terms. The first term is the delay expression when traffic arrives at a uniform rate, which agrees with low arrival rate conditions but underestimates delay for high arrival traffic conditions. The second term is the delay derivation of an M/D/1 queuing system (Poisson arrival/uniform service/one server). The first two terms can give reasonable delay estimation except overestimating delay by about 15 percent under medium and high flow levels. The third term is an empirical correction to the first two terms to give a closer fit for all levels of flow. Since Webster's method relies heavily on the arrival distribution, an improvement made by Miller [*34*] is employing the variance-to-mean ratio and the diffusion theory to derive a delay approximation insensitive to the detailed stochastic characteristics of arrival flow. A further improved method of stochastic approximation proposed by Newell [*35*] is to represent the queue as a continuous fluid with deterministic or stochastic properties and apply the central limit theorem. The result agrees systematically with Webster's formula and solves the issue of delay approximation under steady-state condition.

When traffic demand is time-dependent and fluctuates around saturation, the above delay approximation tends to become infinity. A coordinate transformation technique adopted by Kimber and Hollis [*36*] to the residual queue length and the delay expression can smooth the delay under steady-state condition into near-saturated and over-saturated conditions. The resultant formula is in a general form but too complicated for practical use, which is simplified by Akcelik [*37*] and eventually adopted in the Highway

Capacity Manual (HCM) 2010 [*38*]. The analytical formulas work as the deterministic equivalent of stochastic measures and can effectively approximate delay estimation while providing tractability and ease of computation in optimization modeling. However, the underlying assumptions in the derivation do not hold for all signal timing scenarios in practice.

An alternative traffic representation method is the simulation, either macroscopic or microscopic, of traffic dynamics in response to signal settings. One of the most famous macroscopic models is the cell transmission model (CTM) proposed by Daganzo [*39*, *40*]. The CTM is a finite-differencing solution scheme for the LWR (i.e., the Lighhill-Whitham-Richards) first-order hydrodynamic theory of traffic flow [*41*, *42*]. The model divides the roadways into homogeneous cells with the cell length equal to the duration of time step multiplied by the free-flow speed. Then a set of recursive equations provides a convergent approximation to the LWR kinematic flow representation. Many studies [*4346*] have applied this model in signalized traffic control analysis for isolated intersections, coordinated arterials and networks. A different application of the LWR theory for macro-simulation model is to incorporate platoon dispersion models [*47, 48*] in the shock wave propagation along the arterial [*49*]. This method models arterial traffic evolvement as a two-step Markov decision process. HCM adopts an incremental queue accumulation (IQA) method proposed by Rouphail et al. [*50, 51*] to depict queue evolvement by time for delay estimation, which is an extension of Webster's method. HCM adopts Robertson's geometric distribution model for platoon dispersion along the

arterial [*48*] and defines a platoon ratio to describe progression quality of signal coordination. TRANSYT-7F and Synchro programs both use macroscopic simulations in generating optimized coordination timing plan.

Microscopic simulation models are also widely used for performance evaluation of traffic signals. This type of models considers driving behaviors of individual vehicles (vehicle speed, acceleration, and deceleration) and interactions between vehicles (headway and spacing). Distributions of spot speed and time headway are often the key concern in microscopic flow models. Spot speed data often follow the normal distribution. Headways can be divided into three states: random state for low volume traffic, intermediate state for mid-range volume traffic, and interacting state for high volume traffic [*52*]. Random headways often follow the negative exponential distribution whereas interacting headways often follow the normal or lognormal distribution. The intermediate headway is more complicated, and the Pearson type III distributions and the composite model approach are often adopted [*52*]. These models often apply to uninterrupted flows. For interrupted traffic flows, description of queue discharge characteristics serves as the basis of determining saturation flow rate and capacity. At isolated intersections, queue discharge speed, flow rate, and headway may be expressed as a function of the time since the start of green using exponential distributions [*53*]. The headway distribution by different lane groups and queue positions may follow the Type I extreme value distribution [*54*]. For arriving traffic platoons, platoons can be described by analyzing headway, speed, and arrival flows. The number

of vehicles in a platoon may follow negative exponential distribution; platoon headway and speed follow normal distribution; the interplatoon headway follow lognormal distribution; and the number of platoons follows Poisson distribution [*55*]. CORSIM [*23*, *56*] and VISSIM [*57*] are time-based microscopic simulation tools which capture the stochastic feature of individual vehicles in both interrupted and uninterrupted flows. They are commonly used for performance evaluation.

Maximizing bandwidth is the most widely used objective of arterial coordination optimization to provide good progression quality, and the MULTI-BAND model is one of the best approaches for achieving this goal. A majority of these bandwidth-based optimization models are mixed integer linear programming problems and have good efficiency. Webster's delay formulation is the most widely used analytical model adopted in signal optimization and evaluation. HCM's description of platoon ratio and the queuing diagram provide practical approaches of representing arterial traffic and estimating delay. Considering delay in the coordination optimization often involves nonlinear programming.

CHAPTER III

BASIC MODELING OF ARTERIAL COORDINATION WITH UNEVEN DOUBLE CYCLING*

As stated in the literature review, bandwidth based modeling is most widely used to optimize signal coordination. This research adopts the bandwidth geometry described in the MAXBAND program and utilizes the multiobjective optimization strategy to enable the double cycling capability. The model is based on the following assumptions:

1. Prevailing traffic conditions are under-saturated;
2. No lane blockage or spillback occurs for left turn or through movement;
3. Arriving and discharging traffic flow on cross street approaches are constant.

The three assumptions are intended to describe stable and recurring arterial traffic operation conditions for the optimization model to be applicable. Usually, the under-saturation assumption is met by using a long cycle length to achieve a volume-to-capacity ratio between 0.8 and 0.9 at the critical (often the major-major) intersection. This long background cycle length results in sometimes much smaller volume-to-capacity ratio at the major-minor intersections where the UDC scheme might be beneficial. Given enough turning bay length and link length, the assumption of no

* Part of the content in this chapter is reprinted from *Arterial Signal Coordination with Uneven Double Cycling*, by H. Zhou and G. Hawkins, 2014. Texas A&M Transportation Institute Report (SWUTC/15/600451-00024-1), Texas A&M University System, 3135 TAMU, College Station, TX 77843

blockage or spillback can be satisfied. The constant arrival flow assumption for cross street traffic is to simplify delay estimation for computation efficiency. Future work can build on this foundation to address exceptions to these assumptions.

Compared with conventional signal timing, uneven double cycling needs a different design of the ring-barrier diagram and has more complicated bandwidth geometry. This chapter introduces mathematical formulations that are different from MAXBAND programming. Input parameters for the modeling include geometry and traffic information, signal timing parameters under SC control for fixed timing operation. The modeling process follows two steps.

1. Intuitively model a mixed integer nonlinear programming (MINLP) problem with fewer number of decision variables and constraints and solve the model using the genetic algorithm (GA);
2. Convert the model into a mixed integer quadratic programming (MIQP) problem through disjunctive programming and solve the model with branch and bound (BB) method to global optimum.

The Appendix I has a full list of detailed notations in alphabetical order for parameters, decision variables, and indices involved in the mathematical models developed in this and next chapters. The unit of all phase time related variables is in cycles.

OBJECTIVE FUNCTION

The proposed model considers two objectives: the maximal two-way progression and the minimal total average delay of through traffic on cross streets. For simplicity, delay estimation only considers the uniform delay and applies the queuing diagram to derive the delay formula for a double cycled intersection (thus the under-saturated assumption).

A background cycle under UDC has two sub-cycles, each of which consists of services on the arterial and the cross streets (e.g., cross street service #1 and arterial service #1 make a sub-cycle in Figure 1). Define the sub-cycle containing the outbound green band as the first sub-cycle $C1$ and thus the one without outbound green band as the second sub-cycle $C2$. Then the green split and red split for through movement in $C1$ are defined as first sub-green split $g1$ and first sub-red split $r1$, and the second sub-green split $g2$ and sub-red splits $r2$ are accordingly defined. With a given list of double-cycled intersections, for the j^{th} through movement at the u^{th} double cycled intersection, there exists two possible queuing diagrams for cross street through movement as shown in Figure 4, depending on whether the first sub-green time is large enough to discharge vehicles queuing in the first sub-cycle. Given the assumption of constant flow on cross streets, average delay per background cycle for this through movement is then calculated using Equation 1.

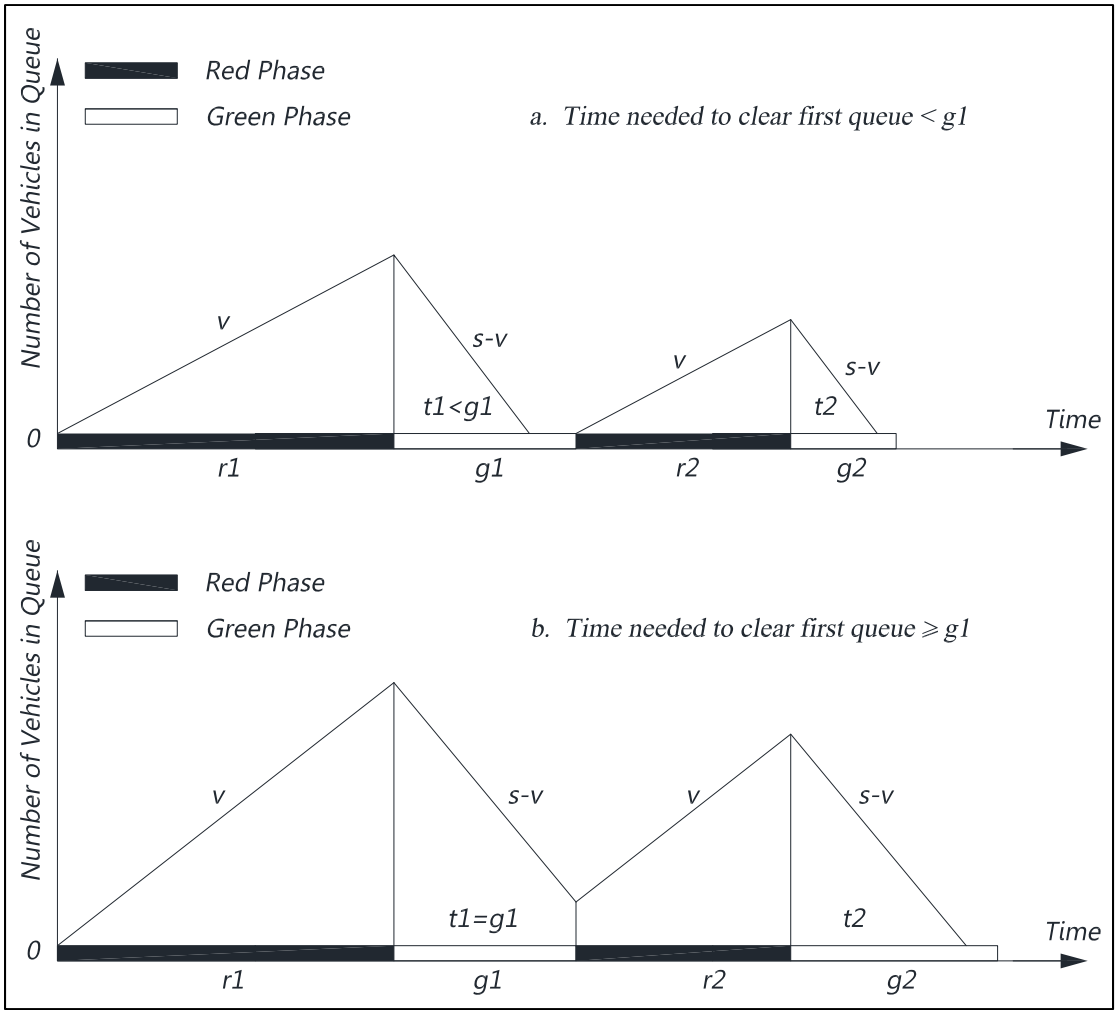

Figure 4. Queuing diagram of cross street through at a UDC intersection

$$AD_{u,jc}^{Tc} = \begin{cases} \dfrac{(r1_{u,jc}^2 + r2_{u,jc}^2)}{2(1-y_{u,jc}^T)z} & if \ \dfrac{r1_{u,jc}}{1/y_{u,jc}^T - 1} < g1_{u,jc} \\ \dfrac{(r1_{u,jc} + r2_{u,jc})^2}{2(1-y_{u,jc}^T)z} - \dfrac{r2_{u,jc}\, g1_{u,jc}}{y_{u,jc}^T z} & if \ \dfrac{r1_{u,jc}}{1/y_{u,jc}^T - 1} \geq g1_{u,jc} \end{cases} \quad \text{Equation 1}$$

where $y_{u,ja}^T$ is the volume-to-saturation (v/s) flow ratio of through traffic. Equation 1 is equivalent to Equation 2.

$$AD_{u,jc}^{Tc} = \frac{(r1_{u,jc} + r2_{u,jc})^2}{2(1 - y_{u,jc}^T)z} - \frac{t1_{u,jc} r2_{u,jc}}{y_{u,jc}^T z} \quad \text{Equation 2}$$

where $t1_{u,jc}$ is the actual queue discharge time in the first sub-cycle $C1$ and is calculated using Equation 3, which is equivalent to Equation 4.

$$t1_{u,jc} = \min\left\{\frac{r1_{u,jc}}{1/y_{u,jc}^T - 1},\ g1_{u,jc}\right\} \quad \text{Equation 3}$$

$$\begin{cases} t1_{u,jc} \le \dfrac{r1_{u,jc}}{1/y_{u,jc}^T - 1} \\ t1_{u,jc} \le g1_{u,jc} \end{cases} \quad \text{Equation 4}$$

Summation of all cross street approaches and intersections gives the total average through delay on cross street AD^{Tc} as shown by Equation 5.

$$AD^{Tc} = \sum_{u=1}^{Nu} \sum_{jc=3}^{4} AD_{u,jc}^{Tc} \quad \text{Equation 5}$$

Use the total average through delay on cross streets under SC control $AD_{\max}^{Tc}$ shown in Equation 6 to get the normalized total average through delay AD_n^{Tc} on cross streets as indicated by Equation 7.

$$AD_{\max}^{Tc} = \sum_{u=1}^{Nu} \sum_{jc=3}^{4} \frac{(1 - g_{u,jc}^s)^2}{2(1 - y_{u,jc}^T)z} \quad \text{Equation 6}$$

$$AD_n^{Tc} = \frac{AD^{Tc}}{AD_{\max}^{Tc}} \quad \text{Equation 7}$$

The definition of bandwidth is the same as used in the basic MAXBAND programming and is also normalized in the objective function. Normalization of the bandwidth uses the weighted sum of directional maximum greens possibly available for green band passage $BW_{\max}$, which is determined by using Equation 8 and Equation 9. Parameter $g_{ja}^{\max}$ is the maximum available green time for green band passage on the arterial.

$$BW_{\max} = g_1^{\max} + kg_2^{\max} \qquad \text{Equation 8}$$

$$g_{ja}^{\max} = \min\left\{\min_i\{g_{i,ja}^s\},\ \min_u\{g_{u,ja}^d - g_{u,ja}^{\min}\}\right\} \qquad \text{Equation 9}$$

Parameter *k* in Equation 8 is the target ratio of inbound to outbound bandwidth on the arterial and is taken as the ratio of total inbound to total outbound volumes along the arterial. Parameter $g_{u,ja}^d$ in Equation 9 is the total green time of a through phase under double cycling. $g_{i,ja}^s$ is the through green split without UDC control, and $g_{u,ja}^{\min}$ is the minimum through green time. Assuming the ratio of outbound (inbound) arterial total through green to cross street total through green being the same under double cycling and single cycling, parameter $g_{u,ja}^d$ is determined using Equation 10. This equation indicates that the ratio of total through green splits in a ring under UDC to that under SC is assumed to be the same as the ratio of the total green splits of a through movement under UDC to that under SC. Deducting the total lost time from the background cycle length gives the total through green splits in a ring. The total lost time is the sum of original lost time plus the additional lost time resulted from the introduction of two sub-

phases in a ring (assuming the same per-phase lost time for all through phases). Equation 10 also calculates this parameter for cross streets which will be used later in the constraint section.

$$g_{u,j}^{d} = \begin{cases} \dfrac{\left(1-4Y-L_{u,3-j}-L_{u,5-j}\right)g_{u,j}^{s}}{g_{u,j}^{s}+g_{u,j+2}^{s}}, & j = ja = 1,2 \\ \dfrac{\left(1-4Y-L_{u,7-j}-L_{u,5-j}\right)g_{u,j}^{s}}{g_{u,j}^{s}+g_{u,j-2}^{s}}, & j = jc = 3,4 \end{cases} \qquad \text{Equation 10}$$

where Y is the total per phase lost time, $L_{u,j}$ is the effective left turn split plus per-phase lost time. Then the normalized bandwidth objective BW_n is calculated using Equation 11.

$$BW_n = \frac{b_1 + kb_2}{BW_{\max}} \qquad \text{Equation 11}$$

where b_1 and b_2 are outbound and inbound bandwidths. With λ^B being the weight of bandwidth, the objective function is the weighted sum of the opposite of normalized bandwidth and normalized total average delay as indicated in Equation 12.

$$\min: \ \lambda^B(-BW_n) + (1-\lambda^B)AD_n^{Tc} \qquad \text{Equation 12}$$

CONSTRAINTS

New constraints introduced in this model are mainly for describing the new bandwidth geometry and enabling selection of one of the sub-green phases for green band passage.

Sub-phase Splits and Synchronization

The objective function involves calculating the sub-red splits for all approaches at a UDC intersection. Both left-turn phase duration and left-turn patterns affect the sub-red time of through movement at a double cycled intersection. The left turn pattern depends on which of the two sub-cycles contains the left turn phases and whether the left turn leads or lags in that sub-cycle.

With $\theta_{u,j}$ being the binary variable for protected left turn to select a sub-cycle, $\delta_{u,j}$ being selecting lag or lead left turn pattern, and $R1_{u,ja}(R2_{u,ja})$ being the total phase splits in the first (second) sub-cycle on the cross street, Table 1 and Equation 13 through Equation 17 show the determination of sub-red splits for arterial through phases. Calculation of sub-red splits of cross-street through movements follows the same method.

Table 1. Opposing left turn patterns and arterial through sub-red splits

LT Pattern	$\theta_{u,2}(\theta_{u,1})$	$\delta_{u,2}(\delta_{u,1})$	$r1_{u,1}(r1_{u,2})$	$r2_{u,1}(r2_{u,2})$
Lead in $C1_u$	1	0	$r1_{u,ja} = R1_{u,ja} + L_{u,3-ja} + Y$	$r2_{u,ja} = R2_{u,ja} + Y$
Lag in $C2_u$	0	1		
Lag in $C1_u$	1	1	$r1_{u,ja} = R1_{u,ja} + Y$	$r2_{u,ja} = R2_{u,ja} + L_{u,3-ja} + Y$
Lead in $C2_u$	0	0		

$$r1_{u,ja} = R1_{u,ja} + \left|\theta_{u,3-ja} - \delta_{u,3-ja}\right| L_{u,3-ja} + Y \quad \text{Equation 13}$$

$$r2_{u,ja} = R2_{u,ja} + \left(1 - \left|\theta_{u,3-ja} - \delta_{u,3-ja}\right|\right) L_{u,3-ja} + Y \quad \text{Equation 14}$$

where:

$$R1_{u,ja} = g1_{u,ja+2} + Y + \theta_{u,5-ja} L_{u,5-ja} \quad \text{Equation 15}$$

$$R2_{u,ja} = g2_{u,ja+2} + Y + (1 - \theta_{u,5-ja}) L_{u,5-ja} \quad \text{Equation 16}$$

$$L_{u,j} = \begin{cases} (l_{u,j} + Y)\beta_u^a & if\ j = ja = 1,2 \\ (l_{u,j} + Y)\beta_u^c & if\ j = jc = 3,4 \end{cases} \quad \text{Equation 17}$$

where $l_{u,j}$ is the effective left turn split, and β_u^a (β_u^c) is the binary parameter of protected left turn on arterial (cross streets). Similarly, sub-red time follows the same procedure and are calculated using Equation 18 through Equation 21.

$$r1_{u,jc} = R1_{u,jc} + \left(1 - \left|\theta_{u,7-jc} - \delta_{u,7-jc}\right|\right) L_{u,7-jc} + Y \quad \text{Equation 18}$$

$$r2_{u,jc} = R2_{u,jc} + \left|\theta_{u,7-jc} - \delta_{u,7-jc}\right| L_{u,7-jc} + Y \quad \text{Equation 19}$$

where:

$$R1_{u,jc} = g1_{u,jc-2} + Y + \theta_{u,5-jc} L_{u,5-jc} \quad \text{Equation 20}$$

$$R2_{u,jc} = g2_{u,jc-2} + Y + \left(1 - \theta_{u,5-jc}\right) L_{u,5-jc} \quad \text{Equation 21}$$

Substituting the sub-red splits into the objective function may affect the convexity of it because of the absolute function. This is improved by replacing the absolute function with a binary variable $\alpha_{u,j}^{I1}$ as indicated in Equation 22.

$$\alpha_{u,j}^{I1} = \left| \theta_{u,j} - \delta_{u,j} \right| \qquad \text{Equation 22}$$

Using a large value of $M = 2$, this disjunctive constraint is equivalent to Equation 23.

$$\begin{cases} \alpha_{u,j}^{I1} - \theta_{u,j} + \delta_{u,j} \le 2\left(1 - \lambda_{u,j}^{D1}\right) \\ -\alpha_{u,j}^{I1} + \theta_{u,j} - \delta_{u,j} \le 2\left(1 - \lambda_{u,j}^{D1}\right) \\ -\theta_{u,j} + \delta_{u,j} \le 2\left(1 - \lambda_{u,j}^{D1}\right) \\ \alpha_{u,j}^{I1} + \theta_{u,j} - \delta_{u,j} \le 2\lambda_{u,j}^{D1} \\ -\alpha_{u,j}^{I1} - \theta_{u,j} + \delta_{u,j} \le 2\lambda_{u,j}^{D1} \\ \theta_{u,j} - \delta_{u,j} \le 2\lambda_{u,j}^{D1} \end{cases} \qquad \text{Equation 23}$$

where $\lambda_{u,j}^{D1}$ is a binary decision variable for the absolute Equation 22. The two sub-green splits sum to equal the total green split (determined by Equation 10) as shown in Equation 24, and each of the sub-green splits should meet the minimum green requirements as indicated in Equation 25 and Equation 26.

$$g1_{u,j} + g2_{u,j} = g_{u,j}^{d} \qquad \text{Equation 24}$$

$$g1_{u,j} \ge g_{u,j}^{\min} \qquad \text{Equation 25}$$

$$g2_{u,j} \ge g_{u,j}^{\min} \qquad \text{Equation 26}$$

In each of the sub-cycles, two-way services (through and left turn movements) on the major street start and end simultaneously, so do the cross street services. For the first sub-green phase, Equation 27 holds:

$$\begin{cases} g1_{u,1} + \theta_{u,2} L_{u,2} = g1_{u,2} + \theta_{u,1} L_{u,1} \\ g1_{u,3} + \theta_{u,4} L_{u,4} = g1_{u,4} + \theta_{u,3} L_{u,3} \end{cases}$$ Equation 27

Given Equation 10 of proportional determination of total through green $g_{u,j}^{d}$ all other synchronization and summation to the background cycle length automatically hold.

Bandwidth Geometry

The bandwidth geometry of two paired SC intersections is the same as the original MAXBAND formulation. When involving the UDC scheme, the bandwidth geometry becomes more complicated than conventional coordination because the green band can choose to pass through either one of the two sub-green phases. This makes the bandwidth geometry very complex with conventional definitions of timing parameters. Figure 5 shows nine scenarios of two-way green band progression under UDC-enabled arterial coordination. In naming the scenarios, the first (second) name indicates the upstream (downstream) intersection control scheme, either SC or UDC control; if an intersection is UDC control, UDC1 and UDC2 further indicates the two-way green bands pass the same and different sub-cycles, respectively. For example, scenario (2) UDC1_SC means the upstream intersection is of UDC control with the two-way green bands passing through the same sub-cycle and the downstream intersection is of SC control. Given the definition of the first sub-green phase of outbound green band passage, UDC1 and UDC 2 also means that the inbound green band pass the first sub-green phase and second sub-green phase, respectively.

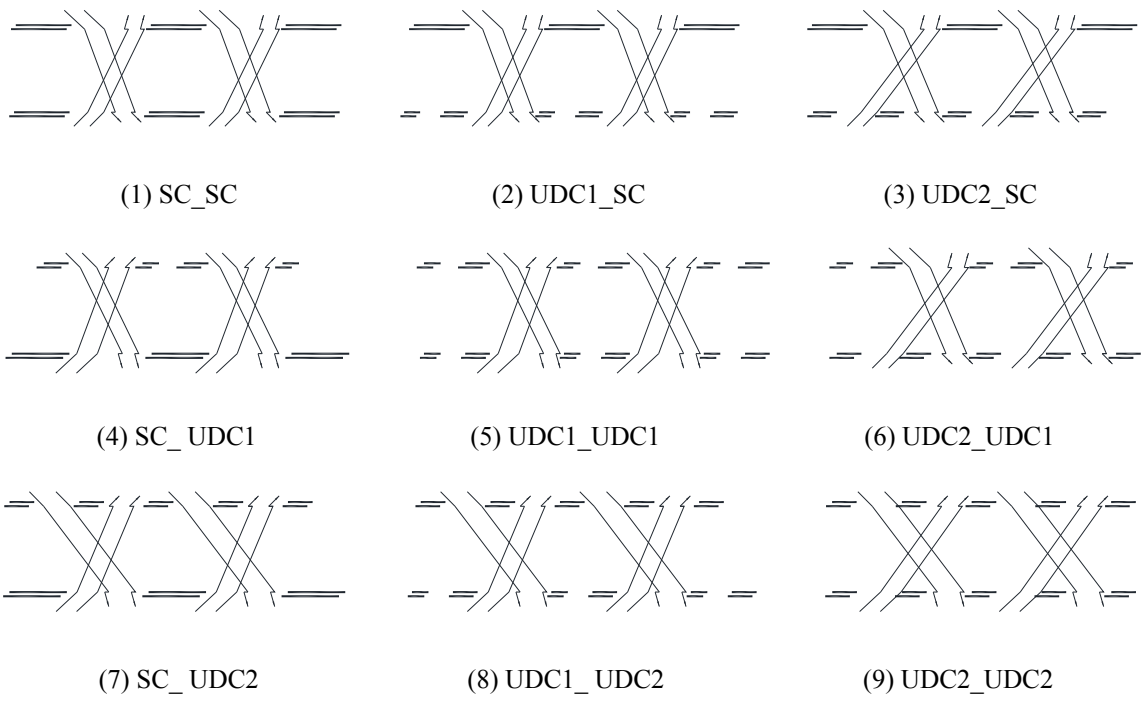

Figure 5. Scenarios of UDC-enabled arterial progression

This model introduces the concept of nominal red $r_{i,ja}^{N}$ to describe the bandwidth geometry of all the above nine scenarios. Nominal red is the time range in a background cycle where a possible green band chooses not to pass. At a UDC intersection, it equals the background cycle length minus the sub-green phase time chosen for green band passage. Equation 28 and Equation 29 determines the outbound and inbound nominal red, respectively. For a single cycled intersection, the nominal red follows the calculation of the conventionally defined red splits of arterial through movement.

$$r_{u,1}^{N} = 1 - g1_{u,1} \qquad \text{Equation 28}$$

$$r_{u,2}^{N} = \begin{cases} 1 - g1_{u,2} & if\ b_2\ chooses\ g1_{u,2} \\ 1 - g2_{u,2} & if\ b_2\ chooses\ g2_{u,2} \end{cases}$$ Equation 29

The concept of the nominal red allows to describe the above nine progression scenarios conveniently without involving too many new terms to the original MAXBAND model. Figure 6 shows the bandwidth geometry at a UDC intersection *i* and a SC intersection *i*+1 for example.

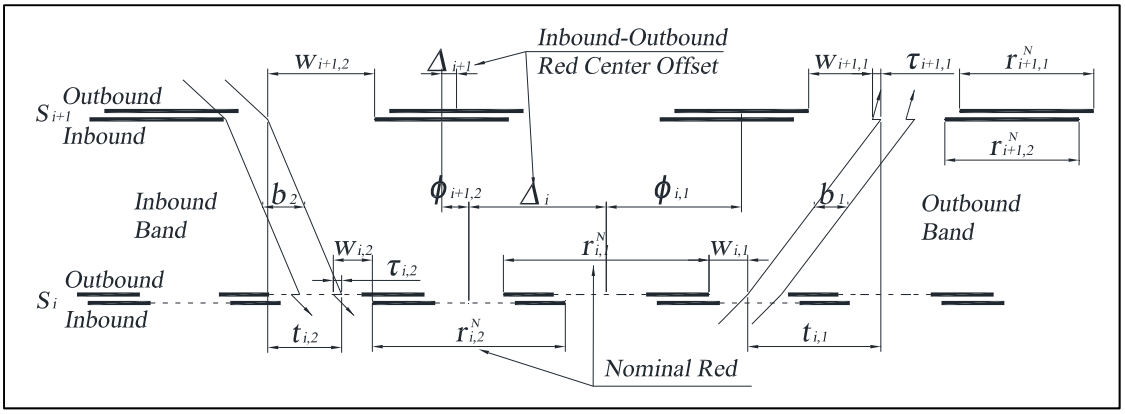

Figure 6. Geometry of constant bandwidth at SC and UDC intersections

(revised from MAXBAND geometry [*12*])

At the UDC intersection, the original definition of inbound and outbound red center offset Δ_i at a UDC intersection is modified as the time from the center of inbound nominal red $r_{i,2}^N$ to the nearest center of outbound nominal red $r_{i,1}^N$. To facilitate the calculation of Δ_i, define that the outbound (inbound) arterial through sub-green of the green band starts at a time point $t_{i,1}^o(t_{i,2}^o)$, and the difference between the two time points

is $t_{i,1}^{o}-t_{i,2}^{o}$ (positive if the outbound coordinated green start point is to the right of the inbound coordinated green start point). Then Δ_i is determined using Equation 30.

$$\Delta_i = t_{i,1}^{o} - t_{i,2}^{o} - \frac{1}{2}\left(r_{i,1}^{N} - r_{i,2}^{N}\right) \qquad \text{Equation 30}$$

For SC control, Equation 31 still applies.

$$\Delta_s = \frac{1}{2}\left[\left(2\delta_{s,1}-1\right)L_{s,1} - \left(2\delta_{s,2}-1\right)L_{s,2}\right] \qquad \text{Equation 31}$$

For UDC control, Table 2 and Equation 32 show the determination of $t_{u,1}^{o}-t_{u,2}^{o}$ in association with different left turn patterns at the UDC intersection. $\theta_{u,ja}$ is a binary decision variable for left turn phase to choose in the first or the second sub-cycle. Other variables are as previously defined.

Table 2. Start time difference of coordinated through green phases

Left Turn Pattern		$\theta_{u,1}$	$\theta_{u,2}$	$\delta_{u,1}$	$\delta_{u,2}$	$t_{u,1}^{o} - t_{u,2}^{o}$	
$L_{u,1}$	$L_{u,2}$					b_2 in $g1_{u,2}$	b_2 in $g2_{u,2}$
lead in $C1_u$	lag in $C1_u$	1	1	0	1	$-L_{u,1}$	$-\left(R2_{u,1} + g1_{u,1} + L_{u,2} + Y\right)$
lag in $C1_u$	lead in $C1_u$	1	1	1	0	$L_{u,2}$	$-\left(R2_{u,1} + g1_{u,1} + Y\right)$
lead in $C1_u$	lead in $C1_u$	1	1	0	0	$L_{u,2} - L_{u,1}$	$-\left(R2_{u,1} + g1_{u,1} + Y\right)$
lag in $C1_u$	lag in $C1_u$	1	1	1	1	0	$-R2_{u,1} + g1_{u,1} + L_{u,2} + Y$
lead in $C1_u$	lag in $C2_u$	1	0	0	1	$-L_{u,1}$	$-\left(R2_{u,1} + g1_{u,1} + Y\right)$
lag in $C1_u$	lead in $C2_u$	1	0	1	0	0	$-\left(R2_{u,1} + g1_{u,1} + Y\right)$
lead in $C1_u$	lead in $C2_u$	1	0	0	0	$-L_{u,1}$	$-\left(R2_{u,1} + g1_{u,1} + Y\right)$
lag in $C1_u$	lag in $C2_u$	1	0	1	1	0	$-\left(R2_{u,1} + g1_{u,1} + Y\right)$
lead in $C2_u$	lag in $C1_u$	0	1	0	1	0	$-\left(R2_{u,1} + g1_{u,1} + L_{u,1} + L_{u,2} + Y\right)$
lag in $C2_u$	lead in $C1_u$	0	1	1	0	$L_{u,2}$	$-\left(R2_{u,1} + g1_{u,1} + Y\right)$
lead in $C2_u$	lead in $C1_u$	0	1	0	0	$L_{u,2}$	$-\left(R2_{u,1} + g1_{u,1} + L_{u,1} + Y\right)$
lag in $C2_u$	lag in $C1_u$	0	1	1	1	0	$-\left(R2_{u,1} + g1_{u,1} + L_{u,2} + Y\right)$
lead in $C2_u$	lag in $C2_u$	0	0	0	1	0	$-\left(R2_{u,1} + g1_{u,1} + L_{u,1} + Y\right)$
lag in $C2_u$	lead in $C2_u$	0	0	1	0	0	$-\left(R2_{u,1} + g1_{u,1} + Y\right)$
lead in $C2_u$	lead in $C2_u$	0	0	0	0	0	$-\left(R2_{u,1} + g1_{u,1} + L_{u,1} + Y\right)$
lag in $C2_u$	lag in $C2_u$	0	0	1	1	0	$-\left(R2_{u,1} + g1_{u,1} + Y\right)$

$$t_{u,1}^{o}-t_{u,2}^{o}=\begin{cases}if\ \ b_2\ \ in\ g1_{u,2}: \\ \left(-\theta_{u,1}+\theta_{u,1}\delta_{u,1}\right)L_{u,1}+\left(\theta_{u,2}-\theta_{u,2}\delta_{u,2}\right)L_{u,2} \\ if\ \ b_2\ \ in\ g2_{u,2}: \\ -\left[R2_{u,1}+g1_{u,1}+\left(1-\theta_{u,1}-\delta_{u,1}+\theta_{u,1}\delta_{u,1}\right)L_{u,1}+\theta_{u,2}\delta_{u,2}L_{u,2}+Y\right]\end{cases} \quad \text{Equation 32}$$

Eliminate the nonlinearity in Equation 32 by replacing the product of the two binary variables $\theta_{u,ja}\delta_{u,ja}$ with a new binary variable $\alpha_{u,ja}^{I2}$ as shown in Equation 33.

$$\alpha_{u,ja}^{I2}=\theta_{u,ja}\delta_{u,ja} \quad \text{Equation 33}$$

which is equivalent to Equation 34 by using a binary decision variable $\lambda_{u,j}^{D2}$ for the product relation.

$$\begin{cases}\alpha_{u,ja}^{I2}+\theta_{u,ja}+\delta_{u,ja}^{d}-3\le 3\left(1-\lambda_{u,ja}^{D2}\right) \\ -\alpha_{u,ja}^{I2}-\theta_{u,ja}-\delta_{u,ja}^{d}+3\le 3\left(1-\lambda_{u,ja}^{D2}\right) \\ \theta_{u,ja}+\delta_{u,ja}^{d}-1\le 3\lambda_{u,ja}^{D2} \\ \alpha_{u,ja}^{I2}\le 3\lambda_{u,ja}^{D2} \\ -\alpha_{u,ja}^{I2}\le 3\lambda_{u,ja}^{D2}\end{cases} \quad \text{Equation 34}$$

Linearize the calculation of inbound nominal red $r_{u,2}^{N}$ and red-center offset Δ_u through disjunctive programming again using Equation 35 and Equation 36 with a binary decision variable λ_u^{D3} for selecting the first or second sub-green phase:

$$\begin{cases} r_{u,2}^{N} - 1 + g1_{u,2} \le 1 - \lambda_u^{D3} \\ -r_{u,2}^{N} + 1 - g1_{u,2} \le 1 - \lambda_u^{D3} \\ r_{u,2}^{N} - 1 + g2_{u,2} \le \lambda_u^{D3} \\ -r_{u,2}^{N} + 1 - g2_{u,2} \le \lambda_u^{D3} \end{cases}$$ Equation 35

$$\begin{cases} \Delta_u - \left(-\theta_{u,1} + \alpha_{u,1}^{I2}\right) L_{u,1} - \left(\theta_{u,2} - \alpha_{u,2}^{I2}\right) L_{u,2} + \frac{1}{2}\left(r_{u,1}^{N} - r_{u,2}^{N}\right) \le \frac{11}{2}\left(1 - \lambda_u^{D3}\right) \\ -\Delta_u + \left(-\theta_{u,1} + \alpha_{u,1}^{I2}\right) L_{u,1} + \left(\theta_{u,2} - \alpha_{u,2}^{I2}\right) L_{u,2} - \frac{1}{2}\left(r_{u,1}^{N} - r_{u,2}^{N}\right) \le \frac{11}{2}\left(1 - \lambda_u^{D3}\right) \\ \Delta_u + g2_{u,3} + 2Y + \left(1 - \theta_{u,4}\right) L_{u,4} + g1_{u,1} + \left(1 - \theta_{u,1} - \delta_{u,1} + \alpha_{u,1}^{I2}\right) L_{u,1} \\ \qquad + \alpha_{u,2}^{I2} L_{u,2} + \frac{1}{2}\left(r_{u,1}^{N} - r_{u,2}^{N}\right) \le \frac{11}{2} \lambda_u^{D3} \\ -\Delta_u - g2_{u,3} - 2Y - \left(1 - \theta_{u,4}\right) L_{u,4} - g1_{u,1} - \left(1 - \theta_{u,1} - \delta_{u,1} + \alpha_{u,1}^{I2}\right) L_{u,1} \\ \qquad - \alpha_{u,2}^{I2} L_{u,2} - \frac{1}{2}\left(r_{u,1}^{N} - r_{u,2}^{N}\right) \le \frac{11}{2} \lambda_u^{D3} \end{cases}$$ Equation 36

Other constraints in the original MAXBAND program remain the same as shown in Equation 37 through Equation 41, except that conventionally defined red split is replaced herein with the nominal red split accordingly.

$$\left(w_{i,1} + w_{i,2}\right) - \left(w_{i+1,1} + w_{i+1,2}\right) + \left(t_{i,1} + t_{i,2}\right) + \Delta_i - \Delta_{i+1} + \frac{1}{2}\left(r_{i,1}^{N} + r_{i,2}^{N}\right) - \frac{1}{2}\left(r_{i+1,1}^{N} + r_{i+1,2}^{N}\right) - \left(\tau_{i+1,1} + \tau_{i,2}\right) = m_i$$ Equation 37

$$(1-k)b_2 \ge (1-k)kb_2$$ Equation 38

$$w_{i,ja} + b_{ja} \le 1 - r_{i,ja}^{N}$$ Equation 39

$$\left(\frac{d_{i,ja}}{f_{i,ja}}\right) z \le t_{i,ja} \le \left(\frac{d_{i,ja}}{e_{i,ja}}\right) z$$ Equation 40

$$\left(\frac{d_{i,ja}}{h_{i,ja}}\right)z \le \left(\frac{d_{i,ja}}{d_{i+1,ja}}\right)t_{i+1,ja} - t_{i,ja} \le \left(\frac{d_{i,ja}}{o_{i,ja}}\right)z \qquad \text{Equation 41}$$

SOLUTION ALGORITHMS

In comparison to the mixed integer linear programming (MILP) used in the MAXBAND problem, the initial optimization model contains arithmetic minimum functions (e.g., Equation 3), absolute functions (e.g., Equation 13), logical if-then functions (e.g., Equation 29), and production of variables involving decision variables. Without considering disjunctive programming, the model is a mixed integer nonlinear programming (MINLP) problem. The author solved the MINLP problem using the Genetic Algorithm (GA) by coding the program in MATLAB [*58*]. Using the field data described in the case study (see Chapter IV), the algorithm did not always converge depending upon the parameter settings, and the solution was not global optimal.

After applying the disjunctive programming technique, the model becomes a mixed integer quadratic programming (MIQP) problem with quadratic terms in the objective function as indicated by Equation 2. The key to solve a MIQP problem is to determine its convexity. Simplify the MIQP problem into the conventional format shown in Equation 42.

$$\begin{aligned} &\min: \quad \frac{1}{2}X^T QX + c^T X \\ &\text{Subject to:} \quad AX \sim B \\ &\qquad\qquad\quad L \le X \le U \end{aligned} \qquad \text{Equation 42}$$

where $X = (r1_{u,jc}, r2_{u,jc}, t1_{u,jc}, b_{ja})$ is the vector of decision variables in the objective function; Q and c^T are the matrix of objective function coefficients; *A* and *B* are constants in the constraints; *L* and *U* are the lower and upper bounds of decision variables.

The convexity of the MIQP problem depends on whether the matrix Q is positive semi-definite (PSD); that is, whether $\frac{1}{2} X^T Q X \geq 0$ for every vector *X*. If Q is separable, the problem is convex when the diagonal elements are all nonnegative and the off-diagonal elements are zeros. If Q is nonseparable, the off-diagonal elements are not all zeros, and determining the convexity needs further judgment. Since the second term of Equation 2 is the production of two decision variables, this is a nonseparable problem. Also, it can be approved that Equation 2 does not satisfy the nonnegativity for all vectors of *X*. Therefore, the problem is nonconvex. The author programmed the model using the OPL language in the IBM ILOG CPLEX studio [*59*] which can solve nonconvex MIQP models to global optimums by using the branch and bound (BB) algorithm. The two key techniques used for global solutions to nonconvex MIQP problems are factorized eigenvalue formulation and McCormick relaxation [*60*]. Limited by the scope of the research, these techniques are not discussed here. Interested readers please refer to the literature for more details.

Using the case study data to compare the two algorithms, solving the MIQP problem with BB algorithm is more efficient than using GA to solve the MINLP problem. The MINLP problem has fewer decision variables and constraints than the MIQP problem, but solving the MIQP problem takes shorter time than the MINLP problem. Although the comparison is based on different solver engines (CPLEX solver for the MIQP problem vs. MATLAB solver for the MINLP problem), the BB algorithm outperforms GA with constant convergence and global optimal solutions. Further study continues to confine the modeling to MIQP problems.

Practically, the arterial signal timing optimization process follows the steps below. If a list of UDC intersections is available before hand, Step 2 can be skipped.

1. Run MAXBAND model to produce maximum bandwidth and delay under single cycling;
2. Run the proposed basic UDC model by trying double cycling one intersection at a time with a large value of λ^B less than 1.0 (e.g., 0.9) for all noncritical intersections; choose those giving a ratio of UDC bandwidth to MAXBAND bandwidth greater than a prescribed threshold to determine a list of UDC intersections.
3. Use the list of UDC intersections and varied λ^B to rerun the proposed model until a preferred combination of BW_n and AD_n^c is reached.

CHAPTER IV

ENHANCED MODELING OF ARTERIAL COORDINATION WITH UNEVEN DOUBLE CYCLING

The basic model developed in Chapter II describes the bandwidth geometry of the UDC control scheme and suffices for generating coordination needed control parameters. The model is based on the constant bandwidth along the arterial and minimizes delay only on cross street approaches without considering long pedestrian timing needs at wider intersections. This chapter first improves the modeling by considering pedestrian needs in one of the sub-cycles. Then the variable bandwidth is incorporated and the concept of secondary bandwidth is proposed. Also, a simplified delay estimation method is used for arterial approaches at UDC intersections. These formulations enables optimization of multiple objectives in addition to maximal bandwidth and minimal delay on cross streets in an attempt to explore the merits of multicriterion optimization.

SATISFYING PEDESTRIAN NEEDS

The basic UDC model can be applied at intersections with short pedestrian clearance time (pedestrian time no greater than normal minimum green time). At wider intersections with longer pedestrian clearance time, the model imposes additional constraints to satisfy such pedestrian needs. The model solves the issue by servicing the pedestrian time of an approach in one of the sub-green through phases. For the phase not

servicing pedestrian traffic, the minimum green requirement should be satisfied. So Equation 43 holds, which is equivalent to Equation 44 through disjunctive programming.

$$\begin{cases} g1_{u,j} \geq g_{u,j}^{ped} \\ g2_{u,j} \geq g_{u,j}^{\min} \end{cases} \text{ or } \begin{cases} g1_{u,j} \geq g_{u,j}^{\min} \\ g2_{u,j} \geq g_{u,j}^{ped} \end{cases} \qquad \text{Equation 43}$$

$$\begin{cases} g_{u,j}^{ped} - g1_{u,j} \leq 1 - \lambda_{u,j}^{D4} \\ g_{u,j}^{\min} - g2_{u,j} \leq 1 - \lambda_{u,j}^{D4} \\ g_{u,j}^{ped} - g2_{u,j} \leq \lambda_{u,j}^{D4} \\ g_{u,j}^{\min} - g1_{u,j} \leq \lambda_{u,j}^{D4} \end{cases} \qquad \text{Equation 44}$$

Note that the model requires that pedestrian phases on both sides of a street be serviced in the same sub-cycle (i.e., $\lambda_{u,1}^{D4} = \lambda_{u,2}^{D4}$ and $\lambda_{u,3}^{D4} = \lambda_{u,4}^{D4}$) to meet pedestrian expectations. However, if justified by future studies on human factors, relaxing this requirement can provide more flexibility in left turn phasing sequence. Normally, the sum of pedestrian walk time and pedestrian clearance time (flash don't walk time) determines the pedestrian phase time $g_{u,j}^{ped}$ of an approach. For narrow cross streets, part of the pedestrian clearance time could use the buffer interval which could be the sum of yellow change interval and red clearance interval at most [*4*]. Equation 44 replaces Equation 25 and Equation 26 of the basic UDC model developed in Chapter II, and the resultant model serves the basis of the improved model.

MULTICRITERION OBJECTIVE FORMULATION

The additional objectives considered in the modeling include maximal variable bandwidth, maximal secondary bandwidth, and minimal arterial average delay and number of stops at UDC intersections. Along with maximal constant bandwidth and minimal cross street delay, different combinations of these objectives are expected to have different model performances.

Simplified Estimation of Arterial Through Arrival Flows

As a premise, the major simplification of formulating these additional objectives is that internal arterial through traffic takes two different arrival flows at UDC intersections in a background cycle. The sub-green through phase which the green band passes has one constant platoon arrival flow $v_{u,ja}^{Tcd}$, and all the other phases (including the sub-green phase without green band passage and the red phases) has one constant random arrival flow rate $v_{u,ja}^{Tuc}$.

For an internal link approach, assuming platoon ratio $R_{u,ja}^{p}$ as defined in the HCM [*38*], with average through arrival rate per cycle $v_{u,ja}^{T}$, and maximum green times available for coordinated phases $g_{i,ja}^{\max}$ (will be determined later in this chapter), flow rates $v_{u,ja}^{Tcd}$ and $v_{u,ja}^{Tuc}$ are estimated using Equation 45 and Equation 46.

$$v_{i,ja}^{Tcd} = R_{i,ja}^{p} v_{i,ja}^{T} \qquad \text{Equation 45}$$

$$v_{u,ja}^{Tuc} = \frac{v_{u,ja}^{T}\left(1 - R_{u,ja}^{P} g_{u,ja}^{\max}\right)}{1 - g_{u,ja}^{\max}} \qquad \text{Equation 46}$$

Equation 46 indicates that arrival flow rate in uncoordinated phases is approximated by assuming that the coordinated green phase uses the maximum green time available for green band passage. This approximation overestimates the coordinated flow rate and is expected to underestimates arterial disutilities (delay or number of stops). The approximation is deemed feasible because of two reasons. On the one hand, this simplification avoids complicated modeling of traffic representation along the arterial and ensures that the MIQP model structure still applies. On the other hand, the optimization results out of fixed timing models developed in this study will more likely be implemented in an actuated signal controller where the coordinated green phase often has green time longer than its maximum green time setting.

Variable Bandwidth Optimization

The variable bandwidth objective applies the concept of MULTI-BAND [*15-17*] to consider a continuous green band along the directional arterial but with varied bandwidths on individual roadway links in the coordinated sub-green phase. Figure 7 shows the outbound bandwidth geometry under variable bandwidth concept for coordination of three intersections with a UDC intersection between two SC intersections. The inbound bandwidth geometry is similar.

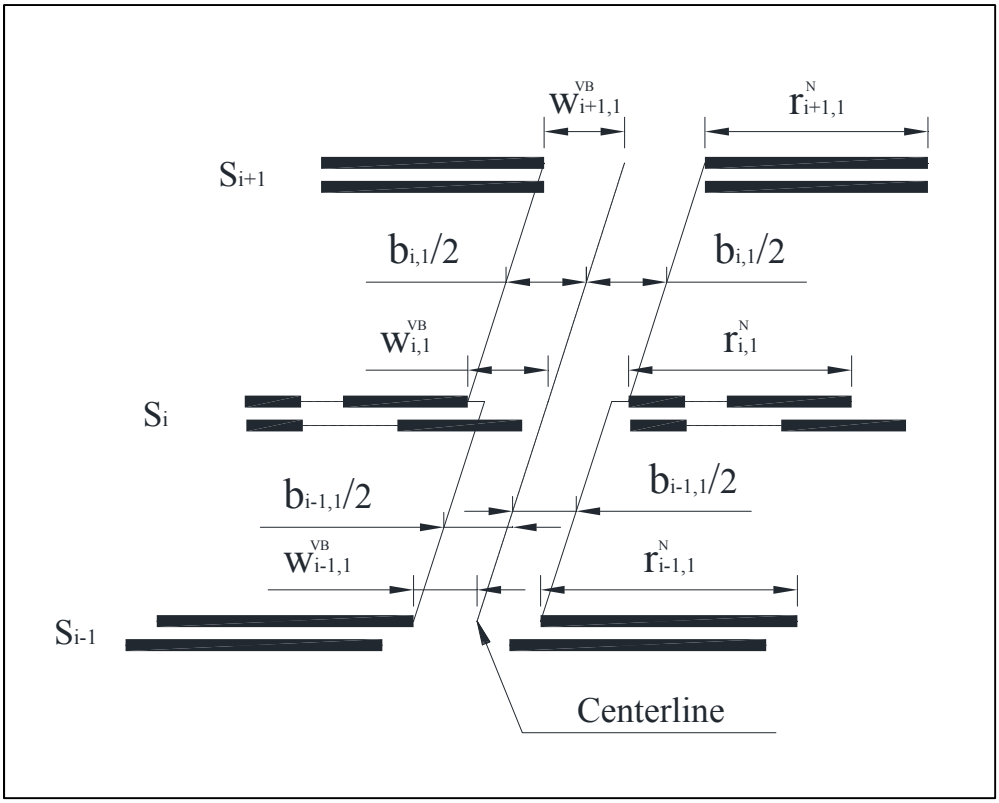

Figure 7. Geometric relations of variable bandwidths with UDC control

(revised from MULTI-BAND geometry [*15*])

With $b_{i,ja}$ being the bandwidth on the directional link i and $a_{i,ja}$ as the link-specific weight for link bandwidth $b_{i,ja}$, Equation 47 expresses the variable bandwidth objective. The superscript "*VB*" differentiates the variable bandwidth objective from the constant bandwidth in the basic model.

$$BW_n^{VB} = \frac{\sum_{i=1}^{N-1}(a_{i,1}b_{i,1} + a_{i,2}b_{i,2})}{BW_{\max}^{VB}} \qquad \text{Equation 47}$$

The bandwidth weight parameter $a_{i,ja}$ uses the link *v*/*s* flow ratio [*15*] of through volume in the coordinated green phase $v_{i,ja}^{Tcd}$ over link saturation flow $s_{i,ja}^{l}$ (upstream link of intersection *i*). Normalizing the two-way bandwidth weights with the sum of the two-way *v*/*s* flow ratios, parameter $a_{i,ja}$ is calculated using Equation 48.

$$a_{i,ja} = \frac{v_{i+1,ja}^{Tcd} \Big/ s_{i,ja}^{l}}{\sum_{ja=1}^{2} \left(v_{i+1,j}^{Tcd} \Big/ s_{i,ja}^{l} \right)} \qquad \text{Equation 48}$$

The denominator $BW_{\max}^{VB}$ in Equation 47 is the weighted sum of two-way maximum available green times $g_{i,ja}^{l\max}$ for green band passage on a directional link as indicated by Equation 49. $g_{i,ja}^{l\max}$ is bounded by the smaller of the maximum green times $g_{i,ja}^{\max}$ and $g_{i+1,ja}^{\max}$ available for coordinated phases at both end intersections of this link as indicated by Equation 50. Calculation of $g_{i,ja}^{\max}$ depends on whether the intersection is single cycled or double cycled as shown in Equation 51.

$$BW_{\max}^{VB} = \sum_{i=1}^{N-1} \left(a_{i,1} g_{i,1}^{l\max} + a_{i,2} g_{i,2}^{l\max} \right) \qquad \text{Equation 49}$$

$$g_{i,ja}^{l\max} = \min\{ g_{i,ja}^{\max},\ g_{i+1,ja}^{\max} \} \qquad \text{Equation 50}$$

$$g_{i,ja}^{\max} = \begin{cases} g_{i,ja}^{s} & if\ SC \\ g_{u,ja}^{d} - g_{u,ja}^{\min} & if\ UDC \end{cases} \qquad \text{Equation 51}$$

For the bandwidth geometry in Figure 7 to hold, define a new decision variable $w_{i,ja}^{VB}$ by revising the definition of $w_{i,ja}$ to the time from the right (left) side of red at intersection i to the centerline of outbound (inbound) green band. Therefore, Equation 52 and Equation 53 must hold for both end intersections of a link and replace the bound constraint of bandwidth Equation 39 in the basic model.

$$\frac{1}{2}b_{i,ja} \le w_{i,ja}^{VB} \le (1-r_{i,ja}^{N}) - \frac{1}{2}b_{i,ja} \qquad \text{Equation 52}$$

$$\frac{1}{2}b_{i,ja} \le w_{i+1,ja}^{VB} \le (1-r_{i+1,ja}^{N}) - \frac{1}{2}b_{i,ja} \qquad \text{Equation 53}$$

With the target ratio of inbound to outbound link bandwidth k_i taken as the ratio of inbound volume to outbound volume on link *i*, bandwidth ratio constraint of Equation 38 is replaced with Equation 54. All other constraints in the basic UDC model remain the same.

$$(1-k_i)b_{i,2} \ge (1-k_i)k_i b_{i,1} \qquad \text{Equation 54}$$

Secondary Bandwidth Optimization

When consecutive UDC intersections exist along the arterial, it might be beneficial to formulate the geometry of secondary bandwidth for optimization along with the main bandwidth and other objectives. The secondary bandwidth is defined as the proportion of background cycle length in which a vehicle can travel to pass consecutive UDC

intersections. The directional secondary bandwidth $b_{u,ja}^{SB}$ on link *u* passes the sub-green phase without the main bandwidth at a UDC intersection. Figure 8 illustrates the secondary bandwidth geometry with a set of decision variables similar to the geometry of main bandwidth defined.

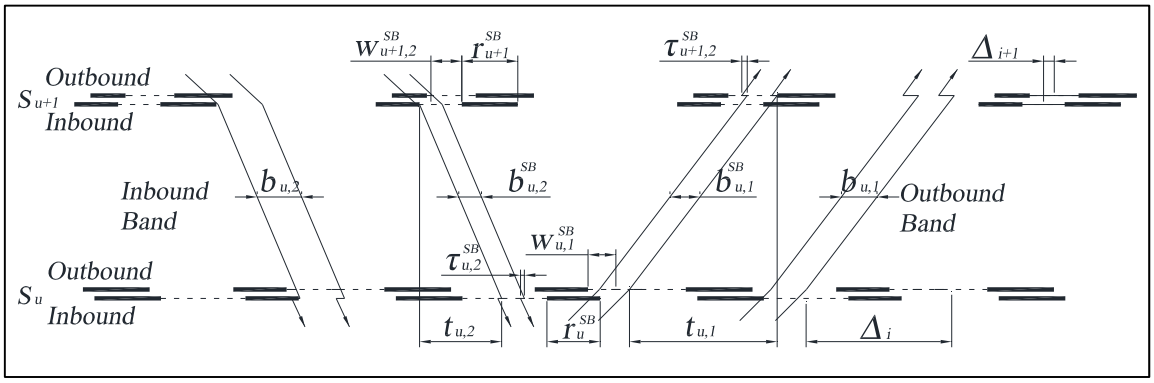

Figure 8. Geometry relations for secondary bandwidth with UDC control

(revised from MAXBAND geometry [*12*])

Similar to the main bandwidth, the normalized objective of secondary bandwidth BW_n^{SB} takes the form shown as Equation 55. With weight λ^{SB} for secondary bandwidth, the weighted sum of two bandwidth objectives participate in the whole objective function in the form of Equation 56.

$$BW_n^{SB} = \frac{\sum_{u=1}^{Nup}(a_{u,1}^{SB} b_{u,1}^{SB} + a_{u,2}^{SB} b_{u,2}^{SB})}{BW_{\max}^{SB}} \qquad \text{Equation 55}$$

$$BW_n^{VSB} = \left(1-\lambda^{SB}\right) BW_n^{VB} + \lambda^{SB} BW_n^{SB} \qquad \text{Equation 56}$$

Determining link weight for $a_{u,ja}^{SB}$ uses the random through flow rate $v_{u+1,ja}^{Tuc}$ outside of the smallest of main bandwidth and saturation flow rate $s_{u,ja}^{l}$ on link u (upstream link of intersection $u+1$). To avoid unnecessary nonlinear terms for simplicity here, approximate the smallest of main bandwidth using the smallest maximum green $g_{i,ja}^{\max}$ among all intersections and calculate the random through flow rate $v_{u,ja}^{Tr}$ and corresponding link weight $a_{u,ja}^{SB}$ using Equation 57.

$$a_{u,ja}^{SB} = \frac{v_{u+1,ja}^{Tuc} \Big/ s_{u,ja}^{l}}{\sum_{j=1}^{2} \left(v_{u+1,j}^{Tuc} \Big/ s_{u,ja}^{l} \right)} \qquad \text{Equation 57}$$

Normalizing the secondary bandwidth uses the maximum achievable link bandwidth $g_{u,ja}^{l\max}$ determined the same way as that for the main bandwidth objective shown in Equation 58, although the actual maximum achievable link bandwidth for secondary bandwidth would probably be smaller than $g_{u,ja}^{l\max}$.

$$BW_{\max}^{SB} = \sum_{u=1}^{Nup} \left(a_{u,1}^{SB} g_{u,1}^{l\max} + a_{u,2}^{SB} g_{u,2}^{l\max} \right) \qquad \text{Equation 58}$$

As indicated in Figure 8, the secondary bandwidth is bounded in the same way as that of the main bandwidth, except that the inbound secondary bandwidth can only pass the sub-green phase without being chosen for the main bandwidth passage. Since the nominal red does not contain the sub-green phase with main bandwidth, the sub-green phase with

secondary bandwidth equals the nominal red less the sum of two sub-red phases. Equation 52 and Equation 53 are revised into Equation 59 and Equation 60 for this difference. Also, using the same target bandwidth ratio, Equation 61 shows the ratio constraint.

$$\frac{1}{2}b_{u,ja}^{SB} \le w_{u,ja}^{SB} \le r_{u,ja}^{N} - r1_{u,ja} - r2_{u,ja} - \frac{1}{2}b_{u,ja}^{SB} \quad \text{Equation 59}$$

$$\frac{1}{2}b_{u,ja}^{SB} \le w_{u+1,ja}^{SB} \le r_{u+1,ja}^{N} - r1_{u+1,ja} - r2_{u+1,ja} - \frac{1}{2}b_{u,ja}^{SB} \quad \text{Equation 60}$$

$$\left(1-k_u^{SB}\right)b_{u,2}^{SB} \ge \left(1-k_u^{SB}\right)k_u^{SB}b_{u,1}^{SB} \quad \text{Equation 61}$$

To derive the loop function to describe the secondary bandwidth, the sub-red phase on the right side of the inbound secondary bandwidth is defined as r_u^{SB}, which depends on whether the secondary bandwidth is in the first or second sub-green phase and could be $r1_{u,2}$ or $r2_{u,2}$. Similar to the disjunctive programming technique used for the nominal red split in Equation 29 and Equation 35, Equation 62 and Equation 63 are formulated.

$$r_u^{SB} = \begin{cases} r1_{u,2} & if\ b_2\ chooses\ g1_{u,2} \\ r2_{u,2} & if\ b_2\ chooses\ g2_{u,2} \end{cases} \quad \text{Equation 62}$$

$$\begin{cases} r_u^{SB} - r1_{u,2} \le 1 - \lambda_u^{D3} \\ -\left(r_u^{SB} - r1_{u,2}\right) \le 1 - \lambda_u^{D3} \\ r_u^{SB} - r2_{u,2} \le \lambda_u^{D3} \\ -\left(r_u^{SB} - r2_{u,2}\right) \le \lambda_u^{D3} \end{cases} \quad \text{Equation 63}$$

Starting from the left end of r_u^{SB}, the loop function is derived and rearranged into a similar form to that in the basic model as shown in Equation 64.

$$\left(w_{u,1}^{SB}+w_{u,2}^{SB}\right)-\left(w_{u+1,1}^{SB}+w_{u+1,2}^{SB}\right)+\left(t_{u,1}+t_{u,2}\right)+\Delta_u-\Delta_{u+1}-\frac{1}{2}\left(r_{u,1}^{N}+r_{u,2}^{N}\right)$$
$$+\frac{1}{2}\left(r_{u+1,1}^{N}+r_{u+1,2}^{N}\right)-\left(\tau_{u+1,1}^{SB}+\tau_{u,2}^{SB}\right)+r_u^{SB}-r_{u+1}^{SB}+r2_{u,1}-r2_{u+1,1}=m_u^{SB} \quad \text{Equation 64}$$

Comparing with the loop functions of main bandwidth, Equation 64 has four additional terms at the right hand side of the equation. Also note that the same travel time decision variables are presented in the loop function. This indicates that the secondary green bands progress in the same speed as that of the main green bands. Equation 40 and Equation 41 still hold for the secondary green band. In case of different progression speeds preferred, one can easily relax this constraint by using a different set of travel time decision variables in Equation 64 and adding two new constraints similar to Equation 40 and Equation 41.

Minimal Delay and Number of Stops of Arterial Through Movements

The basic UDC model described in Chapter II minimizes average delay on cross streets. This section provides formulation of minimizing arterial disutilities of through delay and number of stops. Given the simplified estimation of arterial through arrival flows, the queuing diagrams are similar to Figure 4, expect that one of the sub-green phases has steeper slop of queue dissipation curve than the other sub-green phase.

From the queuing diagram, average delay $AD_{u,ja}^{Ta}$ and average number of stops $AS_{u,ja}^{Ta}$ of through traffic on an arterial approach ja at a UDC intersection is determined using Equation 65 and Equation 66, respectively.

$$AD_{u,ja}^{Ta} = \frac{v_{u,ja}^{Tuc}}{2v_{u,ja}^{T}z}\left[r1_{u,ja}^{2} + t1_{u,ja}r1_{u,ja} + r2_{u,ja}^{2} + t2_{u,ja}r2_{u,ja}\right] \quad \text{Equation 65}$$

$$AS_{u,ja}^{Ta} = \frac{1}{v_{u,ja}^{T}}\left[v_{u,ja}^{Tuc}\left(r1_{u,ja} + r2_{u,ja}\right) + v_{u,ja}^{g1}t1_{u,ja} + v_{u,ja}^{g2}t2_{u,ja}\right] \quad \text{Equation 66}$$

Through arrival flow $v_{u,ja}^{Tuc}$ in uncoordinated phases is used for both red phases as indicated in Equation 46; $v_{u,ja}^{g1}$ and $v_{u,ja}^{g2}$ is the through arrival flow in sub-green phase $g1$ and $g2$, respectively; $t1_{u,ja}$ and $t2_{u,ja}$ is the actual queue discharge time of the sub-cycle $C1$ and $C2$, respectively. All other variables are defined previously.

For the outbound direction, the first sub-green is always coordinated, so the outbound arrival flow rate equals the coordinated flow $v_{u,ja}^{Tcd}$ in the first sub-green and equals the uncoordinated flow $v_{u,ja}^{Tuc}$ in the second sub-green phase. For the inbound direction, the arrival flow rate depends on whether the main green band passes the first or the second sub-green phase. Equation 67 and Equation 68 calculate arrival flow rate for each of the sub-green phases in both directions. On arterial approaches, external arrival flow (traffic entering the arterial at the end intersections) is assumed random and uses the same delay estimation method as that on cross street approaches.

$$v_{u,ja}^{g1} = \begin{cases} v_{u,ja}^{Tcd}, & if\ ja = 1 \\ \lambda_u^{D3} v_{u,ja}^{Tcd} + \left(1 - \lambda_u^{D3}\right) v_{u,ja}^{Tuc}, & if\ ja = 2 \end{cases} \quad \text{Equation 67}$$

$$v_{u,ja}^{g2} = \begin{cases} v_{u,ja}^{Tuc}, & if\ ja = 1 \\ \left(1 - \lambda_u^{D3}\right) v_{u,ja}^{Tcd} + \lambda_u^{D3} v_{u,ja}^{Tuc}, & if\ ja = 2 \end{cases} \quad \text{Equation 68}$$

Note that λ_u^{D3} is treated as a parameter to make the MIQP structure in the enhanced models as opposed to decision variable in the basic model. But this can be improved by using disjunctive programming again in further research. With the arrival flows determined, the queue discharge time in the first sub-green $t1_{u,ja}$ and second sub-green $t2_{u,ja}$ are calculated using Equation 69 and Equation 70, which are equivalent to Equation 71 and Equation 72.

$$t1_{u,ja} = \min\left\{\frac{v_{u,ja}^{Tuc} r1_{u,ja}}{s_{u,ja} - v_{u,ja}^{g1}},\ g1_{u,ja}\right\} \quad \text{Equation 69}$$

$$t2_{u,ja} = \min\left\{\frac{v_{u,ja}^{Tuc}\left(r1_{u,ja} + r2_{u,ja}\right) - \left(s_{u,ja} - v_{u,ja}^{g1}\right) t1_{u,ja}}{s_{u,ja} - v_{u,ja}^{g2}},\ g2_{u,ja}\right\} \quad \text{Equation 70}$$

$$\begin{cases} t1_{u,ja} \le \dfrac{v_{u,ja}^{Tuc} r1_{u,ja}}{s_{u,ja} - v_{u,ja}^{g1}} \\ t1_{u,ja} \le g1_{u,ja} \end{cases} \quad \text{Equation 71}$$

$$\begin{cases} t2_{u,ja} \le \dfrac{v_{u,ja}^{Tuc}\left(r1_{u,ja} + r2_{u,ja}\right) - \left(s_{u,ja} - v_{u,ja}^{g1}\right) t1_{u,ja}}{s_{u,ja} - v_{u,ja}^{g2}} \\ t2_{u,ja} \le g2_{u,ja} \end{cases} \quad \text{Equation 72}$$

For the objective of average delay, normalization uses the total average delay $AD_{\max}^{Ta}$ under single cycling of MAXBAND results. For the objective of number of stops, consider a hypothetical operation of stopping all arrival vehicles in a cycle, i.e., the cycle time is all red. Then the total average number of stops $AS_{\max}^{Ta}$ under such hypothetical operation is used for normalizing the objective of number of stops. The normalized arterial disutilities are determined using Equation 73 and Equation 74.

$$AD_n^{Ta} = \frac{AD^{Ta}}{AD_{\max}^{Ta}} = \frac{\sum_{u=1}^{Nu}\sum_{ja=1}^{2} AD_{u,ja}^{Ta}}{AD_{\max}^{Ta}} \qquad \text{Equation 73}$$

$$AS_n^{Ta} = \frac{AS^{Ta}}{AS_{\max}^{Ta}} = \frac{\sum_{u=1}^{Nu}\sum_{ja=1}^{2} AS_{u,ja}^{Ta}}{AS_{\max}^{a}} \qquad \text{Equation 74}$$

MULTICRITERION OPTIMIZATION MODELS

Combining different objectives, multicriterion optimization modeling in this section considers three model sets each of which contains three models. Table 3 shows the combinations of different objectives of each model within each model set.

Table 3. Objective combinations of multicriterion optimization

Model Name	Objectives					
	Maximal Bandwidth			Minimal disutilities of through traffic		
	Constant main bandwidth	Variable main bandwidth	Variable secondary bandwidth	Average delay on cross street	Average arterial delay	Average arterial # stops
Improved basic UDC models						
UDCo	X			X		
UDC_D	X			X	X	
UDC_DS	X			X	X	X
UDC models enhanced with variable bandwidth optimization						
UDC_V		X		X		
UDC_VD		X		X	X	
UDC_VDS		X		X	X	X
UDC models enhanced with variable and secondary bandwidth optimization						
UDC_SV		X	X	X		
UDC_SVD		X	X	X	X	
UDC_SVDS		X	X	X	X	X

All nine models have a common objective of minimal average delay of through traffic on cross streets as defined in the basic UDC model and take pedestrian needs into consideration. Based on this, each model set differs from other sets by one among three objectives, i.e., maximal constant bandwidth, maximal variable main bandwidth, and maximal main and secondary bandwidth. The first model in each model set maximizes bandwidth and minimizes average through delay on cross streets. Based on the first

model, the second model of each model set also minimizes average delay of arterial through traffic. The third model of each model set additionally minimizes average number of stops of arterial through traffic.

As indicated by Table 3, the multicriterion optimization in this study is not intended to enumerate all possible combinations of all six objectives considered. Instead, basic objectives of maximal bandwidth and minimal through delay on cross streets are first covered before making improvement by revising the bandwidth objectives and additional objectives of minimal arterial disutilities.

CHAPTER V

NUMERICAL EXPERIMENTS OF BASIC UDC MODEL*

The UDC control is relative new and has not been widely used. It is desirable to study factors affecting the model performance and provide preliminary guidelines for its implementation. Also, the performance of UDC control needs to compare with conventional SC control to quantify the impact of UDC in terms of different measures of effectiveness. To these ends, this chapter first describes numerical experiments designed to examine the impact of different *v*/*s*-related parameters on the applicability of the UDC control scheme. Running the basic UDC model generates the experiment results in terms of preliminary guidelines. The guidelines then serve in the case study using field data before running various multicriterion models for performance evaluation in Chapter V.

Factors affecting UDC application may include through and left turn volume levels on both arterial and cross streets, capacity of different lane groups, distance between intersections, traffic differences between major-major and major-minor intersections, and traffic differences between arterial streets and minor cross streets at the major-minor intersections, among other factors. Exploratory analyses indicates that the model performance is sensitive to parameters calculated using *v/s* flow ratio, therefore this

* Part of the content in this chapter is reprinted from *Arterial Signal Coordination with Uneven Double Cycling*, by H. Zhou and G. Hawkins, 2014. Texas A&M Transportation Institute Report (SWUTC/15/600451-00024-1), Texas A&M University System, 3135 TAMU, College Station, TX 77843

chapter uses several of these parameters to test the model trying to find certain traffic thresholds and develop preliminary criteria for UDC implementation guidance.

EXPERIMENT DESIGN

To find the effective indicators for UDC application, three sets of parameters are considered: (1) left turn percentage on the arterial and minor cross streets; (2) traffic ratio between arterial streets and minor cross streets at the UDC intersections; and (3) traffic difference between UDC and SC intersections. Each of them is discussed as follows.

Left turn percentage on an approach is calculated as the left turn *v/s* ratio on this approach divided by the sum of this left turn *v/s* and the opposing through *v/s*. Left turn percentage for the critical approach of arterial (*ArtLT*) and of cross streets (*CrstLT*) are used as a set of controlling parameters for a candidate UDC intersection. The two parameters actually reflect the weight of through movement in demand of green time allocation. Numeric experiments consider protected left turn only on the arterial and protected or permitted left turn on cross streets. Both *ArtLT* and *CrstLT* range from 1 percent to 70 percent.

Traffic ratio between arterial streets and cross streets (*AtC*) is defined as the ratio between the sum of critical *v/s* for arterial phases and the sum of critical *v/s* for the

whole intersection. This parameter reflects the relative demand in green time allocation on arterial and cross streets. *AtC* ranges from 0.5 to 0.9 in the numeric experiments.

Three parameters are investigated for traffic difference between SC and UDC intersections. Arterial traffic ratio between UDC and SC intersections (*UtS*) is defined as the ratio of critical *v/s* for arterial phases between the candidate UDC intersection and the critical SC intersection in the arterial (the intersection dictating arterial background cycle length). This parameter serves to generate various traffic flow levels at the UDC intersection in comparison with the critical single-cycled intersection. *UtS* ranges from 0.8 to 1.2 in the numeric experiments. The second parameter is the ratio of volume-to-capacity ratio (*Xc*) between candidate UDC and the critical intersections (*Xc-ratio*). This parameter reflects comprehensively traffic demand and supply for both intersections. Another parameter investigated in the study is the arterial green time ratio between candidate UDC intersection and the critical intersection under SC control (*g-ratio*). It is calculated as the average of the outbound and inbound ratios. This is a more direct parameter reflecting the applicability of UDC control scheme since changes in all other parameters eventually affect the optimization results by green splits on the arterial. Both *Xc-ratio* and *g-ratio* varies as a result of changes in all the other parameters.

Two measures of effectiveness (MOEs) of arterial progression considered are the bandwidth obtainability as defined in Equation 11 and the relative bandwidth by replacing the denominator in Equation 11 with the optimized bandwidth results of the

MAXBAND model when UDC is not considered. Delay objective as defined in Equation 7 is also investigated.

Consider a hypothetical arterial with three intersections, where the two intersections at both ends are under SC control and the one in between is a UDC candidate. The above defined parameters are varied to generate different flow levels for different movements at the candidate UDC intersection. Other parameters such as background cycle length (C=160 sec) volume-to-capacity ratio (Xc=0.9 and 0.81) at single-cycled intersections, distance between intersections (1000 ft and 2000 ft), inbound and outbound relative flow ratios (0.3 on arterial streets, 0.85 on minor streets), and speed limit boundaries (40 mph ± 2.5 mph) are kept the same throughout the experiments. ILOG-CPLEX [*59*] is used to code and solve the model for its ability to solve global optimum of MIQP problems. The optimization model provides various bandwidth solutions, and the next section discusses the results. It should be noted that the numerical experiments are not designed to cover all possible traffic scenarios in discussing UDC applicability. Instead, the experiments determine ranges of the above parameters by first considering representative scenarios where UDC control might be beneficial and then varying the parameters within proper ranges to observe the model performance.

EXPERIMENT RESULTS

This section first discusses qualitatively and quantitatively each of the above factors to see their impact on the bandwidth solutions and then gives preliminary criteria for UDC application guidance.

Before discussing the results, it is worth explaining the algorithm used in the model to calculate green splits when minimum green requirements are not met using the initial input flow information. The algorithm first calculates the initial *Xc* and the green splits using the input flow information. If the minimum green requirements are not met for a particular phase, *v/s* of this phase is increased by a small increment, and then *v/s* of each phase is updated by redistributing the new critical sum of *v/s* on a street according to the *v/s* in the last step, if necessary. A new *Xc* is then calculated using the updated flow information. This iteration goes until all phases meet the minimum green requirements. Delay calculation still uses the initial *v/s* ratios.

Measures of Effectiveness

The results of bandwidth measures indicate the performance of UDC model on arterial progression, and the delay measure indicates the benefit of UDC model reducing delay on cross streets. Table 4 shows the ranges of MOEs with the changes of all considered parameters in the numerical experiments.

Table 4. Ranges of MOEs of the numerical experiment results

Cross Street Left Turn	Normalized Bandwidth BW_n	Relative Bandwidth BW^r	Normalized Cross Street Delay AD_n^{Tc}
Permitted	[0.858, 0.995]	[0.857, 1.022]	[0.445, 0.636]
Protected	[0.873, 0.993]	[0.780, 1.021]	[0.433, 0.589]

The normalized bandwidth of the UDC model is an indicator of bandwidth obtainability with an upper bounded of 1.0, which is supported by the numerical results. The relative bandwidth, on the other hand, could be above 1.0, which indicates that the UDC model could achieve a sum of two-way bandwidths greater than that of the MAXBAND model. These are the cases when the UDC model provides the same or slightly smaller (difference less than 2 sec) bandwidth in the outbound (peak) direction and greater bandwidth in the inbound (off-peak) direction compared with SC control. There are also scenarios where the MAXBAND model does not converge to provide a solution whereas the UDC model achieves good results. The ranges in delay indicate that the UDC scheme could reduce cross street delay by at least 36.4 (41.1) percent and up to 55.5 (56.7) percent under permitted (protected) left turn operation on cross streets. These results show good potential of the UDC model. Since the progression performance of UDC comparing to single cycling is of interest, the relative bandwidth is emphasized in the following analysis.

Left Turn Factors

Figure 9 shows the changes of bandwidth measures by different cross street left turn ratios *CrstLT* with other factors fixed (*ArtLT* = 0.13, *UtS* = 1.0, *AtC* = 0.6). Figure 9 indicates that bandwidth measures generally increase with *CrstLT* with permitted left turn operation on cross streets but do not change very much with protected left turn operation on cross streets. With permitted left turn on cross streets, the UDC model can more often achieve greater bandwidth than the MAXBAND model.

For permitted left turn on cross streets, with other factors fixed, increasing *CrstLT* decreases *v/s* for through movements on cross streets which reduces the sum of critical *v/s* and thus *Xc* for the intersection. This increases green time allocation for arterial phases and thus available green time for progression. For protected left turn on cross streets, once the minimum green requirements are met, changing *CrstLT* does not affect the sum of critical *v/s* on cross streets or on arterial. Therefore arterial phase splits and bandwidth remain the same.

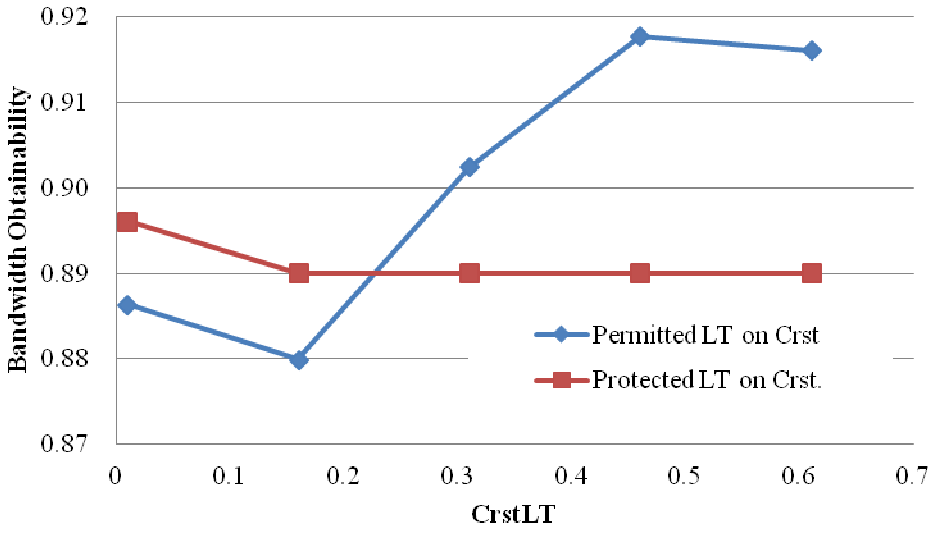

9a. Bandwidth obtainability by cross street left turn ratios

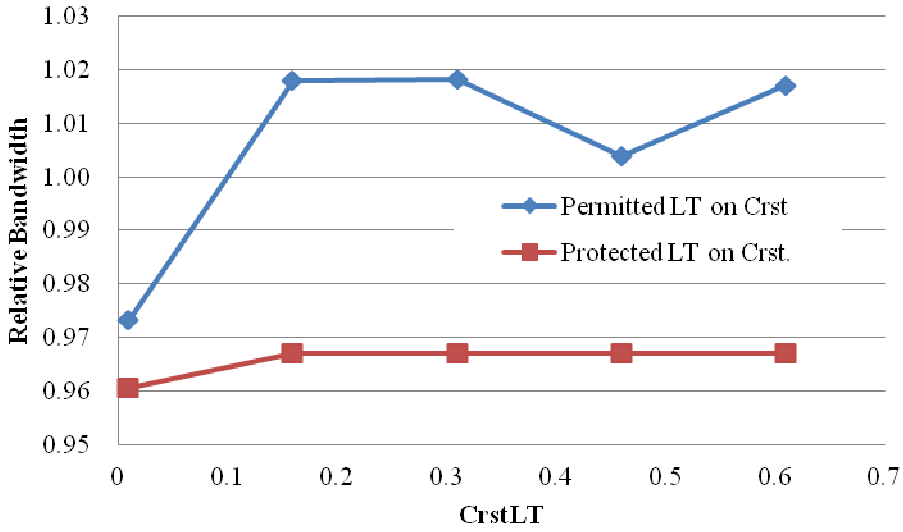

9b. Relative bandwidth by cross street left turn ratios

Figure 9. Bandwidth affected by cross street left turn ratios

As shown in Figure 10, increasing the arterial left turn ratio *ArtLT* has different impacts on bandwidth obtainability and relative bandwidth. Figure 10a indicates that bandwidth

obtainability increases as *ArtLT* increases, whereas Figure 10b shows that relative bandwidth decreases as *ArtLT* increases.

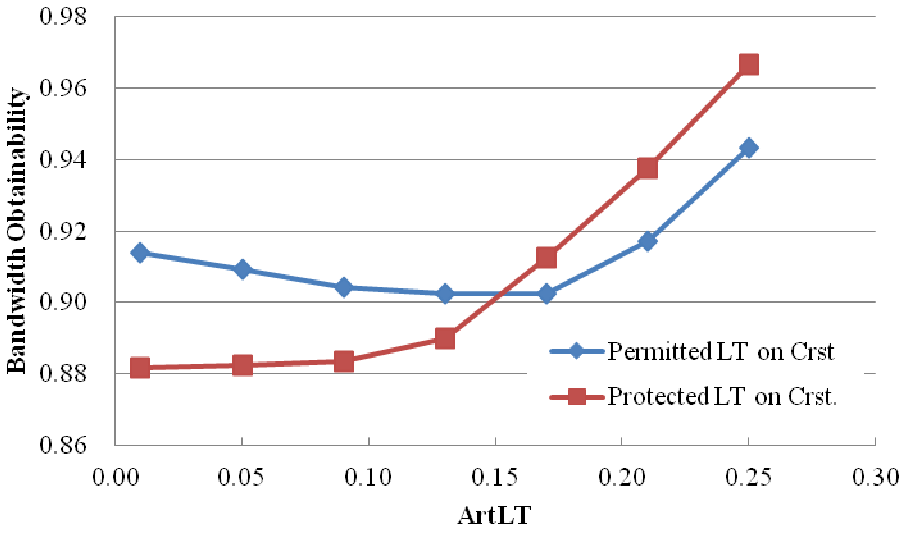

10a. Bandwidth obtainability by arterial left turn ratios

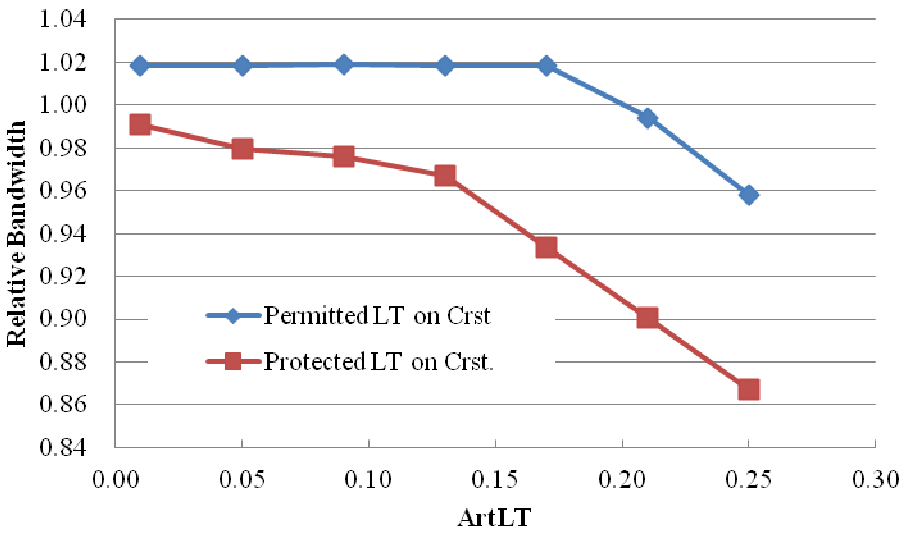

10b. Relative bandwidth by arterial left turn ratios

Figure 10. Bandwidth affected by arterial left turn ratios

Looking at the directional maximum green time possibly available for bandwidth passage $g_{ja}^{\max}$, increasing *ArtLT* directly reduces through phase splits and thus $g_{ja}^{\max}$ on arterial. When $g_{ja}^{\max}$ with UDC control equals that with SC control, bandwidth measures generally decreases as *ArtLT* increases. When $g_{ja}^{\max}$ with UDC control is less than that with SC control, bandwidth availability increases as *ArtLT* increases. This applies to both permitted and protected left turn operations on cross streets. Given all other factors being the same, with permitted left turn operation on cross streets, the available slack green time UDC is greater than that under protected left turn operation and so is the relative bandwidth.

Results for other *CrstLT* and *ArtLT* levels show similar trends. Figure 11 shows the change in relative bandwidth as *CrstLT* (*ArtLT*) under different *ArtLT* (*CrstLT*) levels when other factors are fixed (*UtS*=1.0, *AtC*=0.6) with permitted left turn on cross streets. When *CrstLT* is greater than 0.45 or when *ArtLT* is less than 0.05, the UDC model can provide the same or greater bandwidth results compared with MAXBAND model. If a relative bandwidth of no less than 1.0 is desired, it is possible to observe a threshold of *CrstLT* (*ArtLT*) for each of other *ArtLT* (*CrstLT*) levels.

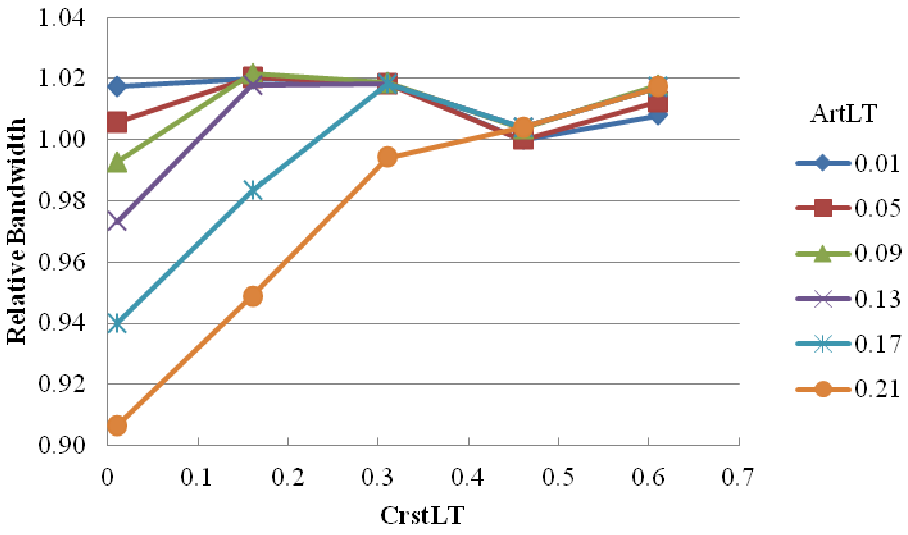

11a. Relative bandwidth by cross street left turn ratios

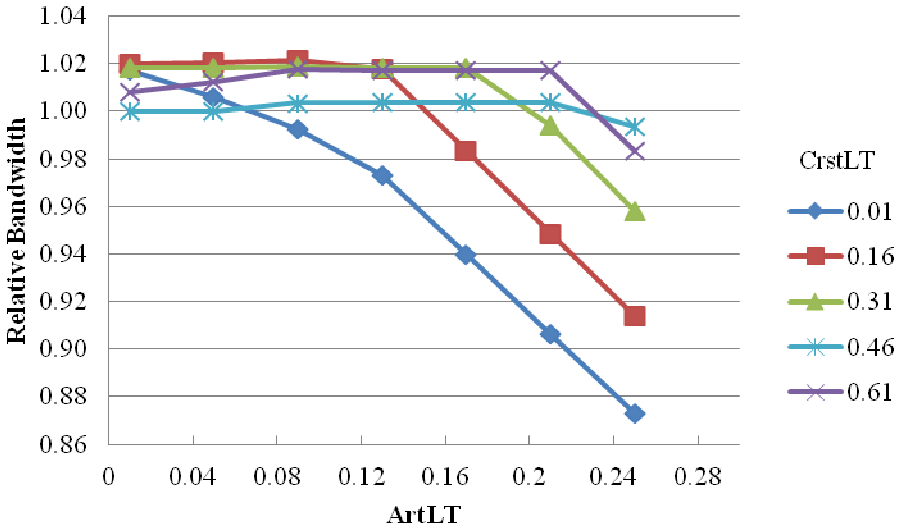

11b. Relative bandwidth by arterial left turn ratios

Figure 11. Relative bandwidth affected by *CrstLT* and *ArtLT* ratios

Traffic Difference between Arterial and Cross Streets at UDC Intersection

Figure 12 shows the changes in relative bandwidth by *AtC* under different levels of arterial left turn percentage (*UtS*=1.0, *CrstLT*=0.31). As *AtC* increases, the curves of relative bandwidth generally increase to above value 1.0 before they drop back to 1.0. When *AtC* is greater than 0.65 with permitted left turn and 0.75 with protected left turn on the cross streets, the UDC model can produce the same bandwidth results as that of MAXBAND model for all levels of *ArtLT* ratios. For individual *ArtLT* levels, individual thresholds of *AtC* ratios can also be obtained if a relative bandwidth of no less than 1.0 is desired.

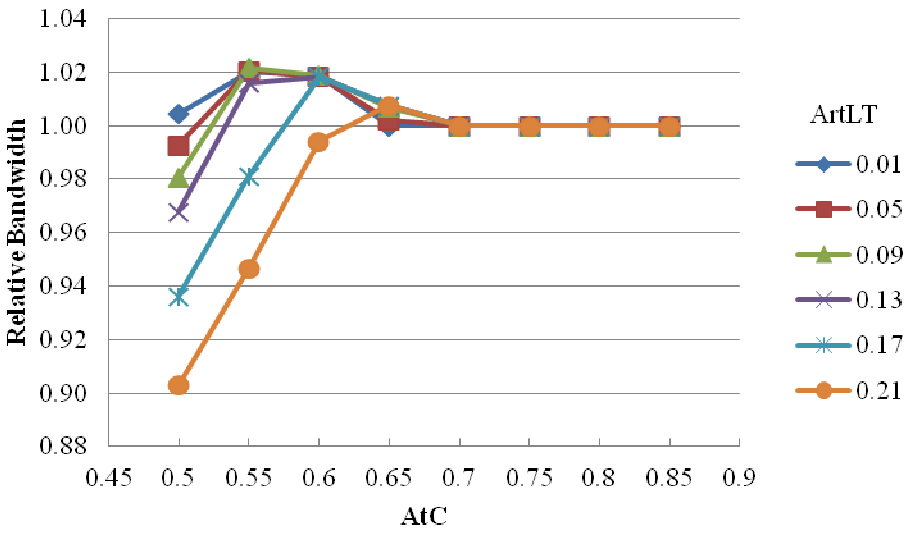

12a. Relative bandwidth by *AtC* ratios with permitted left turn on cross streets

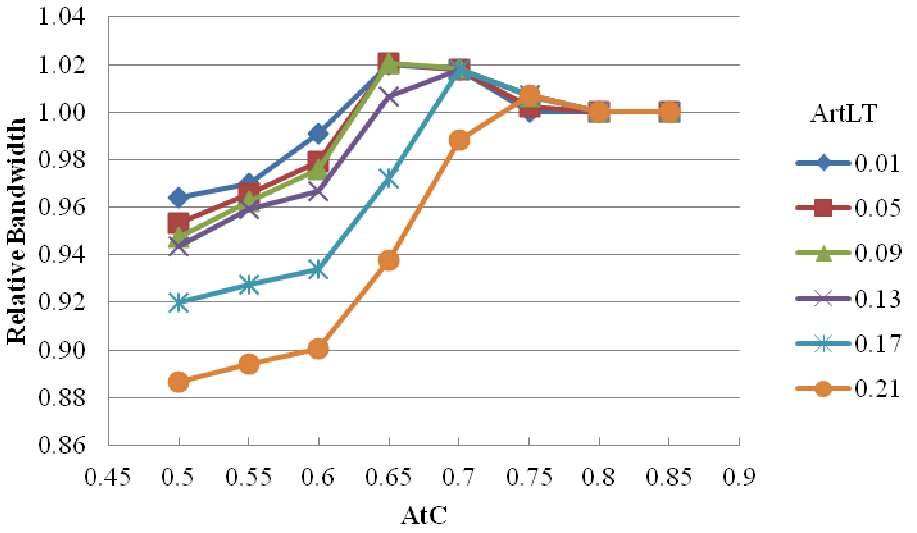

12b. Relative bandwidth by *AtC* ratios with protected left turn on cross streets

Figure 12. Relative bandwidth affected by *AtC* ratios

Traffic Difference between UDC and SC Intersections

Bandwidth efficiency does not change very much as *UtS* varies given all other factors the same. This is because the experiment data is generated in a way that changing *UtS* alone does not change the relative traffic level among different movements on different streets at the UDC intersection, and thus does not necessarily change the green split allocation affecting UDC optimization results.

Changes in *Xc-ratio* have mixed impact on bandwidth performance. Figure 13 shows relative bandwidth varying with *Xc-ratio* when only *AtC* varies (*UtS*=1.0, *CrstLT*=0.01, *ArtLT*=0.13). The figure shows that *Xc-ratio* generally decreases as *AtC* increases when relative bandwidth is less than 1.0 under both permitted and protected left turn operation on cross streets. But there are cases when the relative bandwidth varies while *Xc-ratio* does not change. For instance, when only *ArtLT* varies (*UtS*=1.0, *AtC*=0.65, *CrstLT*=0.31), *Xc-ratio* remains at 0.77 under protected left turn on cross streets, but the relative bandwidth could vary within 10 percent. Therefore, *Xc-ratio* is not a sufficient indicator about whether the UDC control scheme would be beneficial for an intersection.

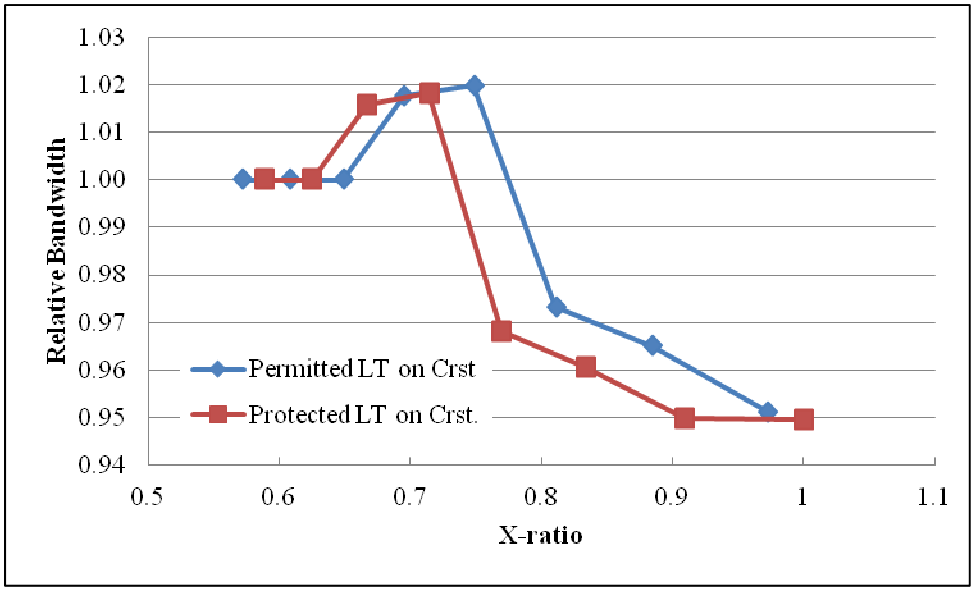

Figure 13. Relative bandwidth affected by *Xc-ratio*

Figure 14 shows changes in relative bandwidth by *g-ratio* under permitted and protected left turn operation on cross streets. As expected, when the relative bandwidth is less than 1.0, the relative bandwidth increases as *g-ratio* increases under most of the scenarios. If a value of at least 1.0 is desired for relative bandwidth, the *g-ratio* is no less than 1.28 (1.18) for permitted (protected) left turn operation on cross streets. The threshold of the *g-ratio* becomes 1.31 if the peak-direction bandwidth of UDC results being the same as that of MAXABND results is also required. A rule of thumb is that if, under SC control, an intersection has an outbound (peak direction) green time longer than that at the critical intersection by at least the sum of minimum green time and per phase lost time, UDC control might be beneficial at this intersection.

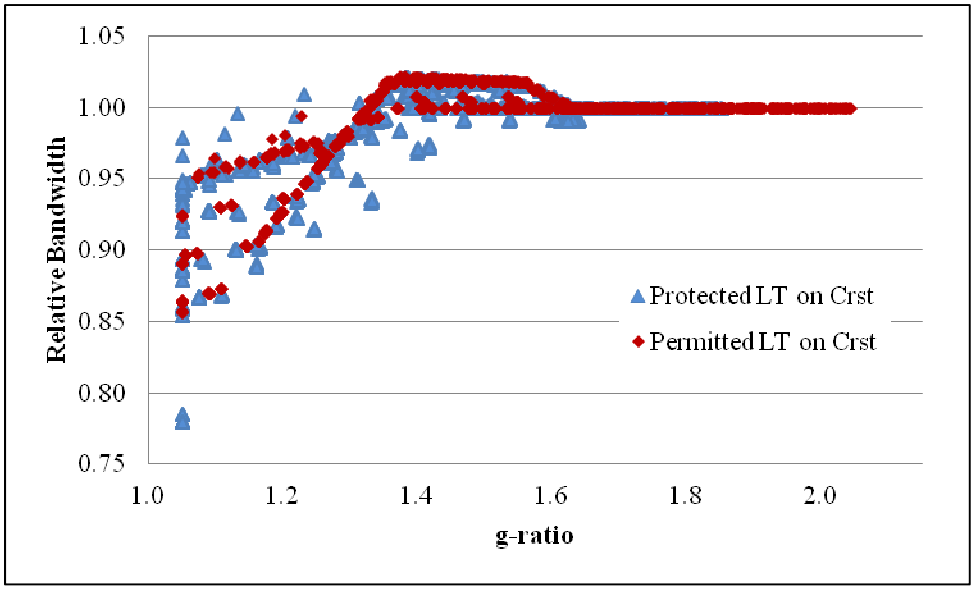

Figure 14. Relative bandwidth affected by *g-ratio*

By imposing the criterion that the bandwidth under UDC control should be no less than that under SC control for both directions, thresholds of the considered parameters can be specified. Table 5 lists the detailed thresholds of *ArtLT* and *g-ratio* for various levels of *AtC*. Because of the way it is designed in this study, bandwidth is not sensitive to *CrstLT* under permitted left turn and thus is not included in the table of thresholds.

Table 5. Thresholds of parameters when UDC control is beneficial[a]

CrstLT		AtC							
		0.50[b]	**0.55**	**0.60**	**0.65[c]**	**0.70**	**0.75**	**0.80**	**0.85**
Permitted	*ArtLT*≤	0.13	0.17	0.21	0.25	0.25	0.25	0.25	0.25
	g-ratio≥	1.32	1.34	1.31	1.32	1.35	1.32	1.41	1.49
Protected	*ArtLT*≤				0.09	0.17	0.21	0.25	0.25
	g-ratio≥				1.33	1.31	1.35	1.37	1.38

a. Beneficial means the UDC model can achieve the same or greater two-way bandwidths compared with SC control

b. Minimum *AtC* for permitted left turn on cross streets

c. Minimum *AtC* for protected left turn on cross streets

d. N/A means no solution under the *AtC* level to meet the beneficial criteria

CHAPTER VI

MODELING EVALUATION: CASE STUDY*

The case study used in this research consists of three parts. The field data is first presented and the preliminary guidelines were applied before running the basic UDC model on the data. Each of the enhanced models was then run on the data under fixed timing operation and the results were evaluated through simulation in comparison with conventional single cycling models. Performance evaluation of these models selected the best model to be applied to the actuated timing operation.

APPLYING THE GUIDELINES WITH BASIC MODEL

After the numerical experiments, the author conducted a case study using field data by first following the preliminary guidelines developed according to the results of numerical experiments and then running the UDC-enabled optimization model on the data to see the actual model results.

Field data for the case study are real traffic and geometric data of an arterial with four intersections (Campbell Rd from N Jupiter Rd to N Plano Rd) in Richardson, Texas provided by city officials. At both ends of the arterial were two major-major

* Part of the content in this section is reprinted from *Arterial Signal Coordination with Uneven Double Cycling*, by H. Zhou and G. Hawkins, 2014. Texas A&M Transportation Institute Report (SWUTC/15/600451-00024-1), Texas A&M University System, 3135 TAMU, College Station, TX 77843

intersections (at N Jupiter Rd and N Plano Rd) requiring 160 sec for good two-way progression, while the two major-minor intersections (at Yale Blvd and Owens Blvd) in between experiences unnecessary delays under signal cycling. Table 6 shows the adjusted flow rate at each of the four intersections along this arterial during AM peak hours. Volume and saturation flow adjusted according to the HCM [*38*].

Table 6. Traffic flow (vph) data for case study

	EBL	EBT	EBR	WBL	WBT	WBR	NBL	NBT	NBR	SBL	NBT	SBR
Jupiter	125	167	88	295	1492	68	424	1116	124	100	1364	635
Yale	33	380	33	33	2228	33	109	65	43	33	33	65
Owens	33	413	0	54	2283	54	65	65	43	43	43	65
Plano	76	340	155	400	2155	203	429	801	109	60	1750	236

The two major-minor intersections are considered as the candidate UDC intersections. Both intersections have permitted left turn operation on the cross streets. Table 7 lists the calculated values of suggested parameters for checking UDC applicability criteria. The results indicates that UDC control might be beneficial at both intersections for achieving the same or greater bandwidth as single cycling while reducing delay on the cross streets.

Table 7. Checking UDC application criteria for the case study

Parameter	Threshold	Actual parameter value	
		Owens	Yale
$AtC \geq$	0.5	0.89	0.81
$ArtLT \leq$	0.13	0.16*	0.11
g-ratio $\geq$	1.32	1.72	1.70
UDC?		Yes	Yes

* Asterisk indicates threshold criterion not met.

Running the optimization model on the data gives the expected results. The model chooses double cycling at both of the major-minor intersections. The UDC model provides the same bandwidth as that of single cycling for both inbound and outbound directions while reducing the total average delay on cross streets of the two UDC intersections by 44.7 percent (AD_n^{Tc} = 55.3%).

FIXED TIMING

Fixed timing plan optimization considers three sets of models: the improved basic models, the variable bandwidth enhanced models, and the variable and secondary bandwidth enhanced models. Each model set optimizes three sets of objectives: maximal bandwidth and minimal average delay on cross streets, maximal bandwidth and minimal total average delay, and maximal bandwidth and minimal total average delay and arterial stops.

Pareto Front and Time-space Diagram

The objective weight is of interest in the numerical experiment for the case study. The improved basic model UDCo is used to construct a Pareto Front between bandwidth efficiency and estimated average through delay on cross streets. The optimization results are not sensitive to changes in the objective weight (λ^B) when it is outside the range of [0.08, 0.4]. Within this range, the model yielded a smooth Pareto Front. Figure 15 shows the Pareto Front in the case study. It indicates that the UDC control scheme could save at least 44.7 percent of average cross street delay at UDC intersections without reducing bandwidth efficiency at all; and it could save up to 47.9 percent of delay by sacrificing 6.7 percent of bandwidth achieved under single cycling. Another trend found with the objective weight analysis is that, as the contribution of delay component to the model objective increases, the difference between the two sub-green splits on arterial decreases in order to minimize delay. The range of objective weight needed to construct a Pareto Front varies depends on the input traffic and geometric data. Usually a larger value of λ^B should be preferred since arterial progression often has higher priority over reducing delay on cross streets.

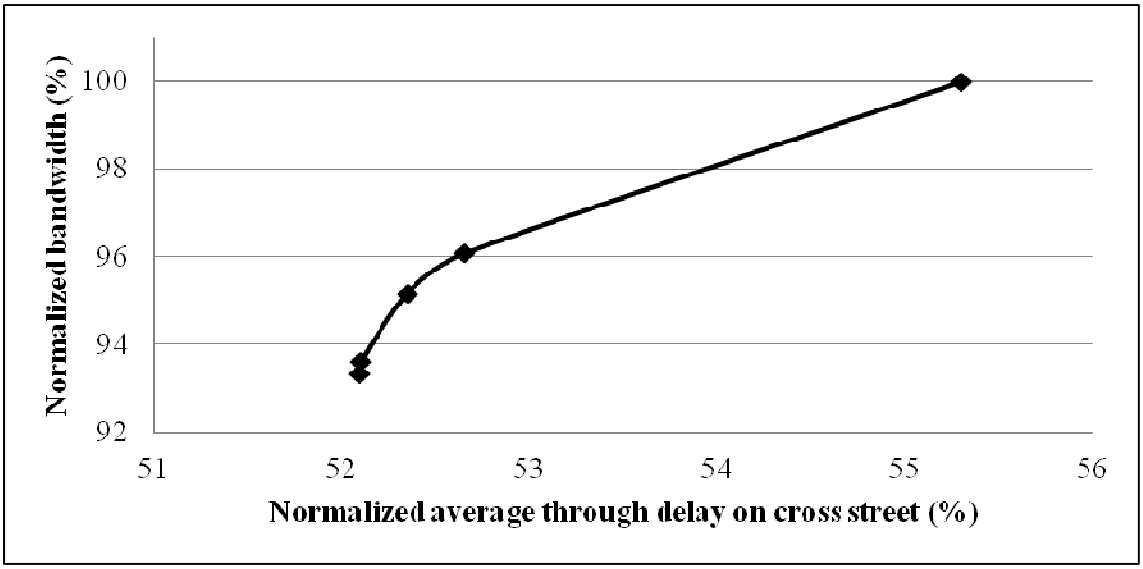

Figure 15. Pareto Front of bandwidth and delay objectives

With the multicriterion modeling results, Figure 16 shows the time-space diagrams produced by the improved basic model UDC_DS and the enhanced model UDC_SVDS. The inbound (eastbound) and outbound (westbound) green bands pass different sub-cycles at Yale Blvd and pass the same sub-cycle at Owen Blvd using both models (and all other models). The outbound bandwidth under constant bandwidth optimization is larger than that under variable bandwidth optimization, but variable bandwidth optimization gives larger outbound bandwidth at the noncritical intersections. The UDC_SVDS model produces a secondary green band that is coordinated locally at the two consecutive UDC intersections.

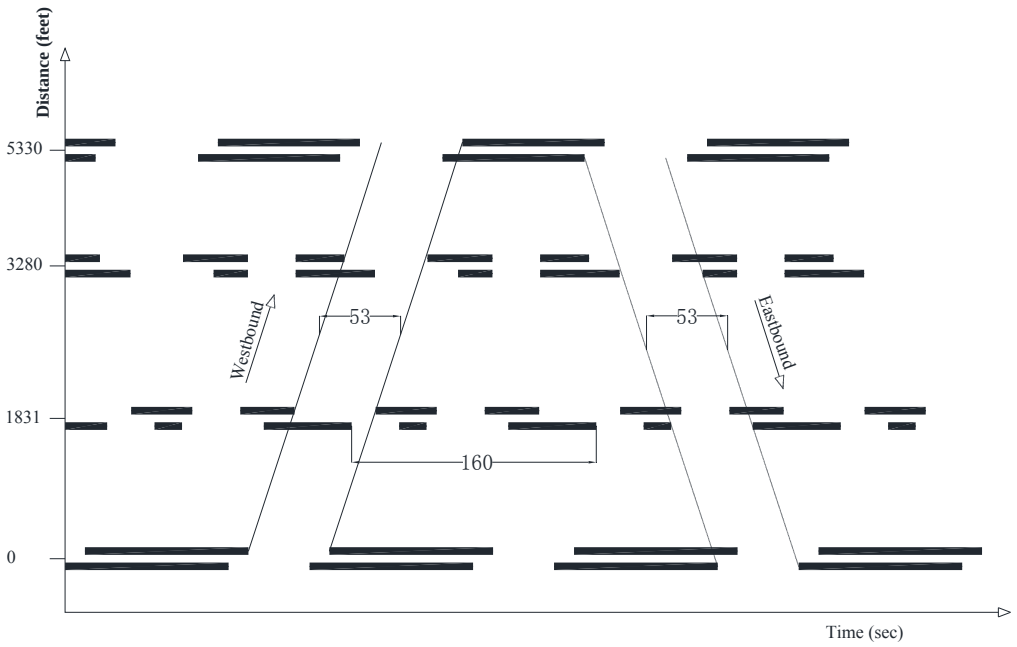

16a. Time-space diagram generated with the improved basic model UDC_DS

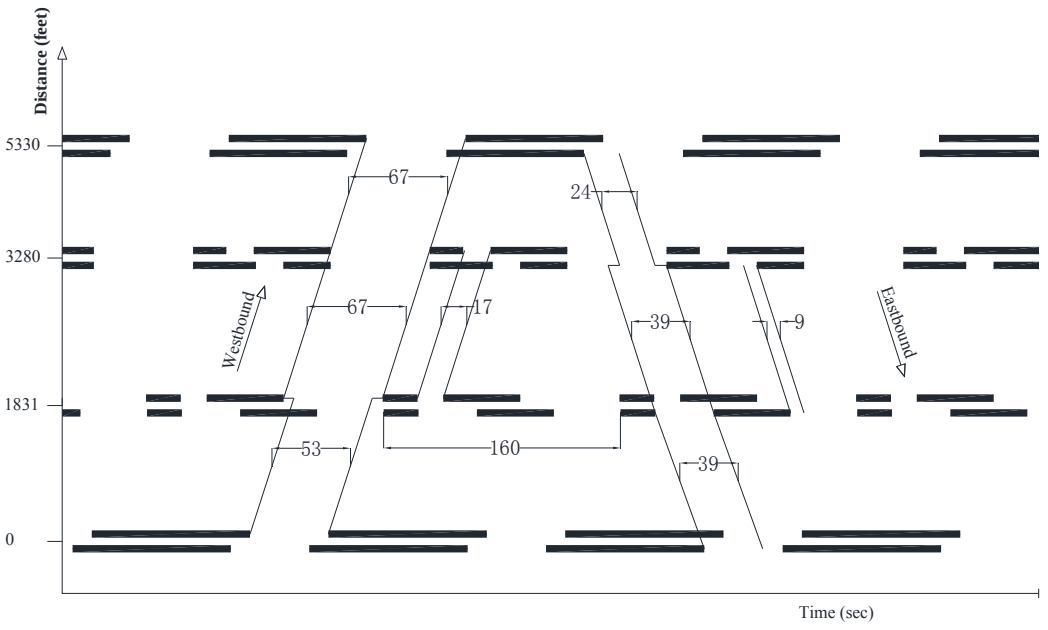

16b. Time-space diagram generated with the enhanced model UDC_SVDS

Figure 16. Time-space diagrams of multiple-objective optimization

Simulation Evaluation of Model Performance

The optimization results of various models are evaluated using SimTraffic 6 [*61*]. The seeding (warm-up) period is four minutes and the simulation duration is fifteen minutes. Each case has five random seed runs, and the average of the five runs is used for evaluation. The evaluation compares the proposed models with the conventional single cycling plans optimized using MAXBAND and MULTI-BAND. Performance measures used are average delay, number of stops, and travel times. Delay and stop statistics are calculated for all lane groups at all approaches; travel times are summarized for arterial through traffic and for total traffic. Appendix II contains the details simulation results. Table 8 shows the summarized results for through delay.

Table 8. Simulation results of through delay (sec/veh) with fixed timing

	Arterial			Cross streets		
	All	UDC	SC	All	UDC	SC
Base models with single cycling						
MAXBAND	25.99	10.87	47.68	66.39	40.44	67.63
MULTI-BAND	23.42	9.83	42.97	66.13	41.55	67.30
Improved basic UDC models						
UDCo	26.64	12.01	47.51	59.55	23.13	61.28
UDC_D	29.29	10.21	44.93	59.28	15.46	61.03
UDC_DS	25.58	11.97	44.93	59.23	21.24	61.03
UDC models enhanced with variable bandwidth optimization						
UDC_V	23.16	9.29	43.07	58.69	24.67	60.29
UDC_VD	23.40	9.22	43.83	60.36	23.61	62.09
UDC_VDS	23.43	9.22	43.89	58.54	23.51	60.19
UDC models enhanced with variable and secondary bandwidth optimization						
UDC_SV	23.92	9.50	44.65	59.98	23.21	61.70
UDC_SVD	24.40	9.61	45.65	57.44	22.84	59.06
UDC_SVDS	24.43	9.19	46.29	59.00	23.16	60.68

Comparing various model results with the base MAXBAND model gives the relative performance of individual sets of multicriterion optimization. Figure 17 shows the comparison results. All nine models reduce cross street through delay at UDC intersections by at least 39 percent and up to 61.8 percent. The enhanced models also reduce arterial through delay at UDC intersections by at least 11.6 percent and up to 15.4

percent. All nine models also reduce through delay at SC intersections on both arterial and cross streets. This is because, given about the same coordinated green time for bandwidth passage, the UDC scheme reshapes the arrival flows profile at the downstream SC intersection by discharging part of flows later in the cycle. This reduces queue lengths and thus reduces delay compared with MAXBAND model. Generally, models with constant bandwidth optimization perform best in reducing cross street through delay at UDC intersections but worst for arterial through movement. The enhanced models with variable bandwidth optimization yield the most through delay reduction on arterial. Considering secondary bandwidth optimization gives the most through delay reduction on cross streets.

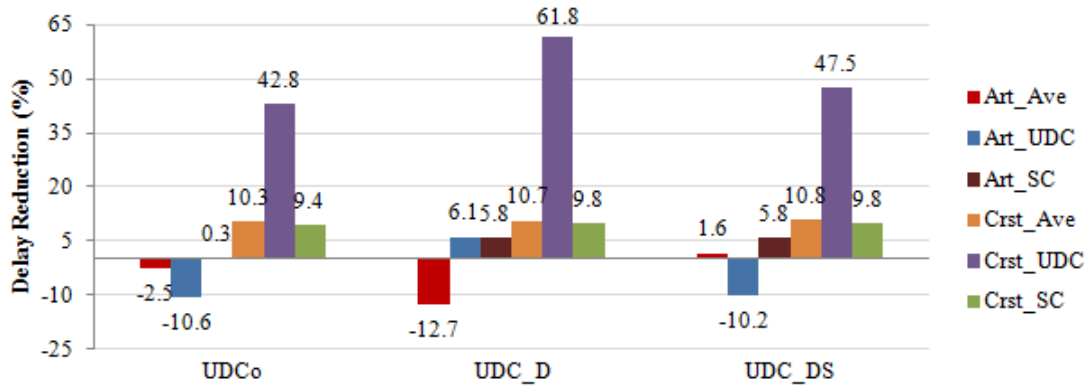

17a. Delay reduction of the improved basic models

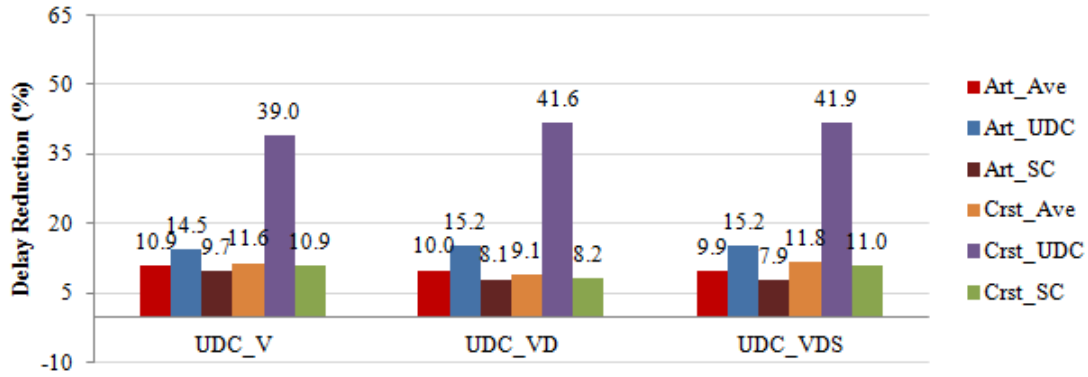

17b. Delay reduced by enhanced models optimizing variable bandwidth

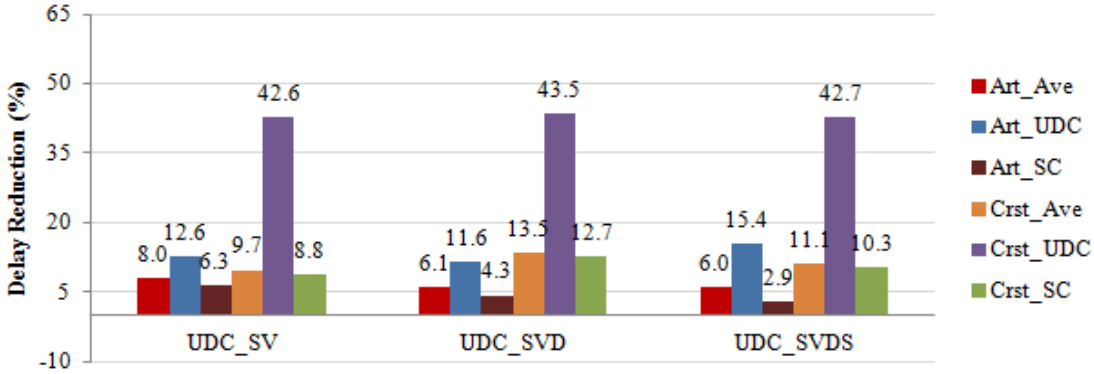

17c. Delay reduced by enhanced models optimizing variable and secondary bandwidth

Figure 17. UDC reduced through delay comparing with MAXBAND

Further comparing the enhanced models with MULTI-BAND model indicates the performance of individual models. Figure 18 shows the comparison results. Both sets of models cross street through delay at all intersections and arterial through delay at UDC intersections. But they slightly increase arterial through delay at SC intersections. Compared with variably bandwidth optimization, the addition of secondary bandwidth optimization slightly betters delay reduction on the cross streets at the cost of increasing delay at SC intersections. The reason that UDC models increase delays at SC intersections is because arrival flow rate at the SC intersections in the red interval is higher with a UDC upstream intersection than with a SC upstream intersection given the MULTI-BAND base condition. Coordinating the secondary green band slightly reduces the main bandwidth and increases flow rate in red and thus offsets some of the benefit of UDC control.

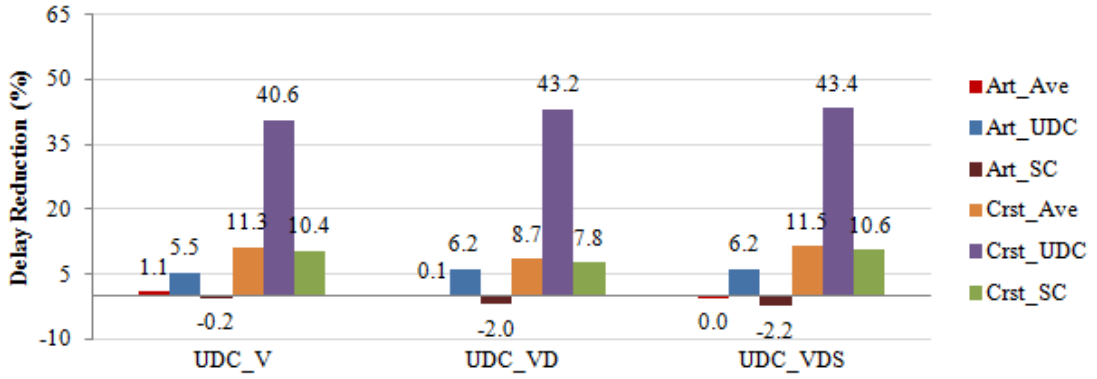

18a. Delay reduced by enhanced models optimizing variable bandwidth

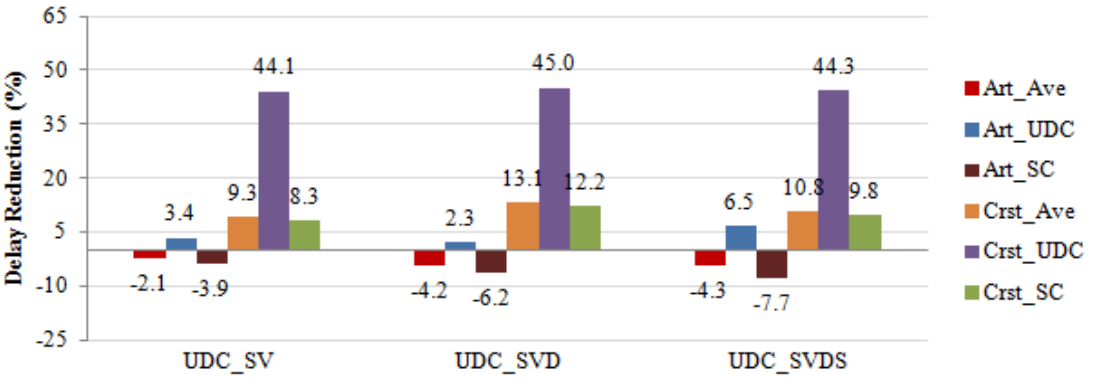

18b. Delay reduced by enhanced models optimizing variable and secondary bandwidth

Figure 18. UDC reduced through delay comparing with MULTI-BAND

Table 9 shows the simulation results for number of stops of through movement. Compared with MAXBAND results, the proposed models reduce the number of stops at single cycled intersections by 8.1 to 15.9 percent for arterial through movement and by 7.7 to 10.8 percent for cross streets through movement. Comparing the enhanced models results with MUTIBAND results, the reduction in stops for cross street through movement at SC intersections ranges from 7.8 percent to 10.9 percent. The reduction of

stops for arterial through movement at SC intersections is not significant (less than five percent).

Table 9. Simulation results of number of stops (stops/veh) with fixed timing

	Arterial			Cross streets		
	All	**UDC**	**SC**	**All**	**UDC**	**SC**
Base models with single cycling						
MAXBAND	0.38	0.16	0.69	0.92	0.70	0.93
MULTI-BAND	0.34	0.15	0.61	0.92	0.74	0.93
Improved basic UDC models						
UDCo	0.42	0.26	0.64	0.84	0.77	0.84
UDC_D	0.49	0.31	0.63	0.84	0.78	0.84
UDC_DS	0.42	0.28	0.63	0.84	0.71	0.84
UDC models enhanced with variable bandwidth optimization						
UDC_V	0.38	0.23	0.58	0.84	0.70	0.84
UDC_VD	0.38	0.23	0.60	0.85	0.68	0.86
UDC_VDS	0.38	0.23	0.59	0.84	0.70	0.85
UDC models enhanced with variable and secondary bandwidth optimization						
UDC_SV	0.38	0.23	0.61	0.85	0.66	0.86
UDC_SVD	0.40	0.25	0.62	0.83	0.70	0.83
UDC_SVDS	0.38	0.22	0.61	0.84	0.68	0.85

This benefit of reducing delay and stops on cross streets at SC intersections mainly comes from the intersection at N Jupiter Rd, where more right turn vehicles make right

turn on red (RTOR) under the UDC model. Figure 19 shows the phasing sequences under single cycling and double cycling at this intersection.

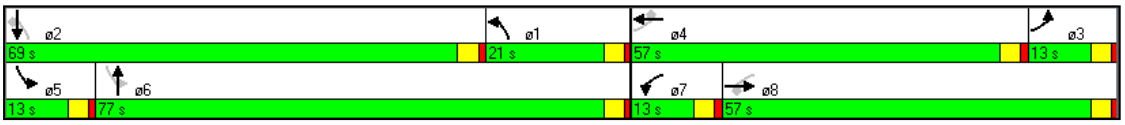

19a. MULTI-BAND optimized phasing sequence

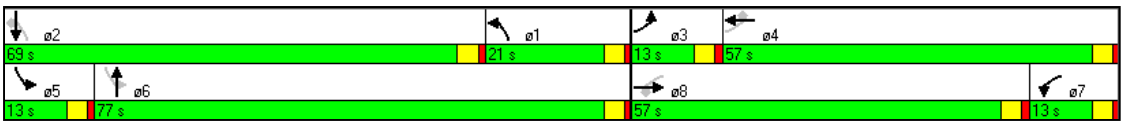

19b. UDC models optimized phasing sequence

Figure 19. Synchro ring-barrier diagrams of the intersection at N Jupiter Rd

In Figure 19, arterial left turn phases have lead-lag pattern for westbound and eastbound directions under the MULTI-BAND results (Figure 19a) and lag-lead pattern under UDC results (Figure 19b). With the lag-lead left turn sequence for northbound and southbound directions, northbound (southbound) right turn traffic is serviced in two separate phases. The two phases are the concurrent northbound (southbound) through phases in green interval and the westbound (eastbound) left turn phase in red interval. The separation by westbound (eastbound) through phase for northbound (southbound) right turn service is beneficial. Similar to UDC control, discharging right turn traffic in two short phases reduces right turn queue length compared with discharging them in a long phase. Given limited storage space (either permitted or exclusive right turn lane), shorter right turn queue gives less friction to the adjacent through traffic and thus shorter through queue.

For instance, compared with the MULTI-BAND results, the UDC_VB results have 44.3 percent shorter right turn queue and 17.0 percent shorter through queue in the outside lane and 19.2 percent in the inside lane on average. It should be noted that this benefit is not considered in the modeling and may not be presented in a different arterial.

The number of through stops on cross streets at UDC intersections is also reduced compared with single cycling because of the reduced through queue length. Total reduction in through stops on cross streets ranges from 7.6 percent to 10.7 percent by various UDC models compared with single cycling models.

However, the UDC control scheme increases arterial through stops at UDC intersections by more than 30 percent under fixed timing operation. This is expected since the slack green time at UDC intersections is shortened which reduces the passage reliability for arrival traffic at the tail of the green band. This shortcoming of UDC scheme is expected to be overcome under actuated control, which will be discussed in the next section.

The UDC control is also beneficial for left turn traffic. The greatest benefit of UDC control for left turn movement is the reduced delay (by more than 35 percent) at UDC intersections on cross streets across all UDC models. Since cross street left turn is permitted at UDC intersections, the reason for its delay reduction is similar to through movement. Another important impact of UDC control on left turn traffic lies in the capacity change in permissive turning duration. For instance, compared with single cycling, the UDC models decrease left turn delay in the peak direction but increase left

turn delay in the off-peak direction at SC intersections. At the intersection of N Plano Rd, through traffic arriving in the peak direction is more spread out in the fixed green time window because of the upstream UDC intersection of Owen Blvd. As a result, the opposing left turn traffic in the off-peak direction has less opportunity making permitted left turns (given the same external traffic input and same timing plan). At the intersection of N Jupiter Rd, through traffic arriving in the off-peak direction is more spread out because of the upstream UDC intersection of Yale Blvd. As a result, the opposing left turn traffic in the peak direction has more opportunity making permitted left turns, even left turn in this direction is lagged with UDC models as oppose to lead with SC models (given the same external traffic input).

The model performance is also evaluated for travel times. Figure 20 shows the simulated travel times of various models for fixed timing operation. Figure 20a shows that all nine models reduce arterial through travel time comparing with the MAXBAND model. Comparing with the MULTI-BAND model, only the model set maximizing variable bandwidth has marginal travel time savings in arterial through traffic. The other two sets of models increase travel time by up to six percent. Figure 20b shows that all nine models reduce total travel time comparing with both MAXBAND and MULTI-BAND models. But the travel time savings are marginal (less than five percent).

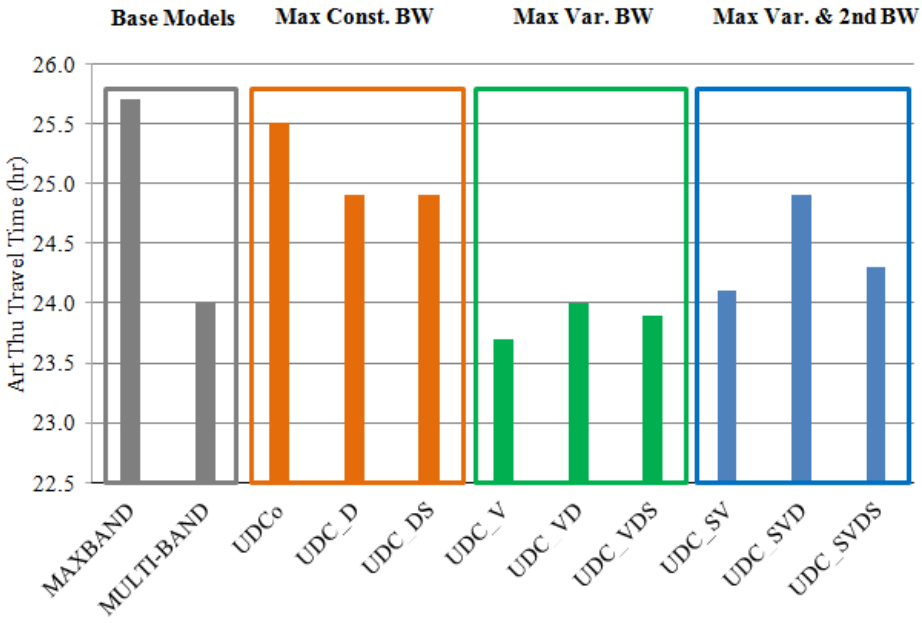

20a. Arterial through travel times

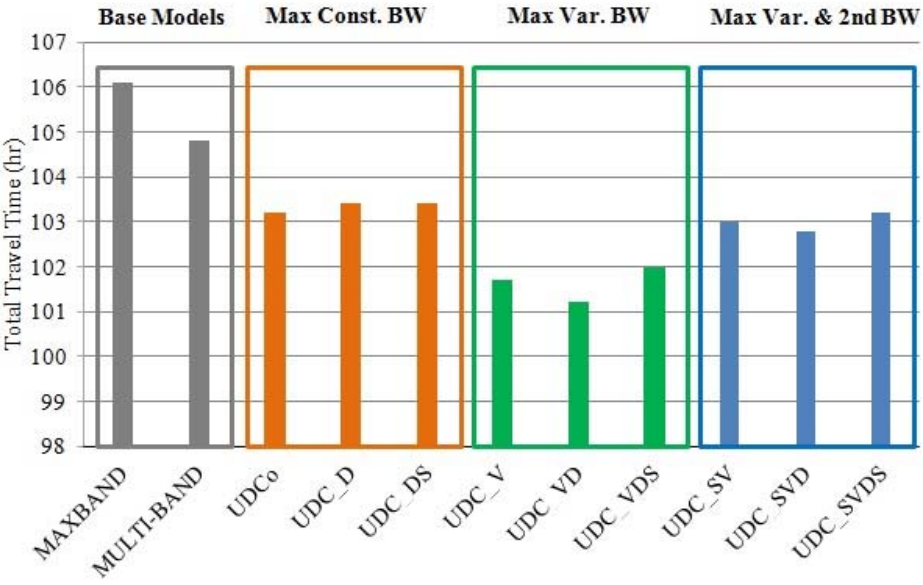

20b. Total travel time of on all streets

Figure 20. Arterial through and total travel times of various models

Overall, the enhanced UDC models optimizing variable bandwidth perform the best. They have the highest delay reduction for arterial through movement and the lowest stop increase for arterial through movement. Their performance for cross through movement is comparable to enhanced models also optimizing secondary bandwidth. They also have the highest reduction in total delay and stops if taking turning movements into consideration. The total throughput and average speed of this set of models are also higher than other models. This model set also has the lowest total travel time and arterial through travel time. Among the three models within this model set, UDC_VB (maximizing variable bandwidth and minimizing UDC cross street delay) gives the highest reduction in delay and stops for arterial through movement. Although UDC_VBTD (also minimizing UDC arterial delay based on UDC_VB) performs best in reducing total delay and stops, it performs worst for arterial through movement. UDC_VBDS (also minimizing UDC arterial stops based on UDC_VBTD) has mediocre performance for most measures except reduces the most cross street through delay. Giving the priority to arterial through traffic, UDC_VB is chosen for further evaluation under actuated timing control.

COORDINATED-ACTUATED TIMING

The case study is also interested in the performance of UDC control scheme under coordinated-actuated operation. The signal controller is assumed to have the following control settings to consider UDC control. Other settings are the same as the conventional single cycling operation.

1. Phases on cross streets are uncoordinated and actuated with floating force-off points and without recalls;
2. Phases on arterial streets are not actuated and have max recalls, and through phases in one of the sub-cycles are coordinated;
3. All phases have the inhibit max feature invoked;
4. Pedestrian phases of both directions of a street are serviced in one of the sub-cycles;

Settings No. 1 through No. 3 make sure that 1) unused green time of an actuated phase due to gap out goes to the first arterial through phase after this actuated phase in sequence; and 2) the arterial through phases in both the sub-cycles get at least the programmed maximum green time. Setting No. 4 is to ensure that pedestrian traffic is serviced upon pedestrian calls. Since none of the vehicular phases have pedestrian recall invoked, actuated phases can still gap out in the absence of calls from the parallel pedestrian phases.

Under real operation conditions, traffic flows at all approaches vary by time, and, as a result, the actuated effective green times also vary. To evaluate the model performance under various traffic conditions, the author first generated traffic input data by adjusting volume data listed in Table 6.

Volume Adjustment

This scenario-based method first creates different cyclic arrival flow rate for external traffic inputs, each of which corresponds to a percentile traffic level. Assume the number through vehicles arriving in a cycle on an approach follow a Poisson distribution with the unadjusted number of arrivals per cycle being the mean. Given the property of Poisson distribution that the variance equals the mean, the standard deviation of equivalent hourly volume of this external through flow $SD_{i,j}^{T}$ is calculated using Equation 75. For external flows, $i = 1..N \cap j = 3,4$ or $i = 1 \cap j = 1$ or $i = N \cap j = 2$.

$$SD_{i,j}^{T} = \sqrt{\frac{v_{i,j}^{T} C}{3600}} \Bigg/ \frac{C}{3600} \qquad \text{Equation 75}$$

Use normal distribution to approximate volumes at a percentile p (10th, 30th, 50th, 70th, and 90th percentiles). Then the adjusted external percentile volumes $v_{i,j}^{Tp}$ are calculated using Equation 76. The adjusted volumes for external left turn $v_{i,j}^{Lp}$ and right turn $v_{i,j}^{Rp}$ can be calculated similarly.

$$v_{i,j}^{Tp} = v_{i,j}^{T} + z_p SD_{i,j}^{T} \qquad \text{Equation 76}$$

where z_p is the z-score of normal distribution for a percentile p. Table 10 contains the five percentile z_p values considered for the volume adjustment.

Table 10. Normal distribution z-score of different percentiles

Percentile	z_p
10	-1.28
30	-0.52
50	0
70	0.52
90	1.28

For internal arrival flows on the arterial, there are two ways of adjusting the volumes. One way is modeling the directional internal arrival flow rate as a random variable which is a function of upstream through and turning traffic. Equation 77 represents this function for outbound arrival rate at the second intersection. For internal flows, $i = 2..N-1 \cap j = 1,2$ or $i = 1 \cap j = 2$ or $i = N \cap j = 1$.

$$v_{2,1}^{m} = \left(v_{1,1}^{T} + v_{1,3}^{L} + v_{1,4}^{R}\right) k_{2,1}^{m} \qquad \text{Equation 77}$$

where $v_{2,1}^{m}$ is the outbound arrival flow rate of a movement *m* (through, left turn, or right turn) at the second intersection and $k_{2,1}^{m}$ is the proportion of flow of this movement *m*. The three terms in the parenthesis are upstream contributing source flow rate.

Assuming the normal distribution approximated external input flow rates are independent from each other, the directional internal flow rate $v_{2,1}^{m}$ also follows a normal distribution. Given the property of normal distribution and the original assumption of Poisson distribution, this normal distribution has parameters of mean and variance

indicated by Equation 78. The corresponding adjusted percentile volumes can be calculated using Equation 79. The inbound internal flow rates can be determined similarly.

$$v_{2,1}^{m} \sim N\left(\left(v_{1,1}^{T}+v_{1,3}^{L}+v_{1,4}^{R}\right)\frac{C}{3600}k_{2,1}^{m}\ ,\ \left(v_{1,1}^{T}+v_{1,3}^{L}+v_{1,4}^{R}\right)\frac{C}{3600}k_{2,1}^{m\,2}\right) \qquad \text{Equation 78}$$

$$v_{2,1}^{m}=\left(v_{1,1}^{T}+v_{1,3}^{L}+v_{1,4}^{R}\right)k_{2,1}^{m}+z_{p}k_{2,1}^{m}\sqrt{\left(v_{1,1}^{T}+v_{1,3}^{L}+v_{1,4}^{R}\right)\frac{C}{3600}}\Big/\frac{C}{3600} \qquad \text{Equation 79}$$

The alternative is to treat the internal flows the same way as the external flows which follow the normal distribution with the variance being equal to the mean and the unadjusted cyclic flow rates being the mean. Comparing with the above method, this treatment is simpler. Although the connection with upstream source flows is not explicitly reflected in calculating the internal flows, using the direct volume inputs on the internal approaches reveals some information about traffic input at access points of links, if any. Also, the volume adjustment is intended for cyclic flow rate, of which the volume balance is of less importance compared with second-by-second processing. Therefore, for simplicity, Equation 75 and Equation 76 are also used for adjustment of internal flows.

Simulation Results

Using the phase splits optimized by model UDC_VB and MULTI-BAND under fixed timing as the maximum splits for actuated controller, the coordinated-actuated timing

plan is obtained by optimizing phasing sequences and offsets in SYNCHRO [*6*]. Simulation evaluation considers the five percentile levels listed in Table 10 for volume adjustment. For each volume level, the simulation consists of three periods: the seeding (warm-up) period of four minutes, three minutes (about one cycle) of adjusted volume level as a sudden demand surge or drop, and the fifteen minutes of recovery period without volume adjustment. Each case has five random seed runs, and the average of the five runs is used for evaluation. Same as the evaluation of fixing timing, measures of effectiveness also use average delay, average stops, and travel time. Appendix III contains the details simulation results.

Table 11. Simulation results of through delay (sec/veh) with actuated timing

%tile Volume	Arterial			Cross streets		
	All	UDC	SC	All	UDC	SC
MULTI-BAND						
10	16.8	4.0	35.0	64.9	69.6	64.8
30	17.9	4.4	37.8	96.3	64.7	97.2
50	26.4	5.3	56.4	82.2	71.8	82.6
70	21.1	5.6	43.3	94.4	68.0	95.2
90	25.8	6.6	53.4	111.5	56.4	114.0
UDC_V						
10	17.8	3.8	37.6	65.9	53.7	66.2
30	20.3	3.9	44.1	94.0	49.6	95.3
50	26.9	4.7	58.5	82.1	46.3	83.4
70	22.8	4.6	48.8	94.0	48.9	95.4
90	26.7	5.7	56.6	108.8	45.0	111.7

Table 11 shows the simulation results of through delay for both models. The greatest benefit of UDC control occurs at UDC intersections compared with conventional control. Cross street through movement at UDC intersections has the highest delay reduction (ranging from 20.2 percent to 35.5 percent under different volume levels, see Table A11 in Appendix III), followed by arterial through delay at UDC intersections (ranging from 4.5 percent to 18.3 percent under different volume levels, see Table A11 in Appendix III). Taking left turn and right turn movements into consideration, total delay reduction at UDC intersection ranges from 12.5 percent to 18.8 percent (4.6 percent to 14.2

percent on arterial and 19.2 percent to 26.1 percent on cross streets) under different volume levels (see Table A19 in Appendix III). This is expected for the similar reason explained for fixed timing.

Delay measures at SC intersections show mixed results because of the spread out arterial arrival flow from upstream UDC intersection. Arterial through and cross street left turn movements at SC intersections have slightly increased delay. This is mainly resulted from less unused green time from cross street turning movement available for coordinated through phases at SC intersections under UDC control. This higher usage of green time of cross street turning movements is because that the spread out arterial through flow rate reduces the RTOR opportunity and increases adjacent through queue length. This further reduces capacity of permitted left turn duration for the opposing approach and thus lowers the chance of skipping phases. The SC intersection at N Jupiter Rd is this case. However, arterial eastbound left turn at the SC intersection of N Plano Rd has significantly reduced delay because more permitted left turn is made. This is because the upstream UDC intersection at Owen Blvd has less early return to green problem compared with SC control under actuated operation. Plus the spread out arrival flow, westbound through queue at the N Plano Rd is shorter and thus needs shorter time to clear the approach compared with single cycling, therefore the opposing eastbound left turn gains more usable permissive turning time.

Compared with fixed timing operation, UDC control has much less negative impact on arterial stops at UDC intersections under coordinated-actuated operation. Table 12 shows the reduction in number of stops on arterial with 50 percentile volume demand compared with single cycling. It shows that applying the UDC control scheme under coordinated-actuated operation slightly increases the number of stops of arterial through movement at UDC intersections, whereas under fixed timing, there is an increment of 57.6 percent (see Table A6 in Appendix II). UDC control also reduces the number of stops for arterial left turn movement at UDC intersections by 10.8 percent, compared with 1.8 percent (see Table A8 in Appendix II) under fixed timing. Although there is a very small increase in stops at SC intersection under actuated timing, total number of stops on arterial is still slightly increased.

Table 12. Reduction in arterial stops of UDC compared with SC (%)

Operation type	Through			Left turn			Total
	Total	UDC	SC	Total	UDC	SC	
Fixed timing	-10.6*	-57.6	4.6	8.0	1.8	8.6	-7.3
Actuated timing	-0.1	1.5	-0.2	1.4	10.8	-0.3	0.7

* Negative values indicate increase in number of stops

Comparing the performance of both models under different volume levels, the UDC model seems to be more robust than SC control. When there is a sudden drop in traffic demand, delay and number of stops generally decrease. When there is a sudden surge in demand, the result is mixed. Arterial through and all left turn movements have decreased

delay and number of stops and cross street through movement has increased delay and stops compared with the 50 percentile volume level for both models. However, the changes in the performance measures tend to be smaller with the UDC model than with the SC model. This is beneficial in that when demand surge happens, which is more of a concern compared with demand drop, the UDC model deteriorates less compared with single cycling. Comparing both models for delay and stops at individual percentile volume levels, the UDC model always has lower delay (ranging from 4.6 percent to 26.1 percent, see Table A19 in Appendix III) and a little more stops at UDC intersections than the SC model. At SC intersections, the SC model performs slightly better than the UDC model.

There is slight travel time savings in both arterial through and total traffic under the 50 percentile volume level comparing with the MULTI-BAND model. Under traffic variation, UDC control still reduce total travel times most of the volume levels (except with the 10 percentile volume adjustment); arterial through travel times are increased under all adjusted volume levels. But all the travel time savings or reduction are marginal.

Overall, incorporating the UDC control scheme to coordinated-actuated operation brings benefits by reducing cross street delay at UDC intersections without increasing the disutilities on other approaches. The LOS on cross street approaches is improved from

LOS E to LOS D for the northbound direction and from LOS D to LOS C for the southbound direction.

CHAPTER VII

CONCLUSIONS AND FUTURE STUDY

CONCLUSIONS

Conventional single cycling coordination often causes excessive delay at major-minor intersections when a long background cycle length is dictated by the major-major intersections. With advances in signal controllers, more enhanced timing optimization models are needed for signal coordination systems to fully utilize the capability of advanced signal controllers for more efficient traffic operation. This dissertation develops mathematical optimization models and programming to enable UDC control in arterial coordination and provides preliminary guidelines for UDC implementation. The proposed models add flexibility to conventional modeling by using UDC to reduce total average delay without significantly compromising progression quality. The provided programming and preliminary guidelines are expected to greatly expedite the process of development and potentially improve the performance of UDC timing plans in current practice.

The basic UDC model solves several major issues to make the UDC control scheme work. Adding delay estimation of cross street through traffic at UDC intersections to the MAXBAND model allows the optimization to not converge at a point that the uncoordinated sub-green phase always gets the minimum green time or less. Introducing

the concept of nominal red and derivation of loop function for UDC intersections makes it easy for the conventional bandwidth geometry to accommodate the new control scheme. The disjunctive programming technique converts a complicated MINLP problem to a MIQP problem to ensure computational efficiency.

The enhanced UDC models improve the basic model in several ways. Considering pedestrian needs in only one instead of both of the sub-cycles allows the UDC control to service more traffic modes and scenarios. Using the platoon ratio to simplify the estimation of arterial through arrival flows makes the MIQP structure still applicable for the enhanced UDC models. The additional objectives considered in the enhanced modeling include maximal variable main bandwidth and secondary bandwidth, minimal average delay, and stops of arterial through movements at UDC intersections. Formulizing the objective of maximal variable bandwidth incorporates the well-known MULTI-BAND model. A new bandwidth geometry is described for the secondary bandwidth provided outside of the main green bands for multiple successive UDC intersections. Combining these objectives generates nine enhanced UDC models depending on whether maximizing constant main bandwidth, variable main bandwidth, and secondary bandwidth as shown in Table 3. Note that the secondary bandwidth is always maximized in addition to maximal main variable bandwidth, and the objective of minimal average delay on cross streets at UDC intersections is included in all models.

With all the models settled, the modeling performance is evaluated through numerical experiments and simulations. In the numerical experiments, three sets of *v/s* ratio based parameters are designed to generate input data for the basic UDC model in an attempt to identify traffic thresholds for UDC implementation. These parameters include left turn percentage on arterial (*ArtLT*) and cross streets (*CrstLT*) at UDC intersections, traffic difference between arterial and cross streets (*AtC*) at UDC intersections, and traffic different between UDC and SC intersections (*Xc-ratio* and *g-ratio*). The experiment results show that the basic UDC model can achieve 99.5 percent bandwidth obtainability and reduce cross street through delay by up to 41.1 percent. In many cases, the UDC model produces the same bandwidth as that of the MAXBAND model. In some scenarios, the sum of two-way bandwidth under UDC can be slightly higher. These are the cases when the basic UDC model provides the same or slightly smaller bandwidth in the peak direction and greater bandwidth in the off-peak direction compared to the MAXBAND model. This benefit is resulted from the more flexibility in phasing sequence under UDC control. Overall, the relative bandwidth of the basic UDC model over the MAXBAND model increases as *ArtLT* decreases, *AtC* increases, and *g-ratio* increases. The *g-ratio* is the most effective indicator of progression quality under UDC control. It is defined as the average of inbound and outbound ratios of arterial through green split at a UDC intersection to that at the critical intersection. *Xc-ratio* might not be an adequate indicator for UDC implementation because there are scenarios when *Xc-ratio* does not change but the relative bandwidth varies within ten percent. The

thresholds of parameters are provided in Table 5 for the basic UDC model to provide the same or greater two-way bandwidths compared with MAXBAND model.

To evaluate the model performance, actual geometry and peak hour traffic data from Richardson, TX is used for a case study. It is an arterial having four intersections with two major-minor intersections located between two major-major intersections. Applying the threshold parameters to check UDC applicability in this arterial suggests UDC control at the two minor-minor intersections. Running the basic UDC model also gives the same recommendation. A smooth Pareto Front is constructed between the bandwidth and delay objectives using MAXBAND results for normalization. Then optimization results of the enhanced models are implemented into fixed timing and actuated operations for simulation evaluation. The simulation results show significant advantages of the UDC control scheme over conventional SC control. For fixed timing operation, all nine enhanced models greatly reduce cross street disutilities (delay and stops) of through and left turn traffic at both UDC and SC intersections. They also reduce arterial through delay at UDC intersections and arterial stops of through and left turn traffic at SC intersections.

Overall, the set of models maximizing constant main bandwidth performs the worst among all three sets of models by increasing the most arterial disutilities of through traffic at UDC intersections and cross street disutilities of left turn traffic comparing with MAXBAND results. It also has the highest travel time in arterial through traffic and total

traffic. The set of models maximizing secondary bandwidth performs better by providing the smallest increase in arterial stops at UDC intersections. The set of models maximizing variable bandwidth but not secondary bandwidth performs the best by giving the largest reduction in average delay and travel time and the smallest increase in average stops on arterial comparing with MULTI-BAND results. The enhanced model maximizing variable main bandwidth and cross street delay (UDC_V in Table 3) has the best overall performance in this model set with large delay reduction and fewer stop increase and lowest arterial through travel time.

UDC control greatly increases the number of stops of arterial through traffic at UDC intersections under fixed timing operation. Fortunately however,, UDC control under actuated operation overcomes this drawback. Actuated UDC control is evaluated by applying results of the UDC model maximizing variable main bandwidth and minimal through delay on cross street at UDC intersections (UDC_V in Table 3) to coordinated-actuated simulation considering traffic variations. To adjust the volume to different percentile levels, the number of vehicles arriving in cycle on cross streets is assumed to follow Poisson distribution, The equivalent standard deviation of hourly volume is determined by applying the Poisson property that the variance equals the mean. Then the hourly volume is assumed to following the normal distribution for hourly volume percentile adjustment. For simplicity and the consideration of traffic input at access points between intersections, the volume adjustment of internal flows uses the same procedure as external flows. Compared to fixed timing operation at UDC intersections,

actuated UDC control results in greater delay reduction and much fewer through stops on the arterial. There are fewer early returns to green at UDC and SC intersections. Shorter queue lengths reduce the probability of lane blockage, which indirectly increases the capacity of permitted phases (RTOR rates on the same approach and permitted left turn on the opposing approach). Also, when there is increase in disutilities due to increase in traffic demand, UDC control scheme tends to deteriorate less than SC control.

Based upon the numerical experiments and case study, this study identifies the following advantages and disadvantages for UDC control.

- The UDC control scheme has the following advantages compared with SC control:
  - It can greatly reduce cross street through and left turn delay at UDC intersections and maintain a similar progression quality on the arterial under coordinated-actuated operation;
  - It can reduce arterial through delay at UDC intersections with a higher reduction rate under actuated operation than that under fixed timing operation;
  - It has more flexibility in phasing sequence which can provide the same or greater bandwidth compared with MAXBAND under certain scenarios;
  - The flexibility in phasing sequence can possibly be beneficial at SC intersections if the same movement can be serviced twice (e.g., northbound right turn movement in Figure 19);

- UDC intersections have shorter through queue lengths and thus fewer lane blockages and spillbacks which is beneficial for intersections with limited turning bay length and link length;
- Arterial through traffic discharged later in the cycle at UDC intersection may have fewer stops and less delay at the downstream SC intersection under fixed timing operation;
- It can increase the capacity of opposing arterial permitted left turn durations and RTOR duration on cross streets at a SC intersection downstream of a UDC intersection because of the increased gap in the arrival flows in the arterial off-peak direction;
- It reduces the impact of the early return to green problem at UDC intersections under actuated operation; and
- Signal operation performance deteriorates less when traffic demand increases.

- The UDC control scheme has the following disadvantages compared with SC control:
  - It can cause significant increase in arterial through stops under fixed timing;
  - It can reduce the capacity of opposing arterial left turn durations and RTOR duration on cross streets at a SC intersection downstream of a UDC intersection. This is because the reduction of unblocked portion of green time in the permitted phase due to the more spread out arrival flows in the arterial peak direction; and

- It can cause higher arterial through delay and stops at SC intersections under actuated operation due to less unused green time from cross street available for arterial coordination.

The research activities also lead to the following preliminary guidelines for the implementation of UDC control:

- Left turn factors indirectly impact the applicability of UDC control. Major-minor intersections with permitted left turn operation on cross streets and/or low left turn demand on the arterial are more likely to have beneficial UDC implementation;
- UDC control tends to be beneficial at intersections with much higher traffic demand on the arterial approaches than the cross street approaches;
- Long slack time (green times in excess of critical green times of through phases on arterial) is a good indicator of UDC applicability;
- UDC control is not recommended when two-way bandwidths under UDC control are smaller than that under SC control;
- The volume-to-capacity ratio might not be a good indicator for UDC application;
- Criteria listed in Table 5 might be considered for prechecking if UDC control would be beneficial at a candidate UDC intersection;
- *g-ratio* is suggested as the primary parameter for checking UDC applicability; *AtC* and *ArtLT* are suggested as the auxiliary parameters;

- When the slack time is longer than the minimum green time plus the per phase lost time, UDC control might be beneficial;
- The above suggestions are based upon limited data and analysis in this study and thus do not necessarily cover all traffic and geometric conditions where double cycling may or may not be beneficial.

FUTURE STUDY

There are limitations in this study, and further research is needed to fully explore the advantages of the UDC control scheme and to improve its optimization models for better results of field implementation.

The underlying assumptions of under-saturation and no blockage or spillback can be relaxed in further study to accommodate more realistic traffic and geometric conditions. The simplification of arrival flows in arterial delay estimation can be improved by considering platoon evolvement along the arterial. The modeling can also consider the impact of the changed arrival flow profiles at single cycled intersections to improve optimization results.

The control scheme allocates the slack green time to a sub-cycle to reduce delay at double cycled intersections. This may affect progression quality due to the reduced reliability of letting platoons pass through the double cycled intersection if large traffic variation is present. Therefore, an interesting research topic would be stochastic analysis

of traffic conditions to evaluate progression reliability of the control scheme and provide additional guidance for the application.

The proposed models do not directly optimize signal parameters for actuated operation, where the UDC control scheme is expected to be of more potential value. A practical solution would be incorporating HCM's method of determining actuated phase green time in the optimization model with stochastic traffic input.

Also, the models could be extended to the network level by adding the network loop function in the constraints. When protected left turn green time is long or if a short turning bay is presented, the model could be improved by providing the option of servicing left turn traffic twice as well.

Last but not the least, further investigation on the safety impacts and human factors of UDC control is recommended. UDC control increases the number of stops of some traffic which may increase the potential of rear-end collisions. The available green times for pedestrians are also reduced which may cause issues for pedestrians with low walking speeds. Before and after crash analysis of existing UDC intersections can be performed to address these concerns. Furthermore, drivers might confuse UDC control with SC control because of phasing changes and sub-green duration in a sub-cycle. For instance, left turns drivers waiting to depart at UDC intersections with a once serviced left turn may perceive the changes of through sub-green phases in a sub-cycle as skip

their left turn phases. Drivers in the shorter sub-green of through phases may feel they are not gaining enough queue discharge time. Public education may be needed for better public acceptance of the UDC control scheme.

REFERENCES

1. US Department of Transportation, Transportation in the United States: Highlights from 2015 Transportation Statistics Annual Report, http://www.rita.dot.gov/bts/publications/transportation_in_the_united_states_2015/performance, accessed January 2, 2016.

2. Kurfees, W. Using Uneven Double Cycles to Improve the Effectiveness of Arterial Traffic Signal Operations, Managing Congestion -- Can We Do Better? Institute of Traffic Engineer (ITE) 2007 Technical Conference and Exhibit, San Diego CA, March, 2007.

3. Urbanik, T., et al, *Signal Timing Manual, Second Edition*, NCHRP report 812, Transportation Research Board, Washington, D.C., 2015.

4. Federal Highway Administration (FHWA). *Manual on Uniform Traffic Control Devices*. FHWA, Washington, DC., 2009.

5. Lan, C. J. and C.J. Messer. Compromise Approach to Optimize Traffic Signal Coordination Problems during Unsaturated conditions, *Transportation Research Record, Journal of the Transportation Research Board*, No. 1360, Transportation Research Board of the National Academies, Washington, D.C., 1992, pp. 112-120.

6. Husch, D. and J. Albeck. *Trafficware Synchro 6.0, Traffic Simulation Software: User Guide*, Trafficware Corporation, Albay, CA, 2003.

7. Bowers, D.A. Progressive Timing for Traffic Signals, *Proceeding of Institute of Traffic Engineers*, 1947, pp. 93-100.

8. Brooks, W.D. Vehicular Traffic Control-Designing Arterial Progressions Using a Digital Computer, *Data Processing IBM*, 1965.

9. Messer, C. J., R.H. Whitson, C.L. Dudek, and E.J. Roman, A Variable Sequence Multiphase Progression Optimization Program, *Highway Research Record*, No. 445, 1973, pp. 24-33.

10. Morgan, J. T. and J.D.C. Little. Synchronizing Traffic Signals for Maximal Bandwidth, *Operations. Research*, Vol. 12, No. 6, December 1964, pp. 896–912.

11. Little, J.D.C. The Synchronization of Traffic Signals by Mixed-Integer Linear Programming. *Operations Research*, Vo. 14, 1966, pp.568-594.

12. Little, J.D.C., M.D. Kelson, and N.H. Gartner. MAXBAND: A Program for Setting Signals on Arteries and Triangular Networks. *Transportation Research Record*: *Journal of the Transportation Research Board*, No. 795, Transportation Research Board of the National Academies, Washington, D.C., 1981, pp. 40-46.

13. Chang E. C. P. et al. MAXBAND 86-Program for Optimizing Left Turn Phase Sequence in Multi-arterial Closed Networks, *Transportation Research Record*: *Journal of the Transportation Research Board*, No. 1181, Transportation Research Board of the National Academies, Washington, D.C., 1988, pp. 61-67.

14. Chaudhary, N.A., A. Pinnoi, and C.J. Messer. Proposed Enhancements to MAXBAND 86 Program. *Transportation Research Record*: *Journal of the Transportation Research Board*, No. 1324, Transportation Research Board of the National Academies, Washington, D.C., 1991, pp. 98-104.

15. Gartner, N. H., S.F. Assman, F. Lasaga, and D.L. Hou. A Multi-Band Approach to Arterial Traffic Signal Optimization, *Transportation Research Part B: Methodological*, Vol. 25,
No. 1, 1991, pp. 55-74.

16. Sripathi, H.K., N.H. Gartner, and C. Stamatiadis. Uniform and Variable Bandwidth Arterial Progression Schemes, *Transportation Research Record*: *Journal of the Transportation Research Board*, No. 1494, Transportation Research Board of the National Academies, Washington, D.C., 1995, pp. 135-145.

17. Stamastiadis, C. and N.H. Gartner. MULTI-BAND-96: A Program for Variable-Bandwidth Progression Optimization of Multiarterial Traffic Networks, *Transportation Research Record*: *Journal of the Transportation Research Board*, No. 1554, Transportation Research Board of the National Academies, Washington, D.C., 1996, pp. 9-17.

18. Chaudhary, N.A., A. Pinnoi, and C.J. Messer. Scheme to Optimize Circular Phasing Sequences, *Transportation Research Record*: *Journal of the Transportation Research Board*, No. 1324, Transportation Research Board of the National Academies, Washington, D.C., 1991, pp. 72-82.

19. Tian, Z. and V. Mangal. Effectiveness of Lead-Lag Phasing on Progression Bandwidth, Presented at 87th Annual Meeting of the Transportation Research Board, Washington, D.C., 2008

20. Tian, Z. and T. Urbanik. System Partition Technique to Improve Signal Coordination and Traffic Progression, *Journal of Transportation Engineering, ASCE*, Vol. 133, No. 2, January. 2007, pp. 119-128.

21. Euler, G.W. Traffic Signal Optimization: Achieving National Objectives through State and Local Government Actions, *Institute of Transportation Engineer (ITE) Journal*, Vol. 54, No. 9, 1983, pp. 14-17.

22. Wallace, C. E., K.G. Courage, D.P. Reaves, G.W. Schoene, and G.W. Euler, *TRANSYT-7F User's Manual,* Federal Highway Administration, Washington, D.C., 1984.

23. Sabra, Z., C.E. Wallace, and F. Lin. Traffic Analysis Software Tools, Transportation Research Board, National Research Council, September, 2000.

24. Hook, D. and A. Albers, *Comparison of Alternative Methodologies to Determine Breakpoints in Signal Progression*, 1999, http://trafficware.infopop.cc/downloads/00029.pdf, accessed June 25, 2015.

25. Wallace, C.E. and K.G. Courage. Arterial Progression, New Design Approach, *Transportation Research Record: Journal of the Transportation Research Board*, No. 881, Transportation Research Board of the National Academies, Washington, D.C., 1982, pp. 53-59.

26. Cohen, S. L., Concurrent Use of MAXBAND and TRANSYT Signal Timing Programs for Arterial Signal Optimization. *Transportation Research Record: Journal of the Transportation Research Board*, No. 906, Transportation Research Board of the National Academies, Washington, D.C., 1983, pp. 81-84.

27. Skabardonis, A. and A.D. May. Comparative analysis of computer models for arterial signal timing, *Transportation Research Record: Journal of the Transportation Research Board*, No. 1021, Transportation Research Board of the National Academies, Washington, D.C., 1985, pp. 45-52.

28. Cohen, S. L. and C.C. Liu. The bandwidth-constrained TRANSYT signal-optimization program. *Transportation Research Record: Journal of the Transportation Research Board*, No. 1057, Transportation Research Board of the National Academies, Washington, D.C., 1986, pp. 1-7.

29. Liu, C.C. Bandwidth-Constrained Delay Optimization for Signal Systems, *Institute of Traffic Engineer (ITE) Journal*, Vol. 58, No. 12, 1988, pp. 21-26.

30. Tsay, H. S. and L.T. Lin (1988) New algorithm for solving the maximum progression bandwidth. *Transportation Research Record: Journal of the Transportation Research Board*, No. 1194, Transportation Research Board of the National Academies, Washington, D.C., 1988, pp. 15-30.

31 Lin, L.T., L.W. Tung, and H.C. Ku. Synchronized Signal Control Model for Maximizing Progression along an Arterial, *ASCE, Journal of Transportation Engineering*, Vol. 136, No. 8, August 1, 2010.

32. McTrans. *Traffic Network Study Tool, Transyt-7F*, United States Version, May 11, 2011, http://mctrans.ce.ufl.edu/featured/transyt-7f/, accessed November 11, 2012.

33. Webster, F.V. *Traffic Signal Settings*, Road Research Technical Paper 39, U.K. Department of Scientific and Industrial Research, Road Research Laboratory, Crowthorne, Berkshire, England, 1958.

34. Miller, A.J. Settings for fixed-cycle traffic signals. *Operational Research Quarterly*, Vol. 14, No. 4, December 1963, pp. 373-386.

35. Newell, G.F. Approximation Methods for Queues with Application to the Fixed−cycle Traffic Light. *SIAM Review*, Vol. 7, No. 2, 1965, pp. 223-240.

36. Kimber, R. and E. Hollis. *Traffic Queues and Delay at Road Junctions*, Technical report, TRRL Laboratory Report No. 909. Transport and Road Research Laboratory, Berkshire, U.K., 1979.

37. Akcelik, R. *Traffic signals: Capacity and Timing Analysis*, Technical report, ARR No.123. Australian Road Research Board, Kew, Victoria, Australia, 1981.

38. Transportation Research Board, *Highway Capacity Manual*, *5th Edition* (HCM 2010), Transportation Research Board of the National Academies, 2010.

39. Daganzo, C. F. The Cell Transmission Model: A Dynamic Representation of Highway Traffic Consistent with the Hydrodynamic Theory, *Transportation Research, Part B*, Vol. 28, 1994, pp. 269-287.

40. Daganzo, C. F. The Cell Transmission Model, Part II: Network Traffic. *Transportation Research, Part B*, Vol. 29, 1995, pp. 79-93.

41. Lighthill, M.J. and J. B. Whitham. On kinematic waves. I: Flow movement in long rivers; II: A theory of traffic flow on long crowded roads. *Proceeding of Royal Society A*, Vol. 229, 1955, pp. 281-345.

42. Richards, P.I. Shockwaves on the highway, *Operations Research*, Vol. 4, 1956, pp. 42-51.

43. Lo, H.K. A novel traffic control formulation, *Transportation Research A*, Vol. 33, 1999, pp. 433-448.

44. Lo, H.K. A Cell-Based Traffic Control Formulation: Strategies and Benefits of Dynamic Timing Plans, *Transportation Science*, Vol. 35, No. 2, 2001, pp.148-164.

45. Zhang, Y. and R. Lou. Signal Timing for Arterials under Day-to-day Demand Variations, *Transportation Research Record: Journal of the Transportation Research Board*, No. 2192, Transportation Research Board of the National Academies, Washington, D.C., 2010, pp. 156-166.

46. Lo, H., E. Chang, and Y. C. Chan. Dynamic Network Traffic Control. *Transportation Research, Part A*, Vol. 35, 2001, pp. 721-744.

47. Pacey, G. M. *The Progress of a Bunch of Vehicles Released from a Traffic Signal*, Research Note Rn/2665/GMP. Road Research Laboratory, London, 1956.

48. Robertson, D.I. *TRANSYT: A Traffic Network Study Tool*, Road Research Laboratory Report LR 253, Road Research Laboratory, Crowthorne, United Kingdom, 1969.

49. Geroliminis, N., A. Skabardonis. Prediction of arrival profiles and queue lengths along signalized arterials by using a Markov decision process, *Transportation Research Record: Journal of the Transportation Research Board*, Transportation Research Board of the National Academies, Washington, D.C., Vol. 1934, 2005, pp. 116-124.

50. Rouphail, N.M., K.G. Courage, and D.W. Strong. New calculation method for existing and extended Highway Capacity Manual delay estimation procedure. Presented at 85th Annual Meeting of the Transportation Research Board, Washington, D.C., 2006.

51. Strong, D.W. and N.M. Rouphail. Incorporating effects of traffic signal progression into proposed incremental queue accumulation method. Presented at 85th Annual Meeting of the Transportation Research Board, Washington, D.C., 2006.

52. May, A. *Traffic Flow Fundamentals*, Englewood Cliffs, N.J. Prentice Hall, 1990

53. Akcelik, R., M. Besley, and R. Roper. *Fundamental Relationships for Traffic Flows at Signalised Intersections*. Research Report ARR 340. ARRB Transport Research Ltd, Vermont South, Australia, 1999.

54. Hung, W.T., F. Tian, and H.Y. Tong. Discharge headway at signalized intersections in Hong Kong, *Journal of Advanced Transportation*, Vol. 37, No. 1, 2003, pp. 105-117.

55. Jiang, Y., S. Li, and D. Shamo. A platoon-based traffic signal timing algorithm for major-minor intersection types, *Transportation Research Part B: Methodological*, Vol. 40, 2006, pp. 543-562.

56. McTrans, *TSIS-CORSIM: Traffic Software Integrated System-Corridor Simulation*. http://mctrans.ce.ufl.edu/featured/tsis/, accessed January, 2015.

57. PTV Traffic Mobility Logistic, *VISSIM 5.30-05 User Manual*, PTV Planung Transport, Verkhr AG, 2011.

58. MathWorks, *MATLAB Documentation: Genetic Algorithm*, 2012 http://www.mathworks.com/help/gads/ga.html, accessed November 2, 2014.

59. IBM, *IBM ILOG CPLEX Optimization Studio V12.6.0 documentation*, October 1, 2013, http://pic.dhe.ibm.com/infocenter/cosinfoc/v12r6/index.jsp, accessed November 10, 2013.

60. Bliek, C. and P. Bonami. IBM CPLEX Global Non-Convex MIQP, INFORMS Annual Meeting, October 6-9, 2013 Minneapolis, Minnesota, 2013.

61. Husch, D. and J. Albeck. *Trafficware SimTraffic 6.0 Traffic Simulation Software: User Guide*, Trafficware Corporation, Albay, CA, 2003.

APPENDIX I

LISTS OF NOTATIONS

INDICES

i = intersection ID, $i = 1, 2, 3...N$;

j = approach ID, $j = 1, 2...4$;

ja = arterial approach ID, 1 for outbound, 2 for inbound;

jc = cross street approach ID, 3 for outbound, 4 for inbound;

s = single cycled intersection ID, $s = 1, 2, 3...Ns$

u = double-cycled intersection ID, $u = 1, 2, 3...Nu$

PARAMETERS

$\beta_i^a (\beta_i^c)$ = 0-1 parameter for protected or permitted-only left turn on arterial (cross streets) at intersection *i*;

λ^B = weight of the normalized bandwidth objective in the objective function;

λ^{SB} = weight of the normalized secondary bandwidth objective in the objective function;

$\tau_{i,ja}$ = queue clearance time in advance of the outbound (inbound) bandwidth at intersection *i*;

$\tau_{u,ja}^{SB}$ = queue clearance time in advance of the outbound (inbound) secondary bandwidth at intersection *u*;

$AD_{\max}^{Ta}$ = total average delay of through traffic on arterial of UDC intersection if with SC control;

$AD_{\max}^{Tc}$ = total average delay of through traffic on cross streets of UDC intersection if with SC control;

$AS_{\max}^{Ta}$ = hypothetical maximum average number of stops of arterial through traffic of UDC

intersection;

$a_{i,ja}$ =weight of variable bandwidth in *ja* direction on the link *i;*

$a^{SB}_{u,ja}$ =weight of secondary bandwidth in *ja* direction on the link *u;*

$BW_{\max}$ = weighted sum of directional maximum greens possibly available for band passage;

$BW^{SB}_{\max}$ = weighted sum of two-way maximum greens possibly available for secondary band passage on link *u*;

$BW^{VB}_{\max}$ = weighted sum of two-way maximum greens possibly available for variable band passage on link *i*;

$d_{i,ja}$ = outbound (inbound) distance between intersection *i* (*i*+1) and intersection *i*+1 (*i*);

$e_{i,ja}$ = lower limit on outbound (inbound) speed on link between intersection *i* (*i*+1) and intersection *i*+1 (*i*);

$f_{i,ja}$ = upper limit on outbound (inbound) speed on link between intersection *i* (*i*+1) and intersection *i*+1 (*i*);

$g^{d}_{i,j}$ = total through green splits on approach *j* at intersection *i* if UDC;

$g^{l\max}_{i,ja}$ = maximum available green time for green band passage on link *i* in the *ja* direction;

$g^{\max}_{ja}$ = maximum available green time for green band passage on the arterial in the *ja* direction;

$g^{\max}_{i,ja}$ = maximum available green time for green band passage at intersection *i* in the *ja* direction;

$g^{\min}_{i,j}$ = minimal through green split on approach *j* at intersection *i*;

$g^{ped}_{u,j}$ = pedestrian phase time on approach *j* at intersection *u*;

$g^{s}_{i,j}$ = through green splits on approach *j* at intersection *i* if single cycled;

$1/h_{i,ja}$ = lower limit on outbound (inbound) reciprocal speed change between adjacent intersections *i* and *i*+1;

k = inbound to outbound target bandwidth ratio for constant main bandwidth optimization;

k_i = inbound to outbound target bandwidth ratio on link *i* for variable main bandwidth optimization;

k_u^{SB} = inbound to outbound target bandwidth ratio on link *u* for variable secondary bandwidth optimization;

$l_{i,j}$ =effective left turn split on approach *j* at intersection *i*;

$L_{i,j}$ =effective left turn split plus per-phase lost time on approach *j* at intersection *i*;

N = number of intersections along the arterial;

Ns = number of single cycled intersections along the arterial;

Nu = number of UDC intersections along the arterial;

$1/o_{i,ja}$ = lower limit on outbound (inbound) reciprocal change between adjacent intersections *i* and *i*+1;

$R_{i,ja}^{P}$ = Platoon ratio on approach *ja* at intersection *i;*

$s_{u,ja}$ = saturation flow of approach *ja* at intersection *i;*

$s_{i,ja}^{l}$ = saturation flow on link *i* in the *ja* direction*;*

$v_{u,ja}^{g1}$ = through arrival volume of the first sub-green phase on approach *ja* at intersection *u;*

$v_{u,ja}^{g2}$ = through arrival volume of the second sub-green phase on approach *ja* at intersection *u;*

$v_{i,ja}^{Tcd}$ = through arrival volume of coordinated phase on approach *ja* at intersection *i;*

$v_{i,ja}^{Tuc}$ = through arrival volume of uncoordinated phase on approach *ja* at intersection *i;*

$v_{i,ja}^{T}$ = through volume on approach *ja* at intersection *i;*

Y = per phase lost time;

$y_{i,j}^{T}$ = v/s ratio for through movement on approach *j* at intersection *i*;

z = inverse of background cycle length.

DECISION VARIABLES

$\alpha_{u,j}^{I1}$ = 0-1 variable for replacing the absolute function for approach *j* at intersection *u*,

$\alpha_{u,ja}^{I2}$ = 0-1 variable for replacing the product function for approach *ja* at intersection *u*,

Δ_i = time from the center of $r_{i,2}^N$ to the nearest center of $r_{i,1}^N$; positive if $r_{i,1}^N$ center is on the right;

$\delta_{i,j}$ = 0-1 decision variable for lagging (1) or leading (0) left turn pattern on approach j at intersection *i*;

$\theta_{u,j}$ = 0-1 variable for selecting the first sub-cycle for protected left turn on approach *j* at intersection *u*;

$\lambda_{u,j}^{D1}$ = 0-1 variable for disjunctive constraint related to $\alpha_{u,j}^{I1}$ for approach *j* at intersection *u;*

$\lambda_{u,j}^{D2}$ = 0-1 variable for disjunctive constraint related to $\alpha_{u,ja}^{I2}$ for approach *j* at intersection *u;*

λ_u^{D3} = 0-1 variable for disjunctive constraint related to selecting inbound sub-green for band passage at intersection *u;*

λ_u^{D4} = 0-1 variable for disjunctive constraint related to selecting sub-green for pedestrian phase at intersection *u;*

b_{ja} = outbound (inbound) bandwidth of constant bandwidth objective;

$b_{i,ja}$ = outbound (inbound) bandwidth of variable bandwidth objective on link *i*;

$b_{u,ja}^{SB}$ = outbound (inbound) secondary bandwidth of on link *u*;

$g1_{u,j}$ = sub-green split in the first sub-cycle for through movement on approach *j* at intersection *u*;

$g2_{u,j}$ = sub-green split in the second sub-cycle for through movement on approach *j* at intersection *u*;

m_i = an integer number for constant and variable main bandwidth optimization at intersection *i*;

m_u^{SB} = an integer number for variable secondary bandwidth optimization at intersection *u*;

$r1_{u,j}$ = sub-red split in the first sub-cycle for through movement on approach *j* at intersection *u*;

$r2_{u,j}$ = sub-red split in the second sub-cycle for through movement on approach *j* at UDC intersection u;

$r_{i,ja}^{N}$ = arterial nominal red split on approach ja at intersection *i*;

r_{u}^{SB} = sub-red phase split on the right side of the inbound secondary bandwidth on at intersection *u*;

$t_{i,ja}$ = arterial outbound (inbound) travel time from intersection *i* (*i*+1) to intersection *i*+1 (*i*);

$t1_{u,j}$ = actual through queue discharge time in the first sub-cycle on approach *j* at intersection *u*;

$t2_{u,ja}$ = actual through queue discharge time in the second sub-cycle on approach *ja* at intersection *u*;

$w_{i,ja}$ = time from right (left) side of red at intersection *i* to left (right) edge of outbound (inbound) green band;

$w_{i,ja}^{VB}$ = time from right (left) side of red at intersection *i* to the centerline of outbound (inbound) green band for variable main bandwidth objective;

w_{iuja}^{SB} = time from right (left) side of red at intersection *i* to the centerline of outbound (inbound) secondary band for variable secondary bandwidth objective;

INTERIM VARIABLES

$AD_{u,ja}^{Ta}$ = average delay of arterial through traffic at intersection *u* on approach *ja*;

AD^{Ta} = weighted total average delay of arterial through traffic at intersections before normalization;

AD_{n}^{Ta} = normalized total average delay of arterial through traffic on cross streets at intersections;

$AD_{u,jc}^{Tc}$ = average uniform delay of cross street through traffic at intersection *u* on approach *jc*;

AD^{Tc} = weighted total average delay of cross street through traffic at intersections before normalization;

AD_{n}^{Tc} = normalized total average delay of cross street through traffic at intersections;

BW_n = normalized objective of constant main bandwidths;

BW_n^{VB} = normalized objective of variable main bandwidths;

BW_n^{SB} = normalized objective of secondary bandwidths;

$R1_{u,ja}$ = total phase splits in the first sub-cycle on approach ja at UDC intersection u;

$R2_{u,ja}$ = total phase splits in the second sub-cycle on approach ja at UDC intersection u;

APPENDIX II

SIMULATION RESULTS WITH FIXED TIMING

Table A1. Simulation results of through delay (sec/veh) with fixed timing

	Arterial			Cross streets		
	All	UDC	SC	All	UDC	SC
Base models with single cycling						
MAXBAND	25.99	10.87	47.68	66.39	40.44	67.63
MULTIBAND	23.42	9.83	42.97	66.13	41.55	67.30
Improved basic UDC models						
UDCo	26.64	12.01	47.51	59.55	23.13	61.28
UDC_D	29.29	10.21	44.93	59.28	15.46	61.03
UDC_DS	25.58	11.97	44.93	59.23	21.24	61.03
UDC models enhanced with variable bandwidth optimization						
UDC_V	23.16	9.29	43.07	58.69	24.67	60.29
UDC_VD	23.40	9.22	43.83	60.36	23.61	62.09
UDC_VDS	23.43	9.22	43.89	58.54	23.51	60.19
UDC models enhanced with variable and secondary bandwidth optimization						
UDC_SV	23.92	9.50	44.65	59.98	23.21	61.70
UDC_SVD	24.40	9.61	45.65	57.44	22.84	59.06
UDC_SVDS	24.43	9.19	46.29	59.00	23.16	60.68

Table A2. Simulation results of reduction in through delay (%) with fixed timing

	Arterial			Cross streets		
	All	UDC	SC	All	UDC	SC
Improved basic UDC models vs MAXBAND model						
UDCo	-2.5*	-10.6	0.3	10.3	42.8	9.4
UDC_D	-12.7	6.1	5.8	10.7	61.8	9.8
UDC_DS	1.6	-10.2	5.8	10.8	47.5	9.8
UDC models enhanced with variable bandwidth optimization vs MULTI-BAND model						
UDC_V	1.1	5.5	-0.2	11.3	40.6	10.4
UDC_VD	0.1	6.2	-2.0	8.7	43.2	7.8
UDC_VDS	0.0	6.2	-2.2	11.5	43.4	10.6
UDC models enhanced with variable and secondary bandwidth optimization vs MULTI-BAND model						
UDC_SV	-2.1	3.4	-3.9	9.3	44.1	8.3
UDC_SVD	-4.2	2.3	-6.2	13.1	45.0	12.2
UDC_SVDS	-4.3	6.5	-7.7	10.8	44.3	9.8

Note:* negative figure indicates increase in disutilities

Table A3. Simulation results of left turn delay (sec/veh) with fixed timing

	Arterial			Cross streets		
	All	UDC	SC	All	UDC	SC
Base models with single cycling						
MAXBAND	48.15	24.41	52.01	105.00	58.57	117.20
MULTIBAND	45.29	25.08	48.58	127.75	63.77	144.60
Improved basic UDC models						
UDCo	47.20	17.98	51.93	102.89	33.50	121.88
UDC_D	22.90	14.69	50.83	110.72	21.83	136.22
UDC_DS	46.42	19.62	50.83	114.46	34.82	136.22
UDC models enhanced with variable bandwidth optimization						
UDC_V	48.23	23.58	52.39	116.16	36.41	137.61
UDC_VD	47.28	25.10	51.03	97.68	35.03	114.13
UDC_VDS	50.56	26.65	54.58	113.10	33.87	134.25
UDC models enhanced with variable and secondary bandwidth optimization						
UDC_SV	48.94	20.87	53.68	123.64	36.63	147.12
UDC_SVD	57.14	27.35	62.25	108.76	34.66	128.54
UDC_SVDS	56.69	26.75	61.76	116.92	31.71	139.84

Table A4. Simulation results of reduction in left turn delay (%) with fixed timing

	Arterial			Cross streets		
	All	UDC	SC	All	UDC	SC
Improved basic UDC models vs MAXBAND model						
UDCo	2.0	26.4	0.2	2.0	42.8	-4.0*
UDC_D	52.4	39.8	2.3	-5.4	62.7	-16.2
UDC_DS	3.6	19.6	2.3	-9.0	40.5	-16.2
UDC models enhanced with variable bandwidth optimization vs MULTI-BAND model						
UDC_V	-6.5	6.0	-7.8	9.1	42.9	4.8
UDC_VD	-4.4	-0.1	-5.0	23.5	45.1	21.1
UDC_VDS	-11.6	-6.3	-12.3	11.5	46.9	7.2
UDC models enhanced with variable and secondary bandwidth optimization vs MULTI-BAND model						
UDC_SV	-8.0	16.8	-10.5	3.2	42.6	-1.7
UDC_SVD	-26.2	-9.0	-28.1	14.9	45.6	11.1
UDC_SVDS	-25.2	-6.7	-27.1	8.5	50.3	3.3

Note:* negative figure indicates increase in disutilities

Table A5. Simulation results of through stops (stops/veh) with fixed timing

	Arterial			Cross streets		
	All	UDC	SC	All	UDC	SC
Base models with single cycling						
MAXBAND	0.38	0.16	0.69	0.92	0.70	0.93
MULTIBAND	0.34	0.15	0.61	0.92	0.74	0.93
Improved basic UDC models						
UDCo	0.42	0.26	0.64	0.84	0.77	0.84
UDC_D	0.49	0.31	0.63	0.84	0.78	0.84
UDC_DS	0.42	0.28	0.63	0.84	0.71	0.84
UDC models enhanced with variable bandwidth optimization						
UDC_V	0.38	0.23	0.58	0.84	0.70	0.84
UDC_VD	0.38	0.23	0.60	0.85	0.68	0.86
UDC_VDS	0.38	0.23	0.59	0.84	0.70	0.85
UDC models enhanced with variable and secondary bandwidth optimization						
UDC_SV	0.38	0.23	0.61	0.85	0.66	0.86
UDC_SVD	0.40	0.25	0.62	0.83	0.70	0.83
UDC_SVDS	0.38	0.22	0.61	0.84	0.68	0.85

Table A6. Simulation results of reduction in through stops (%) with fixed timing

t	Arterial			Cross streets		
	All	UDC	SC	All	UDC	SC
Improved basic UDC models vs MAXBAND model						
UDCo	-9.9*	-61.7	8.1	9.4	-9.8	10.1
UDC_D	-28.5	-90.7	8.6	9.0	-11.4	9.8
UDC_DS	-11.7	-69.8	8.6	9.3	-1.7	9.8
UDC models enhanced with variable bandwidth optimization vs MULTI-BAND model						
UDC_V	-10.6	-57.6	4.6	9.4	5.1	9.6
UDC_VD	-12.1	-55.5	1.7	7.8	7.7	7.8
UDC_VDS	-11.6	-56.0	2.7	9.2	5.1	9.3
UDC models enhanced with variable and secondary bandwidth optimization vs MULTI-BAND model						
UDC_SV	-12.5	-53.7	0.7	8.3	10.3	8.2
UDC_SVD	-16.9	-66.6	-0.8	10.7	5.1	10.9
UDC_SVDS	-11.9	-49.9	0.2	9.0	7.7	9.1

Note:* negative figure indicates increase in disutilities

Table A7. Simulation results of left turn stops (stops/veh) with fixed timing

	Arterial			Cross streets		
	All	UDC	SC	All	UDC	SC
Base models with single cycling						
MAXBAND	0.92	0.63	0.97	1.30	0.83	1.42
MULTIBAND	0.85	0.67	0.88	1.49	0.86	1.66
Improved basic UDC models						
UDCo	0.88	0.70	0.90	1.32	0.81	1.46
UDC_D	0.40	0.25	0.91	1.39	0.74	1.58
UDC_DS	0.88	0.74	0.91	1.43	0.90	1.58
UDC models enhanced with variable bandwidth optimization						
UDC_V	0.78	0.65	0.80	1.46	0.83	1.63
UDC_VD	0.75	0.62	0.78	1.31	0.83	1.43
UDC_VDS	0.80	0.69	0.81	1.43	0.85	1.58
UDC models enhanced with variable and secondary bandwidth optimization						
UDC_SV	0.74	0.55	0.77	1.49	0.81	1.67
UDC_SVD	0.78	0.73	0.79	1.38	0.87	1.52
UDC_SVDS	0.82	0.62	0.86	1.47	0.85	1.64

Table A8. Simulation results of reduction in left turn stops (%) with fixed timing

t	Arterial			Cross streets		
	All	UDC	SC	All	UDC	SC
Improved basic UDC models vs MAXBAND model						
UDCo	5.0	-11.8	6.8	-1.6	2.0	-2.5
UDC_D	56.6	60.1	6.3	-7.3	10.3	-11.1
UDC_DS	4.1	-17.6	6.3	-10.4	-8.7	-11.1
UDC models enhanced with variable bandwidth optimization vs MULTI-BAND model						
UDC_V	8.0	1.8	8.6	2.2	3.4	1.9
UDC_VD	11.4	7.3	11.8	12.5	3.4	13.8
UDC_VDS	6.3	-3.6	7.5	4.3	1.0	4.6
UDC models enhanced with variable and secondary bandwidth optimization vs MULTI-BAND model						
UDC_SV	13.3	18.2	12.5	0.3	5.7	-0.7
UDC_SVD	8.6	-9.1	10.7	7.4	-1.3	8.5
UDC_SVDS	3.4	7.3	2.7	1.7	1.0	1.5

Note: *negative figure indicates increase in disutilities

Table A9. Simulation results of travel times with fixed timing

	Travel times (hr)		Reduction (%)	
	Arterial Through	Total Traffic	Arterial Through	Total Traffic
Base models with single cycling				
MAXBAND	25.7	106.1	-	-
MULTIBAND	24	104.8	-	-
Improved basic UDC models				
UDCo	25.5	103.2	-0.8*	-2.7
UDC_D	24.9	103.4	-3.1	-2.5
UDC_DS	24.9	103.4	-3.1	-2.5
UDC models enhanced with variable bandwidth optimization				
UDC_V	23.7	101.7	-1.2	-3.0
UDC_VD	24	101.2	0.0	-3.4
UDC_VDS	23.9	102	-0.4	-2.7
UDC models enhanced with variable and secondary bandwidth optimization				
UDC_SV	24.1	103	0.4	-1.7
UDC_SVD	24.9	102.8	3.8	-1.9
UDC_SVDS	24.3	103.2	1.3	-1.5

Note: *negative figure indicates increase in disutilities

APPENDIX III

SIMULATION RESULTS WITH ACTUATED TIMING

Table A10. Simulation results of through delay (sec/veh) with actuated timing

%tile Volume	Arterial			Cross streets		
	All	UDC	SC	All	UDC	SC
			MULTIBAND			
10	16.8	4.0	35.0	64.9	69.6	64.8
30	17.9	4.4	37.8	96.3	64.7	97.2
50	26.4	5.3	56.4	82.2	71.8	82.6
70	21.1	5.6	43.3	94.4	68.0	95.2
90	25.8	6.6	53.4	111.5	56.4	114.0
			UDC_V			
10	17.8	3.8	37.6	65.9	53.7	66.2
30	20.3	3.9	44.1	94.0	49.6	95.3
50	26.9	4.7	58.5	82.1	46.3	83.4
70	22.8	4.6	48.8	94.0	48.9	95.4
90	26.7	5.7	56.6	108.8	45.0	111.7

Table A11. Results of reduction in through delay (%) with actuated timing

%tile Volume	Arterial			Cross streets		
	All	UDC	SC	All	UDC	SC
10	-6.0*	4.5	-7.3	-1.4	22.9	-2.2
30	-13.0	10.2	-16.8	2.4	23.3	2.0
50	-2.1	11.0	-3.6	0.2	35.5	-0.9
70	-8.0	18.3	-12.8	0.4	28.1	-0.2
90	-3.5	12.5	-6.1	2.4	20.2	2.0

Note: *negative figure indicates increase in disutilities

Table A12. Simulation results of left turn delay (sec/veh) with actuated timing

%tile Volume	Arterial			Cross streets		
	All	UDC	SC	All	UDC	SC
			MULTIBAND			
10	42.0	13.6	48.8	131.1	68.4	148.1
30	48.2	16.4	55.9	135.6	68.1	153.2
50	59.0	20.8	69.5	173.9	71.2	205.0
70	50.3	20.3	58.7	179.2	69.6	217.1
90	59.2	22.3	69.9	160.2	81.2	184.8
			UDC_V			
10	44.7	12.7	52.3	134.6	57.7	155.6
30	47.1	13.8	55.2	135.8	58.0	156.1
50	54.9	21.3	64.1	184.5	59.5	222.6
70	50.4	23.8	57.9	162.1	57.6	198.1
90	53.3	15.4	64.4	151.0	71.8	175.7

Table A13. Results of reduction in left turn delay (%) with actuated timing

%tile Volume	Arterial			Cross streets		
	All	UDC	SC	All	UDC	SC
10	-6.4*	6.8	-7.1	-2.7	15.6	-5.1
30	2.2	15.8	1.3	-0.1	14.9	-1.9
50	7.1	-2.4	7.8	-6.1	16.5	-8.6
70	-0.3	-17.1	1.4	9.5	17.3	8.8
90	10.0	31.2	7.9	5.8	11.6	4.9

Note: *negative figure indicates increase in disutilities

Table A14. Simulation results of through stops (stops/veh) with actuated timing

%tile Volume	Arterial			Cross streets		
	All	UDC	SC	All	UDC	SC
			MULTIBAND			
10	0.28	0.07	0.57	0.89	0.83	0.89
30	0.29	0.08	0.60	1.18	0.83	1.19
50	0.39	0.11	0.80	1.06	0.86	1.06
70	0.34	0.11	0.66	1.17	0.85	1.18
90	0.39	0.13	0.76	1.33	0.80	1.36
			UDC_V			
10	0.30	0.08	0.61	0.90	0.87	0.90
30	0.31	0.07	0.67	1.17	0.87	1.18
50	0.39	0.11	0.80	1.07	0.85	1.08
70	0.37	0.11	0.73	1.17	0.89	1.18
90	0.39	0.13	0.76	1.33	0.95	1.34

Table A15. Results of reduction in through stops (%) with actuated timing

%tile Volume	Arterial			Cross streets		
	All	UDC	SC	All	UDC	SC
10	-6.4*	6.8	-7.1	-2.7	15.6	-5.1
30	2.2	15.8	1.3	-0.1	14.9	-1.9
50	7.1	-2.4	7.8	-6.1	16.5	-8.6
70	-0.3	-17.1	1.4	9.5	17.3	8.8
90	10.0	31.2	7.9	5.8	11.6	4.9

Note: *negative figure indicates increase in disutilities

Table A16. Simulation results of left turn stops (stops /veh) with actuated timing

%tile Volume	Arterial			Cross streets		
	All	UDC	SC	All	UDC	SC
			MULTI-BAND			
10	0.82	0.62	0.87	1.56	0.96	1.72
30	0.84	0.62	0.90	1.60	0.97	1.77
50	1.03	0.70	1.12	1.89	0.96	2.18
70	0.91	0.62	0.99	1.90	0.99	2.21
90	0.97	0.65	1.07	1.77	0.96	2.02
			UDC_V			
10	0.91	0.60	0.98	1.66	1.04	1.83
30	0.88	0.55	0.96	1.57	1.03	1.71
50	1.01	0.63	1.12	1.96	1.02	2.24
70	0.97	0.68	1.05	1.87	0.98	2.18
90	0.97	0.63	1.08	1.74	1.07	1.95

Table A17. Results of reduction in left turn stops (%) with actuated timing

%tile Volume	Arterial			Cross streets		
	All	UDC	SC	All	UDC	SC
10	-10.0*	2.7	-12.1	-6.7	-7.3	-6.6
30	-4.4	10.7	-6.9	2.2	-6.2	3.3
50	1.4	10.8	-0.3	-3.4	-6.9	-3.1
70	-6.2	-8.8	-5.7	1.5	0.6	1.7
90	-0.4	3.5	-1.2	1.4	-12.1	3.4

Note: *negative figure indicates increase in disutilities

Table A18. Simulation results of total delay (sec /veh) with actuated timing

%tile Volume	UDC Intersection			SC Intersection		
	All	Art.	Crst	All	Art.	Crst
MULTI-BAND						
10	8.4	4.3	51.5	56.1	36.0	71.0
30	8.6	4.7	47.7	74.6	39.4	99.6
50	10.6	5.8	54.9	77.3	57.0	92.8
70	10.9	6.1	51.9	79.1	44.2	104.6
90	12.4	7.1	54.7	89.4	54.2	115.7
UDC_V						
10	7.3	4.1	41.7	58.3	38.6	73.0
30	7.4	4.2	39.0	75.7	44.4	97.9
50	8.8	5.2	40.6	79.1	57.6	95.3
70	8.8	5.2	40.1	79.6	48.8	102.0
90	10.3	6.1	44.1	88.1	56.1	111.9

Table A19. Results of reduction in total delay (%) with actuated timing

%tile Volume	UDC Intersection			SC Intersection		
	All	Art.	Crst	All	Art.	Crst
10	12.5	4.6	19.2	-4.0	-7.3	-2.8
30	13.4	10.2	18.2	-1.5	-12.8	1.8
50	17.5	9.6	26.1	-2.3	-1.1	-2.7
70	18.8	14.0	22.8	-0.7	-10.4	2.4
90	17.3	14.2	19.5	1.5	-3.5	3.2

Note: *negative figure indicates increase in disutilities

Table A20. Simulation results of total stops (stops /veh) with actuated timing

%tile Volume	Arterial			Cross streets		
	All	UDC	SC	All	UDC	SC
MULTI-BAND						
10	0.82	0.62	0.87	1.56	0.96	1.72
30	0.84	0.62	0.90	1.60	0.97	1.77
50	1.03	0.70	1.12	1.89	0.96	2.18
70	0.91	0.62	0.99	1.90	0.99	2.21
90	0.97	0.65	1.07	1.77	0.96	2.02
UDC_V						
10	0.91	0.60	0.98	1.66	1.04	1.83
30	0.88	0.55	0.96	1.57	1.03	1.71
50	1.01	0.63	1.12	1.96	1.02	2.24
70	0.97	0.68	1.05	1.87	0.98	2.18
90	0.97	0.63	1.08	1.74	1.07	1.95

Table A21. Results of reduction in total stops (%) with actuated timing

%tile Volume	Arterial			Cross streets		
	All	UDC	SC	All	UDC	SC
10	-10.0*	2.7	-12.1	-6.7	-7.3	-6.6
30	-4.4	10.7	-6.9	2.2	-6.2	3.3
50	1.4	10.8	-0.3	-3.4	-6.9	-3.1
70	-6.2	-8.8	-5.7	1.5	0.6	1.7
90	-0.4	3.5	-1.2	1.4	-12.1	3.4

Note: *negative figure indicates increase in disutilities

Table A22. Simulation results of travel times with actuated timing

%tile Volume	Travel times (hr)		Reduction (%)	
	Arterial Through	Total Traffic	Arterial Through	Total Traffic
MULTI-BAND				
10	23.7	118.0	-	-
30	24.3	137.7	-	-
50	31.5	143.4	-	-
70	27.1	146.4	-	-
90	31.3	158.5	-	-
Improved basic UDC models				
10	23.8	118.8	0.4	0.7
30	25.3	137.5	4.1	-0.1*
50	31.3	143.1	-0.6	-0.2
70	27.9	145.6	3.0	-0.5
90	31.5	156.0	0.6	-1.6

Note: *negative figure indicates increase in disutilities